Scuola Internazionale Superiore di Studi Avanzati /
International School for Advanced Studies

The interaction between neuronal networks and gene networks

Thesis submitted for the degree of Doctor Philosophiae

Neurobiology sector

October 2008

Candidate
Silvia Pegoraro

Supervisor
Prof. Vincent Torre

Ed. Q1 AREA SCIENCE PARK - S.S.14 Km163,5 - 34012 Basovizza (TS) - ITALY

...a mia mamma...

...a mio papa'...

...ad Andrea...

INDEX

Declaration

The work described in this thesis has been carried out at the International School for Advanced Studies (SISSA/ISAS, Trieste, Italy) between November 2004 and August 2008. All the work in this thesis arises from my own experiments and data analysis with the exception of the microarrays analysis performed in collaboration with Daniele Bianchini and Claudio Altafini and the MEA analysis performed by Frederic Broccard, in the first work. In the second work the calcium imaging and intracellular recordings were performed by Giulietta Pinato.

The results presented in this thesis have been submitted in the following manuscripts:

Broccard FD, **Pegoraro S**, Ruaro ME, Bianchini D, Avossa D, Pastore G, Altafini C, Torre V (2008) Characterization of the time course of the activity pattern and transcriptome in a model of chemical-induced neuronal plasticity triggered by $GABA_A$ antagonists**.**
Submit to BMC Neuroscience

***Pegoraro S**, *Pinato G, Ruaro ME, Torre V (2008) Calcium control of gene regulation in rat hippocampal neuronal cultures.
*equally contributed
Submit to the Journal of Cellular Physiology

Abbreviation

Act D: Actinomycin D

BDNF: Brain-derived neurotrophic factor

Ca^{2+}: Calcium

CaMK: Serine/threonine kinases, Ca^{2+}/calmodulin-dependent kinase

cLTP: Chemically-induced long-term potentiation

CREB: cyclic adenosine monophosphate (cAMP) response element binding protein

D-AP5: d-2-amino-5-phosphonopentanoic acid

DG: Dentate gyrus

DRB: 5,6-dichloro-1-β-D-ribofuranosyl benzimidazole

E-LTP: Early long-term potentiation

ERK: Extracellular signal-regulated kinase

E-Sync: Early synchronization

GABA: γ-aminobutyric acid

GBZ: Gabazine

IEG: Immediate early gene

K^{+}: Potassium

L-LTP: Late long-term potentiation

L-Sync Late: synchronization

LTD: Long-term depression

LTP: Long-term potentiation

MAPK: Mitogen-activated protein kinase

MEA: Multielectrode array

M-LTP: Medium long-term potentiation

mRNA: Messenger RNA

NMDA: N-methyl-D-aspartate

PKC: Protein kinase C

SRE: serum-response element

VGCC: Voltage-gated calcium channel

1 Abstract

Periods of strong electrical activity can initiate neuronal plasticity leading to long-lasting changes of network properties. A key event in the modification of the synaptic connectivity after neuronal activity is the activation of new gene transcription. Moreover, calcium (Ca^{2+}) influx is crucial for transducing synaptic activity into gene expression through the activation of many signalling pathways.

In our work we are interested in studying changes in electrical activity and in gene expression profile at the network level. In particular, we want to understand the interplay between neuronal and gene networks to clarify how electrical activity can alter the gene expression profile and how gene expression profile can modify the electrical and functional properties of neuronal networks. Thus, we investigated the neuronal network at three different levels: gene transcription profile, electrical activity and Ca^{2+} dynamics.

Blockage of $GABA_A$ receptor by pharmacological inhibitors such as gabazine or bicuculline triggers synchronous bursts of spikes initiating neuronal plasticity. We have used this model of chemically-induced neuronal plasticity to investigate the modifications that occur at different network levels in rat hippocampal cultures. By combining multielectrode extracellular recordings and calcium imaging with DNA microarrays, we were able to study the concomitant changes of the gene expression profile, network electrical activity and Ca^{2+} concentration.

First, we have investigated the time course of the electrical activity and the molecular events triggered by gabazine treatment. The analysis of the electrical activity revealed three main phases during gabazine-induced neuronal plasticity: an early component of synchronization (E-Sync) that appeared immediately after the termination of the treatment persisted for 3 hours and was blocked by inhibitors of the MAPK/ERK pathway; a late component (L-Sync) -from 6 to 24 hours- that was blocked by inhibitors of the transcription. And, an intermediate phase, from 3 to 6 hours after the treatment, in which the evoke response was maximally potentiated. Moreover, gabazine exposure initiated significant changes of gene expression; the genomic analysis identified three clusters of genes that displayed a characteristic

temporal profile. An early rise of transcription factors (Cluster 1), which were maximally up-regulated at 1.5 hours. More than 200 genes, many of which known to be involved in LTP were maximally up-regulated in the following 2-3 hours (Cluster 2) and then were down-regulated at 24 hours. Among these genes, we have found several genes coding for K^+ channels and the HNC1 channels. Finally, genes involved in cellular homeostasis were up-regulated at longer time (Cluster 3). Therefore, this approach allows relating changes of electrical properties occurring during neuronal plasticity to specific molecular events.

Second, we have investigated which sources of Ca^{2+} entry were involved in mediating the new gene transcription activated in response to bursting activity. Using Ca^{2+} imaging, a detailed characterization of Ca^{2+} contributions was performed to allow investigating which sources of Ca^{2+} entry could be relevant to induce gene transcription. At the same time, changes of gene expression were specifically investigated blocking NMDA receptors and L-, N- and P/Q-type VGCCs. Therefore, the analysis of the Ca^{2+} contribution and gene expression changes revealed that the NMDA receptors and the VGCCs specifically induced different groups of genes.

Thus, the combination of genome-wide analysis, MEA technology and calcium imaging offers an attractive strategy to study the molecular events underlying long-term synaptic modification.

2 Introduction

2.1 EXPERIENCE CAN ALTER NEURAL CIRCUITRY

Sensory experience and the subsequent synaptic activity within the brain modify the neural circuits. Sensory organs transduce physical or chemical stimuli that change the membrane potential which, in this case, can be integrated to produce an action potential. The precise pattern of neuronal activity, in terms of spatial and temporal characteristics, that a sensory stimulus elicits is thought to regulate specific changes in the structure and function of the nervous system (Fig. 1).

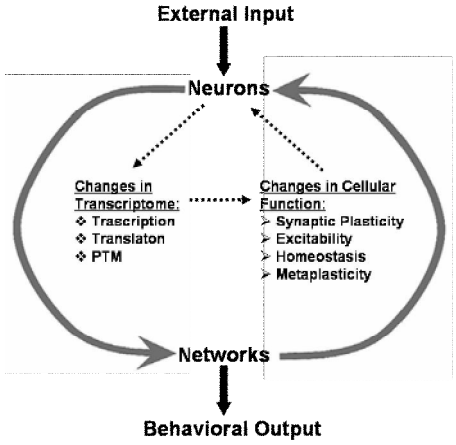

Fig.1: A dynamic model of the molecular, cellular, and systems interactions involved in the establishment and maintenance of memory. Neuronal activation driven by external inputs (e.g, sensory experience) and intrinsic brain network activity (information of the internal state of the organism) activate second messenger systems in brain neurons which modify the gene expression profiling (transcriptome) and the subsequent protein network. These changes occur via rapid post-translational modification (PTM) of pre-existing proteins and through alterations in gene expression (via regulated transcription and translation). Modifications of the protein interactome alter functional properties of neurons within an ensemble to entrain them into a representation encoding a discrete experience. (Modified from Miyashita, 2007).

Synaptic activity leads to membrane depolarization and to Ca^{2+} influx in neurons. This action then triggers a wide variety of cellular changes within these neurons, which are capable of altering the synaptic connectivity of the circuit. To determine which are the cellular mechanisms that underlie these events, has been the

subject of several investigations in recent years. One hypothesis is that neuronal activity may lead to long-lasting changes in neuronal structure and function by regulating the expression of specific genes and proteins. With this theory in mind, over two decades ago, it was shown that the activation of an ion channel could lead rapidly to the expression of a gene (Greenberg et al., 1986).

In the rapid coupling of ion channel activation and gene transcription, Ca^{2+} has a pivotal role. Calcium can activate several Ca^{2+}-sensitive signalling pathways, which lead to post-translation modification of proteins or translation of pre-existing mRNA (Malinow and Malenka, 2002; Sutton and Schuman, 2006). In addition to these local effects, Ca^{2+} entry into the postsynaptic neuron can alter cellular function by activating new gene transcription (Bito et al., 1997). Calcium influx activates a number of signalling pathways that converge on transcription factors within the nucleus; these transcription factors, in turn, control the expression of a large number of neuronal activity-regulated genes that alter the structure and function of the cell. Several works have revealed a number of signalling pathways that mediate activity-dependent transcription (for reviews see Ghosh and Greenberg, 1995; Rosen et al., 1995; Bradley and Finkbeiner, 2002).

Considered all together these features give special relevance to the functional connections among neuronal activity, Ca^{2+} influx and gene expression; and these three main topics will be discussed in the present introduction.

The nervous system has the unique ability to shape and reshape itself in long lasting manners after brief sensory stimulation. Specifically, a large number of studies have provided evidence that neuronal activity plays a critical role in different cellular functions: i) dendrites outgrowth, ii) synaptic maturation or elimination, and iii) synaptic plasticity.

2.1.1 Dendrites Outgrowth

Environmental stimuli can alter dendrites outgrowth. Dendrites commonly sprout new branches and extend or retract existing branches. Blockade of N-methyl-D-aspartate (NMDA) subtype of glutamate receptors slows both new dendritic branch addition and branch extension (Rajan and Cline, 1998). Additional *in vitro* data (Redmond et al., 2002) suggested that synaptic activity promotes dendrites outgrowth. These cellular modifications are mediated by Ca^{2+} via new gene transcription. In fact, in this study the authors have demonstrated that in cortical slice cultures, dendritic growth is attenuated by inhibitors of voltage gated calcium channels (VGCCs) and by dominant negative of cyclic adenosine monophosphate (cAMP) response element binding protein (CREB).

2.1.2 Synapse Maturation/Elimination

Synapses form on the dendrites and undergo extensive maturation. For example, this maturation involves arborisation of the axon at the presynaptic site of neuromuscular junction (Sanes and Lichtman, 1999), whereas on the postsynaptic site, maturation can be detected as an increase in synaptic current (Chen and Regehr, 2000). In addition to synapse maturation, also synapse elimination can occur. In fact, after synaptic activity an excess of synapses are formed but only a subset of these synapses is strengthened while the others are eliminated. Synaptic activity has an important role in mediating both synapse maturation and elimination (Colman et al., 1997; Chen and Regehr, 2000).

2.1.3 Synaptic Plasticity

Experience can alter synaptic connectivity and synaptic efficacy in adults, in fact this is how the information is thought to be stored in the brain. Studies of

associative learning give significant evidence in the experience-dependent memory formation. An example is the Pavlovian fear conditioning paradigm, in which an electrical shock to the foot is administered to an animal shortly after an auditory tone is presented. After several repetitions, the animal learns that the tone and the shock are paired. So, they display a fear response when the tone is presented even in the absence of the electrical shock. Recordings from the dorsolateral nucleus of amygdala, which receives direct inputs from the auditory system, demonstrated that these neurons had an increased firing rate in response to the tone after the paradigm had occurred (Maren and Quirk, 2004). This is a clear example of how, in adult animals, experience can trigger a memory and influence the behaviour, by modifying the synaptic efficiency of neurons.

A very useful experimental model called long-term potentiation (LTP) has given the opportunity to investigate which are the molecular and cellular mechanisms that underlie these changes. This model demonstrated that the activity-dependent plasticity is a fundamental property of the nervous system and it is at the basis of the formation and consolidation of memory and learning (Bliss and Collingridge, 1993).

2.2 MODELS OF ACTIVITY-DEPENDENT SYNAPTIC PLASTICITY

2.2.1 Long-Term Potentiation

In the late 1940s Hebb and Konorsky proposed a rule to produce synapse potentiation: the synapse linking two cells is strengthened if the cells are active at the same time. The first example of such synapse that was identified in the mammalian brain was the excitatory connection made by perforant path fibres onto granule cells of the hippocampus. In 1973 Bliss et al. described a model in which brief trains of high-frequency stimulation to monosynaptic excitatory pathways in the hippocampus caused an increase in the efficacy of synaptic transmission.

This model has been called long-term potentiation (LTP). In the last decades, LTP of synaptic transmission has become the primary experimental model of activity-dependent synaptic plasticity in the mammalian brain. Using this model, the mechanisms underlying its induction and expression were then investigated in order to elucidate the synaptic basis of memory and learning (Bliss and Collingridge, 1993). In fact, hippocampal LTP and processes like memory and learning were compared and several similarities were discovered. These new findings included: rapid induction, synaptic potentiation by repetition of the stimulus, long-lasting persistence, dependence on NMDA receptors in most protocols of induction and correlation of LTP decay with the time course of normal forgetting (Otto et al., 1991; Whitlock et al., 2006; Pastalkova et al., 2006).

LTP is characterized by a persistent increase in the size of the synaptic component of the evoked response, for many hours in the *in vitro* hippocampal slice preparation, and for days or months in freely moving animals (*in vivo* models). Although LTP depends on the cell type, developmental stage and induction protocol, it has also been established that LTP has distinct temporal phases (Abraham, 2003). The first nomenclature created by Racine et al. in 1983 divided LTP in an early phase (E-LTP) and in a late phase (L-LTP). The early phase, beginning immediately after stimulation and lasting for 1 to 3 hours, was induced by a single high-frequency train and did not require protein synthesis. The late phase was long-lasting (more than 3 hours), was induced by three or more high-frequency trains and was dependent on protein synthesis (Racine et al., 1983). During the past two decades, significant evidence supporting a more precise categorization method has been produced. Abraham and Otani analysed the LTP decay in the dentate gyrus (DG) *in vivo*. They observed three discrete groups of LTP-decay time constants that had been defined in order of persistence, as LTP1, LTP2 and LTP3. LTP1 was induced by a weak stimulus protocol and was rapidly decaying, LTP2 was at an intermediate phase of LTP, and LTP3 was defined as the most persistent form of LTP (Otani and Abraham, 1989).

Considerable efforts have been made to understand the biochemical pathways that underlie these forms of LTP and, although differences can still be found in literature, three broad mechanisms are clearly involved in the different forms of LTP: post-translational modification of pre-existing proteins, translation of pre-existing messenger RNA (mRNA) and new gene transcription. Calcium entry through different channels, such as the NMDA receptors and the VGCCs plays a major role in these mechanisms.

It has been established that post-translational modifications, primarily phosphorylation, are important mechanisms in LTP induction. The two most common protein kinases implicated in the early phase of LTP are the serine/threonine kinases, Ca^{2+}/calmodulin-dependent kinase II (CaMKII) and protein kinase C (PKC) (Bliss and Collingridge, 1993). The time window of activity of both these kinases and the relative contribution to different phases of LTP is currently a matter of debate (Lisman et al., 2002; Reymann and Frey, 2007). Although CaMKII is involved in multiple forms of the NMDA receptor dependent LTP (Lisman et al., 2002), the current hypothesis is that this component is the primary effector of LTP1. There are also other kinases that seem to be important for supporting long-lasting LTP. The extracellular signal-regulated kinase (ERK)–mitogen-activated protein kinase (MAPK) pathway has recently become the subject of important LTP studies (Thomas and Huganir, 2004). Even though it seems to be meaningful for long-lasting form of LTP (Rosenblum et al., 2002), Sweatt proposed a model in which ERK plays a role during both early and late phases of LTP. According to this model, ERK seems to modulate E-LTP by regulating voltage-gated potassium channels, and triggers L-LTP by regulating CREB phosphorylation and subsequent gene expression (Sweatt, 2001). In addition to post-translational modification of existing proteins it is also evident that protein synthesis is equally necessary for LTP. Recent works demonstrated that this new protein synthesis does not dependent on gene transcription. So, protein translation must be performed from pre-existing mRNAs present in the dendrites of most neurons (Sutton and Schuman, 2005).

Finally, in 1994 Nguyen et al. demonstrated that the LTP3 or L-LTP depended on new gene transcription and that it was necessary to have a critical time window for this event. They used rat hippocampal slices stimulated with three stimulation trains to induce a long-lasting LTP. To assay the involvement of transcription in L-LTP, they applied for two hours - immediately after LTP induction - two inhibitors of transcription, actinomycin D (Act D) and 5,6-dichloro-1-β-D-ribofuranosyl benzimidazole (DRB) which have distinct mechanisms of action. So, they found that these treatments blocked the induction of L-LTP. Moreover, if the application of the inhibitors was delayed 2 hours after the stimulus, there was no blockade of L-LTP induction, indicating a critical period for gene transcription (Nguyen et al., 1994).

Thus, there are three main mechanisms underlying different forms of LTP: i) post-translational modification (LTP1), ii) dendritic protein synthesis (LTP2) and iii) new gene transcription (LTP3).

2.2.2 Chemically-Induced Long-Term Potentiation

The induction of LTP, as described above, is usually performed by stimulating with brief high-frequency trains a group of axons that converge towards a target neuron. In this way the stimulation is highly localized and only a small number of synapses are potentiated. Moreover, the stimulated synapses are randomly distributed along the dendritic tree and cannot be easily identified. Therefore, in order to study the electrical and transcriptional modification at the network level, it would be necessary to have a model in which the majority of the synapses undergo to plasticity changes. For this reason, there has been considerable interest in inducing LTP following different protocols. In particular, chemical protocols for inducing LTP (cLTP) also exist and have become popular (Ben Ari and Gho, 1988; Ben Ari and Represa, 1990; Fleck et al., 1992; Kang and Schuman, 1995; Abegg et al., 2004; Otmakhov et al., 2004).

Inducing LTP by chemical rather than electrical protocol is advantageous for several reasons. First, a chemical stimulation that activates directly a biochemical process inducing potentiation can indicate a specific involvement of that process in LTP. Second, cLTP ensures potentiation of a large fraction of synapses in the cells cultured. Several protocols are reported to induce synaptic potentiation by bath-application of different chemicals, such as brain-derived neurotrophic factor (BDNF) (Kang and Schuman, 1995), forskolin (Otmakhov et al., 2004), potassium (K^+) (Fleck et al., 1992) and bicuculline (BIC) (Debanne et al., 2006).

The neurotrophins are a group of signalling molecules and are important for the regulation of neuronal survival and differentiation. Moreover, they participate in synaptic plasticity (for review, see Reichardt, 2006). These characteristics indicate that they could be involved in regulate synaptic strength in the adult brain. Kang and Schuman applied BDNF and neurotrophic factor 3 (NT-3) extracellularly for 30 min in hippocampal slices from young adult rats and they observed a rapid enhancement of the excitatory synaptic transmission which persisted for two hours. The rapid onset and the long-lasting duration of the neurotrophin-induced potentiation were similar to those observed during LTP induced by high-frequency stimulation. Hence, the authors tested the ability of each form of potentiation to occlude subsequent induction of the other form, in order to understand whether the neurotrophin-induced potentiation shared common cellular mechanisms with synaptically induced LTP. They found that both protocols did not occlude the induction of potentiation induced by the other form. Thus, these data suggested that these two forms of synaptic enhancement may involve at least partially independent cellular mechanisms (Kang and Schuman, 1995).

A frequently used method for inducing cLTP utilizes a bath application of agents that raise cAMP levels (Frey et al., 1993; Bolshakov et al., 1997; Patterson et al., 2001; Otmakhov et al., 2004). For example, a combination of forskolin, an adenylyl cyclase activator, and rolipram, a phosphodiesterase inhibitor, in the presence of low magnesium (Mg^{2+}), is able to induced cLTP in hippocampal slices

from adult rats, where this cLTP is NMDA receptor-dependent (Otmakhov et al., 2004).

The models of cLTP described above are very useful because not only do they allow the potentiation of the large majority of the synapses in the cells cultured but they also provide important insights into the molecular mechanisms underlying LTP.

Also bursting activity (epileptiform activity) has been shown to induce long-lasting potentiation of excitatory synapses in the hippocampus (Ben Ari and Gho, 1988; Fleck et al., 1992; Morgan and Teyler, 2001; Abegg et al., 2004; Debanne et al., 2006). The bursting activity can be chemically induced by elevating K^+ to increase excitation or by applying γ-aminobutyric acid $(GABA)_A$-receptor antagonists, like bicuculline, to decrease inhibition. For example, the experiments of Morgan and Teyler were performed on hippocampal slices from adult rats treated for 10 min with an elevated K^+ concentration. They confirmed that after washout of elevated K^+ the evoked response increased, resulting in LTP and they also demonstrated that this form of LTP consisted of two components mediated by both NMDA receptor and L-type VGCCs as well as for classical LTP (Morgan and Teyler, 2001).

2.2.3 $GABA_A$ Receptors Inhibition: A Model of Synaptic Plasticity

A prolonged period (3 min to 15 h) of bursting activity is able to induced potentiation at the excitatory synapses in hippocampal slices (Abegg et al., 2004; Debanne et al., 2006). The bursting activity can be initiated decreasing the inhibition by application of a $GABA_A$ receptors antagonist such as bicuculline or gabazine (GBZ). When organotypic hippocampal slices were treated with bicuculline, synchronous bursts of network activity were induced (Abegg et al., 2004). In the experiments of Abegg et al. (2004), simultaneous recordings of field potential in the CA3 region (presynaptic activity) and the membrane potential of a CA1 pyramidal cell (postsynaptic activity) revealed that during bursting pre- and postsynaptic cells

are activated concomitantly. They observed that an overnight of incubation with bicuculline led to an NMDA receptor-dependent activation of silent synapses and a potentiation of functional synapses. In addition, they checked the possibility to induce LTP with a conventional stimulation protocol in slices treated with bicuculline. Their results showed that synapses that were strengthened by bicuculline-treatment cannot be further potentiated. On the other hand, the induction of long-term depression (LTD) was enhanced. Furthermore, Debanne et al. (2006) reported that even a brief (<3 min) exposure of rat hippocampal slices to bicuculline, can induce reversible**,** long-lasting potentiation of glutamatergic transmission at CA3-CA1 and at CA3-CA3 pyramidal cell synapses. They demonstrated that this potentiation, as classical LTP, depended on NMDA receptor activation. In fact, application of bicuculline in the presence of the NMDA receptor antagonist d-2-amino-5-phosphonopentanoic acid (D-AP5) blocked the synaptic potentiation (Debanne et al., 2006).

Moreover, bursting-induced potentiation shares several characteristics with conventional LTP. First, Hebbian conditions for LTP induction are established during bursting, i.e. pre- and postsynaptic cells are activated simultaneously. Second, burst-induced potentiation of synaptic transmission is blocked in a reversible manner by NMDA-receptor antagonist, like conventional LTP. Third, bursting-induced potentiation occludes induction of LTP with standard pairing protocol and like LTP it could be reversed by low-frequency stimulation. Therefore, it is conceivable that bursting-induced synaptic potentiation and LTP share a common expression mechanism. Moreover, this system is able to potentiate a large fraction, virtually all, of the synapses in the cells cultured. This allows the investigation of the response at the network level.

Furthermore, Arnold et al. (2005) developed a cell culture system to study neuronal plasticity. They described a model to induce synaptic plasticity in dissociated hippocampal cultures applying bicuculline for 15 min. They observed that, like in hippocampal slices, bicuculline induced an increase in synaptic efficacy

and a change in network activity from uncoordinated firing (lacking any recognizable pattern) to a highly organized, periodic and synchronized firing. These changes in the network activity persisted for several days after bicuculline washout. This form of plasticity depended on NDMA receptors and for the long-lasting expression required new gene transcription (Arnold et al., 2005). Thus, this could be a useful model to study the changes and the mechanisms underlying synaptic plasticity.

Starting from these considerations we decided to study at larger scale changes that occur in network activity and in gene expression profiling after induction of this form of synaptic plasticity. In our model we used dissociated hippocampal cultures grown on the multielectrode arrays (MEAs) and treated for 30 min with gabazine as $GABA_A$ receptor inhibitor, to induce synchronous bursts. Although bicuculline is generally used in a variety of experimental models, we preferred to use gabazine because it is well known that bicuculline also blocks the afterhyperpolarizing current (IAHP) (Debarbieux et al., 1998).

Dissociated hippocampal neurons are a useful model to study network properties. Although cultured neuronal networks developed *in vitro* lack the functional cytoarchitecture from the region where the cells were dissociated and can be considered as random networks, they retain many features and characteristics of physiological networks (Potter, 2001; Marom and Eytan, 2005). In fact, the primary neuronal cultures from hippocampus have been extensively used as a model of synaptogenesis, in which the electrical activity is dependent on the connectivity of the neurons, rather than the properties of individual cells (Siebler et al., 1993). In addition, results obtained from work in our lab using *in vitro* random networks of rat hippocampal neurons, demonstrated that these networks could perform some basic image processing operations (Ruaro et al., 2005). All together, these results (Ruaro et al., 2005; Marom and Eytan, 2005) indicate that random networks are capable of some form of learning and can be used to investigate their mechanisms of induction and maintenance.

In order to investigate the network functions, it is essential to measure simultaneously the activity of a large number of neurons. In the last two decades, great efforts were made to develop planar multielectrode arrays (MEAs). MEAs are petri dishes with embedded electrodes that allow simultaneous recording from, and stimulation of, a large number of neurons for a long period of time, ranging from hours up to a month, thanks to their non-invasive extracellular electrodes (Pine, 1980; Nisch et al., 1994; Potter, 2001).

2.3 CALCIUM: A MOLECULE FOR SIGNALLING

The acquisition and consolidation of new information is achieved through activity-dependent, and sustained, modification of synaptic strength. Activity at synapses must therefore be communicated to the nucleus and newly synthesized proteins must play a role in modification of synaptic strength. In their pioneering paper on excitation-transcription coupling, Morgan and Curran put forward a hypothesis on how Ca^{2+} entry through L-type VGCCs might activate espression of *c-fos*, an immediate early gene (IEG) (Morgan and Curran, 1986). They suggested that a calmodulin (CaM)-sensitive kinase would phosphorylate a transcription factor that activates gene expression.

Calcium binding to proteins triggers changes in shape and charge, two features that govern protein function. The abilities of Ca^{2+} to alter local electrostatic fields and protein conformation are the two universal tools of signal transduction. A very steep gradient of Ca^{2+}, over four orders of magnitude, exists across the plasma membrane of all eukaryotic cells. Cytosolic free Ca^{2+} is maintained roughly at 100 nM while extracellularly the Ca^{2+} concentration is over 1 mM. This gradient is maintained thanks to the action of plasma membrane Ca^{2+}-ATPases (PMCA) and Na^{+}/ Ca^{2+} exchangers (NCX). In addition, to exert control over cytoplasmic Ca^{2+} concentration, cells chelate and compartmentalize it in the endoplasmic reticulum. Hundreds of

cellular proteins act by binding Ca^{2+}, in some cases simply to buffer or lower Ca^{2+} levels, and in others to trigger cellular processes.

Calcium is an ubiquitous intracellular messenger, controlling a diverse range of cellular processes, such as gene transcription, muscle contraction, cell proliferation and cell survival or apoptosis. It shows the versatility of a simple ion in playing a pivotal role in cell biology results from its spatial and temporal properties (Berridge et al., 2000). The spatial properties refer to the subcellular location of the Ca^{2+} influx (*microdomain*) (Rizzuto and Pozzan, 2006); the temporal properties are defined by the amplitude, kinetics or frequency of the Ca^{2+} signal (Gu and Spitzer, 1995).

The term Ca^{2+} microdomain is generally used, referring to all the increases in cellular Ca^{2+} that do not involve the generality of the cell cytoplasm, but remain localized in a part of the cell (Rizzuto and Pozzan, 2006). The definition of Ca^{2+} microdomain appeared in the 1970s and 1980s to explain results otherwise uninterpretable, but still without a solid experimental support. In fact some observations, such as the high Ca^{2+} buffering capacity of the cytoplasm, the very low Ca^{2+} diffusion rate, 10–50 $\mu m^2/s$ (Allbritton et al., 1992), the existence of highly organized subcellular structures and the clustering of Ca^{2+} channels (both of the plasma membrane and of organelles) in discrete membrane domains, were ideal to describe transient (or even prolonged) local elevations of Ca^{2+}. Only in the late 1980s when fluorescent Ca^{2+} indicators became widely available, localized Ca^{2+} signals within the cytoplasm of living cells were finally measured. One of the first direct measurements of a localized Ca^{2+} increase was reported in 1988: a subplasma membrane Ca^{2+} increase (in the cell body and growth cones) activated in sympathetic neurons by membrane potential depolarization or Ca^{2+} mobilization from intracellular stores (Lipscombe et al., 1988a; Lipscombe et al., 1988b). Then, the existence, amplitude, and functional role of Ca^{2+} microdomains became the subject of intense investigation over the last decades concerning their role in neurotransmitter release (Neher, 1998) and gene expression induction (Dolmetsch et al., 2001; Hardingham et al., 2001; Mellstrom and Naranjo, 2001).

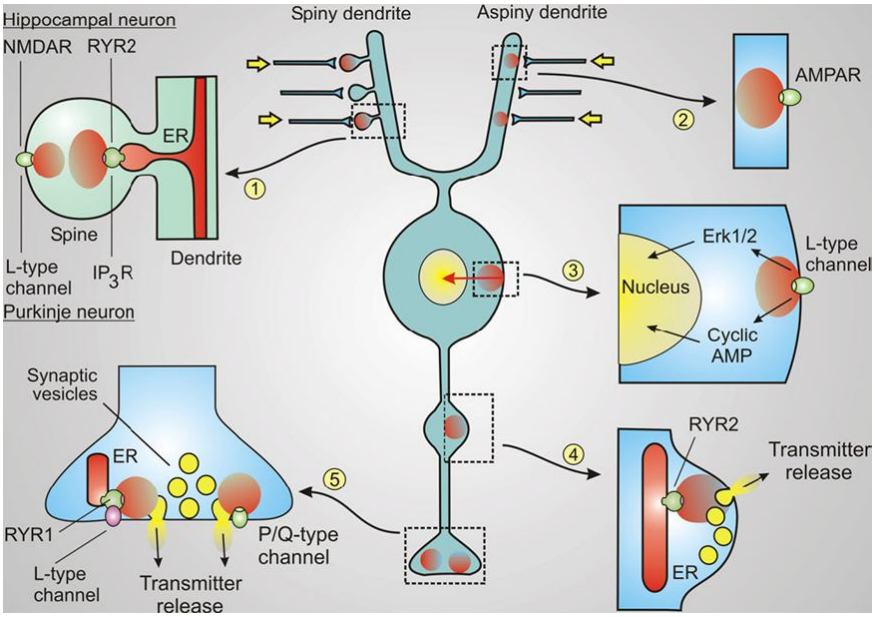

Fig. 2: Neuronal Ca^{2+} domains are responsible for carrying out a large number of highly localized neuronal functions. (1) In the case of spiny dendrites, those spines that are stimulated by a synaptic input (yellow arrows) create a microdomain of Ca^{2+} responsible for the input-specific synaptic plasticity that underlies learning and memory. The microdomain is created by either entry channels, internal release channels or a combination of the two. (2) Similar Ca^{2+} microdomains are found in aspiny dendrites where they are formed by the brief opening of AMPA receptors (AMPARs). (3) The opening of L-type Ca^{2+} channels on the soma create microdomains responsible for activating both the cyclic AMP and MAP kinase signalling pathways to create signals that travel into the nucleus to activate gene transcription. (4) In the case of hippocampal mossy fibres, there are a large number of boutons where transmitter release is triggered by the spontaneous release of Ca^{2+} by RYR2 on the endoplasmic reticulum (ER). (5) At synaptic endings, release of transmitter can be triggered by either the entry of external Ca^{2+} or the release of internal Ca^{2+}. The classical mechanism depends on the opening of P/Q channels associated with the exocytotic apparatus on synaptic vesicles to create a local microdomain responsible for triggering exocytosis. A specialized mechanism based on syntillas produced by RYR1s that are activated by L-type channels in the plasma membrane as described in hypothalamic neurons. (From Berridge MJ 2006).

Calcium microdomains can initially arise as a consequence of Ca^{2+} influx through plasma membrane voltage- and neurotransmitter-activated Ca^{2+} channels or through store-operated Ca^{2+} channels; activation of Ca^{2+} release channels present in intracellular stores can also generate Ca^{2+} microdomains (for review, see Berridge, 2006) (Fig.2). The different outcomes will be the consequences of the action of a wide range of Ca^{2+} sensor proteins, located close to the route of Ca^{2+} entry, which in turn transduce the Ca^{2+} signals into specific changes in cellular function (Dolmetsch et al., 2001; Hardingham et al., 2001; Calin-Jageman and Lee, 2008).

Then, Ca^{2+} influx is essential for synapse-to-nucleus signalling enabling information contained in fast electrical activity at the synapse to be transduced into long-lasting changes (West et al., 2001). Among the Ca^{2+}-regulated processes critical for long-term structural and functional modification of neurons, are changes of gene expression (Morgan and Curran, 1986; Ginty et al., 1992). Therefore, a major aim in the field has been to identify the mechanisms by which Ca^{2+} entry - through specific ion channels -regulates gene expression in order to produce a specific response for long-term synaptic modification.

In the following sections of this introduction I will discuss the possible routes of Ca^{2+} entry and their role in gene expression changes, including the signalling pathways involved in the transduction of the electrical signal in a transcriptional response.

2.4 ROUTES OF CALCIUM ENTRY

Research from many laboratories has shown that Ca^{2+} influx through ion channels can regulate gene expression by multiple and diverse mechanisms. There are four primary routes of calcium entry into the cytoplasm of the postsynaptic neuron: extracellular calcium can enter 1) through the ligand-gated ion channels of the NMDA and 2) a-amino-3-hydroxy-5-methyl-4-isoxazolepropionate- type (AMPA) (Jonas and Burnashev, 1995) glutamate receptors, 3) through VGCCs, or 4) calcium can be released from intracellular stores (Berridge, 1998). The different molecular nature of these channels, their subcellular distribution and their regulation are the key components of the generation of subplasma membrane Ca^{2+} signalling to the nucleus.

The state of the art tells us that there are two main routes of Ca^{2+} entry involved in inducing gene transcription: the NMDA receptors and the VGCCs.

NMDA receptor gating is dependent on the binding of glutamate as the agonist, glycine as a co-agonist, and depolarization to a membrane potential of-50 mV or more to release the Mg^{2+} that blocks the channel. NMDA receptor channels have a high permeability to Ca^{2+} compared to other glutamate receptors and their activation/deactivation kinetics are slow. In the central nervous system (CNS), NMDA receptors are predominantly localized to the postsynaptic region of the dendrites (Benke et al., 1993). It is well established that the Ca^{2+} influx through NMDA receptors plays a critical role in the neuronal survival and refinement of neuronal connections during brain development, as well as in the synaptic plasticity underlying learning and memory (Bliss and Collingridge, 1993; Hardingham and Bading, 2002).

Voltage-gated Ca^{2+} channels mediate Ca^{2+} entry into cells in response to membrane depolarization. Electrophysiological studies revealed different Ca^{2+} currents: the L-type currents are distinguished by high voltage threshold of activation, slow inactivation, and large single-channel conductance, which make them ideal for passing the large amount of Ca^{2+} necessary to increase the Ca^{2+} concentration within the cytoplasm and the nucleus. The N-, P/Q- and R-type currents are distinguished by their intermediate threshold of activation and an inactivation faster than L-type currents. Finally, the T-type currents are characterized by fast activation and inactivation and the lowest threshold of activation (for review on VGCCs, see Catterall, 2000). All major types of VGCCs are present in dendritic arborization of CA1 hippocampal pyramidal neurons (Bloodgood and Sabatini, 2007). Immunohistochemical studies of the distribution of different isoforms of alpha subunits (i.e. the pore forming subunit) constituting VGCCs in rat hippocampal neurons have shown that T and R-types are mainly expressed in the dendrites while L, N and P/Q -types are primarily expressed in the soma or proximal dendrites (Westenbroek et al., 1990; Westenbroek et al., 1992; McKay et al., 2006; Vinet and Sik, 2006).

Activation of NMDA receptors induces the transcription of many immediate-early genes in cultured hippocampal neurons (Cole et al., 1989; Bading et al., 1995). Among the VGCCs, Ca^{2+} influx through the L-type has been extensively studied as mediator of changes in gene expression. In fact, activation of L-type VGCCs has been coupled to gene expression in the cell line pheochromocytoma 12 (PC12), in primary neuron cultures from the cortex, hippocampus, striatum, and cerebellum, as well as neurons within hippocampal and cortical slides (Greenberg et al., 1986; Murphy et al., 1991; Lerea et al., 1992; Bading et al., 1993; Impey et al., 1996; Tao et al., 1998). Besides the involvement of L-type VGCCs in gene transcription, also P/Q-type VGCCs are shown to be involved in the induction of syntaxin-1A (Sutton et al., 1999). By contrast, little is known about the regulation of gene expression by Ca^{2+} channels such as the inositol-1,4,5 trisphosphate receptors (IP3-R) and the ryanodine receptors (RyR) that release Ca^{2+} from intracellular stores.

An important feature of the Ca^{2+} signalling is the specificity. Since neurons are constantly exposed to a variety of extracellular stimuli that can affect cell vitality, morphology and synaptic connectivity, the response to such stimuli has to be specific. So neurons activate specific genes, which in turn produce proteins that alter the structure and function of the cell.

Over the past decade, studies of Ca^{2+}-dependent gene expression in a number of cell types have demonstrated that Ca^{2+} influx may produce specific responses in the nucleus. For example in B-lymphocytes the amplitude of the Ca^{2+} rise controls specific patterns of gene expression (Dolmetsch et al., 1997), whereas different frequencies of Ca^{2+} oscillations in T-lymphocytes were demonstrated to induce the expression of different genes (Dolmetsch et al., 1998). The frequency of spontaneous Ca^{2+} transients was also shown to be essential for the expression of certain genes in embryonic spinal neurons (Watt et al., 2000). Experiments using neurons of the CNS have revealed that the temporal profile of increases in Ca^{2+} may induce specific nuclear responses. As well as Ca^{2+} temporal profile, also the spatial profile is critical for the production of a specific response. Various studies have demonstrated that

Ca^{2+} influx through different types of Ca^{2+} channel activates different biochemical processes that trigger distinct patterns of gene expression (Bading et al., 1993; Gallin and Greenberg, 1995; Finkbeiner and Greenberg, 1998; Dolmetsch et al., 2001). Bading et al. (1993) demonstrated in primary hippocampal cultures that NMDA receptors and L-type VGCCs transmit signals to the nucleus and regulate gene transcription through two distinct Ca^{2+} signalling pathways. In fact, they observed that the relative induction of *c-fos* gene by selective stimulation of NMDA receptors and L-type VGCCs, was dependent on different enhancer elements within the promoter of the gene. The *c-fos* promoter contains two well-characterized enhancer elements, the serum-response element (SRE) and the cyclic adenosine monophosphate response element (CRE). In their experiments, hippocampal neurons were transfected with plasmids that contained mutations in each of these enhancer elements and consequently stimulated while blocking selectively one of the two channels. In this way the authors showed that L-type VGCCs can activate *c-fos* through either SRE or CRE whereas NMDA receptors only activate *c-fos* through SRE. Moreover, also the transcription of *Bdnf* gene is preferentially driven by Ca^{2+} influx through L-type VGCCs, whereas it is weakly induced by NMDA receptors activation (Ghosh et al., 1994). Specific Ca^{2+} channel-dependent gene expression was also demonstrated by Sutton et al. (1999), who found that transfection of HEK293 cells with P/Q-type VGCCs but not with L-, N- and T-type induced transcription of syntaxin-1A. Furthermore, Dolmetsch et al. (2001) using primary cortical neurons demonstrated that, even though after stimulation with high K^+, the global increase in Ca^{2+} concentration was the same in the presence of L-type VGCC blockers as in the presence of N- and P/Q-type VGCC blockers, L-type VGCC blockers completely blocked CREB-dependent reporter gene expression whereas N- and P/Q-type VGCC blockers did not.

All these observations support the idea that Ca^{2+} influx through different types of Ca^{2+} channels can direct the transcription of different genes, and control different

programs of gene transcription. More than ten years ago, the Bading group, after the observations raised about the distinct regulation of gene expression by NMDA receptors and L-type VGCCs, discussed some hypothesis about how Ca^{2+} influx through different channels could be specific for different transcriptional responses. They hypothesized that it may depend on the availability of a particular mechanism for signal processing at the site of Ca^{2+} entry; or it may depend on the different concentration thresholds of Ca^{2+} that differ locally within the neuron (Bading et al., 1993). Dolmetsch et al. (2001) demonstrated that the specificity of Ca^{2+} influx through L-type VGCCs to activate CREB was due to the ability of the channel to bind Ca^{2+}-calmodulin (CaM) through an isoleucine-glutamine ("IQ") motif in its carboxyl terminus. Ca^{2+}-CaM binding to the L-type VGCCs was necessary for the activation of the MAPK pathway, which conveyed local Ca^{2+} signals from the mouth of the channel to the nucleus.

2.5 SIGNALLING FROM SYNAPSE TO THE NUCLEUS

Various studies focused on the pathway triggered by an intracellular Ca^{2+} rise downstream of synaptic activity, and now it has been confirmed that the signal from cytoplasm to the nucleus can be conveyed in several ways. Calcium can interact directly with a transcription factor in the nucleus modifying its DNA-binding properties (i.e. DREAM); or Ca^{2+} can interact with a protein in the cytoplasm, such as calmodulin, to activate signalling pathways involving kinases or phosphatases that finally modify and activate transcription factors. All these pathways result in the activation of well defined gene expression programs allowing the neurons to modify themselves in response to a specific stimulus.

2.5.1 Nuclear Factor of Activated T Cells (NFAT)

Calcium regulation of NFAT is the classical example of signalling through translocation of the transcription factor itself to the nucleus upon changes in its phosphorylation state. Although the NFAT family of transcription factors were characterized in immune tissues, they also play an important role in neuronal plasticity as well as vascular development and muscular hypertrophy (Crabtree and Olson, 2002).

In particular, NFATc4 is expressed within hippocampal neurons, and undergoes activation upon Ca^{2+} influx through L-type VGCCs (Graef et al., 1999). In resting cells, NFATc4 is phosphorylated and resides in the cytoplasm. After L-type VGCCs opening, the cytoplasmic Ca^{2+} rise activated the Ca^{2+}/CaM-dependent phosphatase calcineurin that dephosphorylates NFATc4. This modification causes the unmasking of multiple nuclear localization signals on NFATc4 and the active transportation of the transcription factor into the nucleus.

2.5.2 Downstream regulatory element antagonist modulator (DREAM)

An opposite mechanism of Ca^{2+} regulation of gene expression is represented by the transduction of free Ca^{2+} that can arise in the nucleus after neuronal excitation. The transcription factor DREAM is a Ca^{2+} binding protein that contains three active Ca^{2+} binding motifs (EF hands) (Carrion et al., 1999). DREAM is abundant in the nucleus where it is bound to a downstream regulatory element (DRE) and acts as a gene repressor. This process is controlled by Ca^{2+} concentration, in fact, when nuclear Ca^{2+} is low (0.5 μM) DREAM binds to DRE, whereas dissociates upon elevation of Ca^{2+} (10 μM) causing activation of downstream genes (Osawa et al., 2001). For example, de-repression of DRE causes activation of transcription of prodynorphin and attenuation of pain signalling *in vivo* (Cheng et al., 2002).

2.5.3 Calcium Regulated Protein Kinases: CaMKs and ERK

Activation of NFAT and DREAM describe the extremes in the Ca^{2+} signalling from the plasma membrane to the nucleus, but the predominant mechanism by which Ca^{2+} signals are further processed within cytoplasm and the nucleus, ultimately leading to activation of the transcriptional-regulating machinery, involves protein kinase cascades. Two main signalling pathways regulated by Ca^{2+} are the CaMKs pathway and the ERK pathway (Fig. 3).

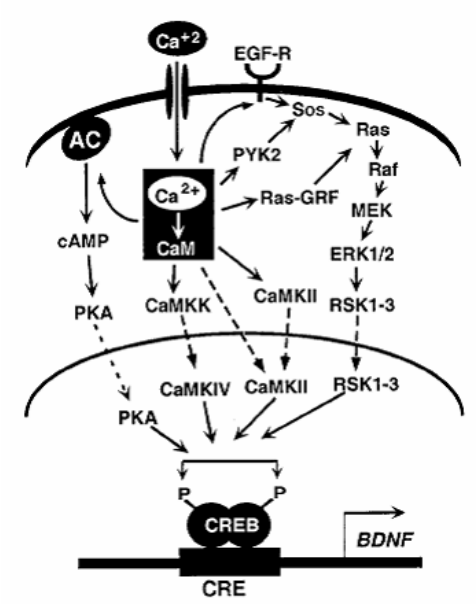

Fig. 3: Calcium-activated signaling pathways that regulate gene transcription. In neurons, neurotransmitter reception and membrane depolarization lead to the opening of ligand- and voltage-gated calcium channels. Subsequent calcium influx across the plasma membrane drives the activation of a number of signaling molecules, including the calcium-sensitive adenylate cyclase, calciumycalmodulin-activated kinases, and Ras. Each of these molecules activates a cascade of signaling proteins that amplifies the calcium signal and carries it to the nucleus. Dashed lines represent the components of each pathway that are proposed to translocate into the nucleus. Nuclear kinases including protein kinase A, CaMK-IV, and members of the Rsk family phosphorylate CREB at Ser-133, rendering it competent to mediate transcription of genes such as *BDNF*. (from Shaywitz and Greenberg 1999).

Calmodulin (CaM) is a small (148 amino acids) acidic protein capable of binding four Ca^{2+} ions. The Ca^{2+}/CaM complex interacts and activates a variety of cellular effectors which include protein kinases and phosphatases (Means et al.,

1991). Deisseroth et al. (1998) showed that synaptic stimulation induced the translocation of calmodulin from dendrites to the nucleus of hippocampal neurons. In addition, the amount of calmodulin in the nucleus correlated with the extent of CREB phosphorylation, suggesting that a calmodulin-kinase regulated CREB (Deisseroth et al., 1998). Most of the studies have correlated CREB activation with the activity of the CaMKIV, which is localized in the nucleus (Matthews et al., 1994; Bito et al., 1996; Chawla et al., 1998). Furthermore, Dolmetsch et al. (2001) demostrated that stimulation of L-type VGCCs mediated CREB phosphorylation and, that this was realized through a direct interaction between the L-type channel and CaM with the subsequent activation of MAPK pathways. Hence, another molecule which may serve as a signal between Ca^{2+} channels and the nucleus is ERK1/2. Their activity is controlled by the MAPK signalling pathway; after activation ERKs translocate from the cytoplasm to the nucleus where they phosphorylate and activate transcription factors, such as CREB (Curtis and Finkbeiner, 1999). In the work of Wu et al. (2001), the authors demonstrated that stimulation of hippocampal neurons with high K^+ resulted in both activation of rapid CaMK and slow MAPK signalling pathways responsible for CREB phosphorylation (Wu et al., 2001).

In summary, the transfer of information from the membrane surface of a neuron to the nucleus can be achieved in two different ways: either Ca^{2+} can directly interact with a transcription factor in the nucleus (i.e. DREAM) modifying its activity, or Ca^{2+} can bind to Ca^{2+}-binding proteins that activate in the cytoplasm signalling pathways conveying to the activation of diverse transcription factor.

2.6 ACTIVITY-REGULATED GENES

Studies of quiescent fibroblast stimulated by growth factors to make it re-enter the cell cycle suggested the first observation that extracellular stimuli can trigger rapid changes in gene transcription. The addition of platelet-derived growth factor (PDGF) or other growth factors to quiescent 3T3 fibroblasts led to the rapid induction of the *c-fos* proto-oncogene (Greenberg and Ziff, 1984).

Then, the importance of stimulus-induced transcriptional response in neuronal cells was first suggested by the observation that *c-fos* transcription could be induced by a number of different stimuli. For example, in PC12 cell line increase in the concentration of extracellular K^+ that leads to membrane depolarization it triggered *c-fos* transcription (Greenberg et al., 1986). The up-regulation of *c-fos* was observed also in neurons from different regions of the brain after seizure induction (Morgan et al., 1987) or after tetanic stimulation in hippocampal slices (Abraham et al., 1993).

One of the steps in gene expression response of the neurons to extracellular stimuli is the induction of the immediate early gene (IEG). The IEGs are defined as those genes whose expression increases rapidly and transiently in a protein synthesis-independent manner in response to extracellular stimuli. IEGs encode a wide range of proteins including activity-induced transcription factors, and effector IEGs such as structural proteins, signal transduction proteins, growth factors and enzymes. Since the discovery of *c-fos* induction, other studies have then focused on the activity-induced transcription factors such as *c-jun*, *Egr1* and *Egr2* (Cole et al., 1989; Abraham et al., 1993; Inokuchi et al., 1996). Among the effector IEGs, *Arc*, *Homer1a* and *Bdnf* can be identified.

The IEGs transcription factors are believed to drive the expression of delayed induced genes (Clayton, 2000), since a separated group of extracellular stimuli-responsive genes is induced with slower kinetics, often showing a peak of transcriptional activity several hours after stimulation. Delayed induced genes may play a role in neurotransmission, cellular maintenance and plasticity. Therefore, this

further suggested that the IE class of genes constituted an early genomic response required to trigger the mechanisms underlying persistent cell modification.

2.6.1 Early growth response: Egr family of Transcription Factors

The *Egr* family is composed of four members: *Egr1* (also known as *Zif268* or *Krox-24*), *Egr2* (also known as *Krox 20*), *Egr3* (also known as *PILOT*) and *Egr4* (also known as *NGFl-C*). Like *c-fos*, the members of the *Egr* family of transcription factors are readily inducible in the mammalian brain by a wide array of stimuli. They were first discovered more than a decade ago and identified as immediate early genes according to their response to growth factors (Milbrandt, 1987; Lemaire et al., 1988). A defining feature of the *Egr* family is the highly conserved DNA-binding domain composed of three zinc-finger motifs that allow the proteins to regulate the transcription of other genes (Christy and Nathans, 1989; Cao et al., 1990). Together, these fingers recognize a nine-base-pair segment of DNA, with each finger spanning three nucleotides. The high homology in the 3 zinc finger sequence in all members of the *Egr* family, suggests that the proteins may well bind to the same sites of at least a subset of the same target genes, even though little is known about those genes.

In general, there is a considerable basal expression of all the *Egr*, which may reflect ongoing physiological processes in the brain. All *Egr* members are expressed at their highest levels in CA1–CA3 in the hippocampus, with negligible levels of *Egr1* and *Egr2* in the dentate gyrus (Mack et al., 1990; Herdegen et al., 1993; Yamagata et al., 1994). The constitutive levels of *Egr2* are higher in layers II and III of the cortex and negligible in layers IV and VI, whereas *Egr3* and *Egr4* are highly expressed in layers II and IV, and *Egr3* was shown to co-localize with *Egr1* (Yamagata et al., 1994).

In neurons, *Egr* genes are robustly and transiently expressed by elevated cytosolic calcium produced by synaptic activity (Ghosh et al., 1994). Much information has been obtained about *Erg1* both in terms of its induction in response

to extracellular stimuli and in the molecular process governing its regulation and function. Numerous studies have shown that *Egr1* was regulated by seizure activity, electroconvulsive shock, kindling and pathological stimuli, or by brain injury. Many studies both *in vivo* and *in vitro* have shown that regulated expression of *Egr1* mRNA was initiated via the activation of different receptors which include at least, all subtypes of glutamatergic receptors (for review, see Hughes and Dragunow, 1995).

In addition, high-frequency stimulation leading to LTP in the ipsilateral hippocampal dentate gyrus *in vivo* markedly increased *Egr1* mRNA in the same area; both LTP and *Egr1* induction were susceptible to be blocked by NMDA receptor antagonists (Cole et al., 1989). Also *Egr2* was induced after a high-frequency stimulation paradigm that produced a longer-lasting synaptic enhancement (Williams et al., 1995). Egr2 protein may be involved in the stabilization of LTP, as the induction of Egr2 protein has been correlated with the persistence of LTP (Williams et al., 1995). Seen the presumed role of *Egr1* and *Egr2* in stabilization of LTP, they could be good candidates in inducing gene transcription of effector genes that would be involved directly in the long-term synaptic modification.

2.6.2 Activity regulated cytoskeletal-associated protein: Arc

Arc (also termed *Arg3.1*) is an IEG that has been cloned from brain on the basis of its rapid induction after seizure stimulation (Lyford et al., 1995; Link et al., 1995). *Arc* received particular attention because of its activation by physiological stimuli including hippocampal LTP induction and absence seizures (Lyford et al., 1995; Link et al., 1995), and because of its tight experience-dependent regulation in behaviourally defined neural networks (Guzowski et al., 1999).

Arc is unique among the known IEGs since its mRNA is rapidly distributed into dendrides after induction, where it is targeted towards recently activated synapses and then locally translated into protein (Steward et al., 1998; Steward and Worley, 2001a; Steward and Worley, 2001b). Given its dynamic regulation by neural activity

in vivo and localization to activate regions or the dendritic arbour, *Arc* is an excellent candidate as critical agent in synaptic plasticity.

Using *Arc* antisense oligodeoxynucleotide to reduce *Arc* expression, Guzowski et al. (2000) demonstrated that, although the early phase of LTP was not affected by the treatment with *Arc* antisense, the late phase decayed rapidly, supporting a critical role of *Arc* expression in synaptic plasticity.

Although *Arc* is likely to play a fundamental role in many natural functions of neurons in the brain, its function is still unknown; several studies demonstrated that Arc protein interacted with cytoskeleton (Lyford et al., 1995) binding with microtubule associated protein 2 (MAP2) (Fujimoto et al., 2004). Such interactions could be important in dendritic remodelling associated with long-lasting alterations of synaptic efficacy. Another *in vitro* study suggested that *Arc* interacted with CaMKII, and that this interaction promoted neurite outgrowth in neuroblastoma cells (Donai et al., 2003).

2.6.3 Brain-derived neurotrophic factor: Bdnf

The activity-regulated gene *Bdnf* encodes a neurotrophin that is secreted at synapses in an activity-dependent manner and can bind to tyrosine kinase receptor B (TrkB) and p75 neurotrophin receptors located in both pre- and postsynaptic membranes. BDNF is predominantly present in the central nervous system, and its mRNA expression is up-regulated by neuronal activity that is accompanied by Ca^{2+} influx into the postsynaptic spines of neurons (Ernfors et al., 1990; Ghosh et al., 1994).

The genomic structure of *Bdnf* is rather complex. To date, as many as nine distinct promoters in the mouse and rat gene have been reported (Aid et al., 2007). Transcripts initiated at each of these promoters splice from their first exon to a common downstream exon, which contains the entire open reading frame encoding the BDNF protein. The complexity of the *Bdnf* gene is larger; in fact, there are two

distinct polyadenylation sites in the 3' untranslated region (UTR) of the common *Bdnf* exon. The biological importance of this diversity remains a mystery, it has been hypothesized that such complicated organization confers additional regulation to BDNF production beyond its transcriptional regulation. For instance, the distinct *Bdnf* mRNA could be localized in different subcellular compartments or translate into proteins under different cellular conditions or regulate by microRNA. Such complex regulation suggests that diversity of *Bdnf* gene expression is required for the fine-tuning of BDNF functions, since BDNF can control a large number of distinct processes in the nervous system, like dendritic outgrowth, synapse maturation, neuronal survival, differentiation and synaptic plasticity (Thoenen, 1995).

2.6.4 Homer1a

Beside activity-regulated genes, either the ones whose product is a secreted protein or those involved in transcription or remodelling of dendrites, neuronal activity regulates also the expression of genes whose products regulate intracellular signalling pathways in the postsynaptic compartment.

Homer1a is an activity-regulated gene produced by the *Homer1* gene locus. Beside the transcription of the *Homer1* gene, Ca^{2+} influx causes a switch in *Homer1* pre-mRNA processing. This switch promotes the use of a premature polyadenylation site in the fifth intron of the *Homer1* gene, which results in the activity-dependent production of *Homer1a*, a truncated mRNA encoding only the N-terminus of Homer1 (Bottai et al., 2002). So, *Homer1a* is expressed at a low level in the resting state and is induced by neuronal activities such as LTP, seizure (Kato et al., 1997), and stimulations like inflammatory pain (Tappe et al., 2006), depolarization (Sato et al., 2001) and dopamine (Yamada et al., 2007).

Overexpression of exogenous *Homer1a* has proved to inhibit spine morphogenesis and reduce the densities of postsynaptic proteins in spines (Sala et al., 2003). Thus, Homer1a is expected to play an important role in the mechanism of

activity-dependent synaptic reorganization. It is generally believed that the primary cause for the morphological changes at postsynaptic sites is the polymerization–depolymerization reactions of actin filaments. Using a short hairpin that specifically blocked the expression of endogenous Homer1a, Inoue et al. (2007) demonstrated that Homer1a was required for the clustering and de-clustering (polymerization–depolymerization) reactions of actin. Hence, Homer1a may play a fundamental role for the long-term change of synaptic structures at synaptic sites (Inoue et al., 2007).

All these activity-dependent genes are clear examples of a fine and complex transcriptional regulation. In fact, *Arc* is rapidly transported to active synapses and only when it gets there it is transcribed into proteins. In the same way, *Bdnf* mRNA is actively transported into dendrites where it can be translate into proteins. Moreover, the genomic organization of the *Bdnf* gene is complicated and it could possibly transcribe twenty-two different *Bdnf* transcripts. Also the function of *Homer1* is modulated by the activity-dependent transcription of a splicing variant of the constitutively form of *Homer1*.

All together, these observations can suggest the complexity and significance of the activity-regulated gene expression program that neurons activate in response to extracellular stimuli, to modify their functional properties.

2.7 ACTIVITY-REGULATED GENE EXPRESSION PROFILE

Detailed studies investigating the function of a single gene have yielded insights into how this activity-induction of gene expression is fundamental and how these genes act to control neuronal modification. However, the concept that synaptic modification, like LTP, could be a function of a single gene is not fully correct, since it rather seem that an orchestrated expression of multiple activity-dependent genes is crucial to integrate several extracellular stimuli and encode new information.

Although, after discovery of *c-fos* induction many additional activity-regulated genes have been discovered (Saffen et al., 1988; Bartel et al., 1989; Nedivi et al., 1993), a comprehensive picture of the gene expression response to external stimuli was not possible until recently, because of technical limitations. The use of cDNA and high-density oligonucleotide microarrays has then allowed high-throughput analysis of gene expression patterns.

The sequence of a genome can be viewed as a gene database for a given organism. Knowing the sequence of its genes, however, is only the first step to understand the function of the genome. The intricate circuitry that governs growth, development, homeostasis, behaviour and the onset of diseases is largely governed by the RNAs and proteins encoded by the genes and the complex and dynamic interactions of the genes with each others and with the environment. This is why the need for a practical, high-capacity gene expression assay encouraged the creation of microarray platforms.

Microarray analysis is based on standard molecular biology, with the principal advantage being higher throughput and greater precision than traditional filter and blotting techniques. In general, microarrays use high-density microscopic array elements, planar glass substrates, low reaction volumes, high-binding specificity, high-speed instrumentation for manufacture and detection, and sophisticated software for data analysis and modelling. Then, gene expression arrays can determine the simultaneous profiling of thousands of transcripts.

At the moment, different studies have been using this technique to identify the gene regulated in response to membrane depolarization, NMDA application, LTP induction and seizure induction (Altar et al., 2004; Hong et al., 2004; Li et al., 2004; Park et al., 2006).

These experiments confirm the presence of several hundreds of neuronal activity-regulated genes. Among these genes, some are transcription factors and many are effector genes that encode for proteins with important functions in dendrites and synapses.

The first work in which a combination of MEA and microarray was used to monitor the electrical activity and the gene expression profile respectively was performed by Valor et al. (2007). The authors were interested in examining synapse formation and the activity-dependent gene regulation of this process in mouse hippocampal neuronal cultures. They followed the temporal profile of synapse formation, of the network activity and of the transcriptome over a period of twenty days *in vitro*. Although the regulated genes found in this screening could be classified in a variety of functional categories, the authors divided them into three subsets with functional and structural relevance to synapses: genes related to the core postsynaptic components; genes linked to synaptic plasticity; genes codified neurotransmitter receptor subunits. They observed then that two distinct sequentially active gene expression programs underlied the genomic response of synapse formation. The concomitant analysis of the network activity and gene expression profile allowed the authors to demonstrate that the first and fastest program did not depend on the network activity and drove the transcriptional synthesis of the synapse genes, whereas the second was slower and activity-dependent. So their results supported the conclusion that network activity was not a major force in the synaptogenesis program, but played a role in the subsequent activity-dependent gene regulation. This conclusion was very attractive, because activity-dependent gene expression was believed to be contributing to synaptogenesis, although blockage of neuronal activity or synaptic transmission did not prevent synaptogenesis in cultured primary neurons (Rao and Craig, 1997; Varoqueaux et al., 2002). An important consideration about this work is that the combination of MEA and microarray provides the ideal condition to correlate in time the gene expression response to the network modifications.

In the context of activity-dependent modification in response to an external stimulus, Hong et al. (2004) provided a molecular dissection of the activity-dependent long-lasting neuronal responses induced by NMDA receptors activation. They used a very sensitive method of differential gene expression analysis (DAzLE)

coupled with custom microarray analysis, to identify late-response plasticity-induced genes. In their protocol, the activation of NMDA receptors was done by brief (5 min) stimulation of primary cortical neurons with NMDA, and DAzLE screening was used to identify NMDA-induced genes 6 hours after stimulation. Subsequent DNA microarray hybridization was used to measure the temporal changes in mRNA levels at five different times ranging from 1 hour to 27 hours after the stimulation. A possible limitation of this work is that with the microarray they analysed only the up-regulated genes, because the initial screening was focused on identifying NMDA-induced genes. Beyond that, they found that the late response of NMDA receptor activation led to changes in many functional groups of genes; many of these were dynamically regulated in the late response of NMDA application. In fact, they observed five different groups of genes based on their temporal expression profile, which probably linked the NMDA receptor activation to long-term changes in neuronal function.

Another example of investigation of the transcriptome and its associated molecular programs that support synaptic plasticity changes was performed by Park et al. (2006). In this work the authors presented the data of a time course DNA microarray analysis of the genomic expression after LTP-inducing tetanic stimulation in the mouse dentate gyrus. A potential problem with this protocol is that LTP induction may not occur in all neurons in the dentate gyrus and slicing process can induce activity-regulated genes, therefore the changes in the gene expression would be partially masked by these factors. They also identified a large number of activity-regulated genes that covered a wide range of cellular processes, responding to LTP induction. In addition, these activity-regulated genes were characterized by a dynamic temporal regulation and were clustered on chromosomes. Then, the authors hypothesized that this gene expression response provided molecular support to propose critical cellular changes associated with LTP. Moreover, there was the fact that the chromosomal clustering of these activity-regulated genes might have been

facilitating the transcriptional coordination of the functionally related genes during LTP.

These last works demonstrated that an external stimulus evokes complex transcriptional cascades that may ultimately lead to changes of cellular and synaptic functions. In fact, genome-wide analyses have revealed that several hundred activity regulated genes can be detected in neurons. Beside those genes that codify for transcription factors, there are genes involved in the regulation of cell surface and adhesion, extracellular matrix, cytoskeleton, cytokine and growth factor signalling. Furthermore, the temporal expression of these genes suggests that they are dynamically regulated in time. These observations suggest that multiple molecular processes are involved in the modification of the synaptic properties of the cell. Therefore, the complete definition of the activity-regulated gene expression program is incomplete; nevertheless this should now be possible thanks to the most recent advances in genomic technology.

3 Results

3.1

Characterization of the time course of the activity pattern and transcriptome in a model of chemical-induced neuronal plasticity triggered by $GABA_A$ antagonists

Broccard FD, **Pegoraro S**, Ruaro ME, Bianchini D, Avossa D, Pastore G, Altafini C and Torre V

Submitted to BMC Neuroscience

Characterization of the time course of the activity pattern and transcriptome in a model of chemical-induced neuronal plasticity triggered by $GABA_A$ antagonists

Running title: Neuronal plasticity and gene regulation

Frédéric D. Broccard[1], Silvia Pegoraro[1], Maria Elisabetta Ruaro[1], Daniele Bianchini[1], Daniela Avossa[1], Giada Pastore[1], Claudio Altafini[1] and Vincent Torre[1,2,#]

[1]International School for Advanced Studies- Area Science Park SS 14 Km 163.5 Edificio Q1 34012- Basovizza, Trieste (Italy), [2] Italian Institute of Technology (IIT)

[#] corresponding author

E-mail addresses :

FDB: broccard@sissa.it, SP: pegoraro@sissa.it, MER: eruaro@sissa.it, DB: bianchid@sissa.it, DA: avossa@sissa.it, GP: jada@sissa.it, CA: altafini@sissa.it, VT: torre@sissa.it

Keywords: network, seizure-induced neuronal plasticity, multielectrode array, gene expression, DNA microarray, electrical activity

Abstract

Background: Periods of intense electrical activity can initiate neuronal plasticity leading to long lasting changes of network properties. By combining a previous reported model of chemically-induced plasticity using multielectrode extracellular recordings and DNA microarrays, we have investigated the time course of neuronal plasticity triggered by a transient exposure to the $GABA_A$ receptor antagonist gabazine (GabT) in rat hippocampal cultures.

Results: GabT induced a synchronous bursting pattern of activity. The analysis of electrical activity identified three main phases during neuronal plasticity following GabT: (i) immediately after termination of GabT, an early synchronization (E-Sync) of the spontaneous electrical activity appears that progressively decay after 3-6 h. E-Sync is abolished by inhibitors of the MAPK/ERK pathways, but not by inhibitors of gene transcription; (ii) the evoked response was maximally potentiated 3-6 hours after GabT (M-LTP); and (iii) at 24 h after GabT, the spontaneous electrical activity became more synchronous (L-Sync). The genomic analysis identified three Clusters of genes: The mRNA of genes in Clusters 1 and 2 is maximally up-regulated respectively after 1.5 and 3 h after GabT and return close to their original level after about 6 h. Many genes of Cluster 1 and 2 are down-regulated 24 h after GabT. Genes in Cluster 3 are up-regulated after 24 h after GabT.

Conclusion: At least five sequential events seem to be initiated by GabT: (i) within 5-10 minutes the MAPK/ERK pathways are activated and likely underlie E-Sync via phosphorylation of several target proteins; (ii) an early rise of transcription factors (Cluster 1), primarily composed by members of the EGR, and Nr4a families, maximally up-regulated 1.5 h after GabT; (iii) a successive up-regulation of some hundred genes many of which known to be involved in LTP (Cluster 2) about 3 h after GabT likely underlying M-LTP; (iv) a late down-regulation of several genes

coding for K+ channels and the HCN1 channels can participate to L-Sync; (v) a late up-regulation occurring 24 h after GabT of several genes (Cluster 3) involved in cellular homeostasis. These results allow relating different phases of neuronal plasticity to specific molecular events.

Background

When the electrical activity of neuronal networks is elevated, even transiently, several properties of synapses and neurons are modified, resulting in neuronal plasticity. Neuronal plasticity provides the basis for memory and learning [1,2]. This activity-dependent neuronal plasticity can be induced either electrically with intracellular and/or extracellular electrodes [3] or via pharmacological manipulations such as for example elevation of extracellular K^+ [4], elevation of the intracellular concentration of second messenger such as cAMP using forskolin [5] or addition of convulsant drugs such as bicuculline [6] or kaininc acid [7]. Neuronal plasticity is mediated by several signaling pathways leading to the modulation of synaptic strength, density of ionic channels and morphological changes of neuronal arborization [8]. This is further complicated by the fact that intrinsic neural properties can alter network dynamics and vice versa. All of these modifications, occurring at different time scales, have important consequences for the activity of neuronal networks in normal and pathological conditions. On a time scale of a few minutes, neuronal plasticity is mediated by local protein trafficking, leading to the insertion or removal of proteins into and from the membrane [9,10], whereas modifications beyond 2-3 h require changes of gene expression [11,12]. These changes occur at different time scales: the mRNA of immediate early genes (*c-fos, jun*), increases within 15 minutes following glutamate application [13,14] but other genes are up-regulated or down-regulated at longer periods of times. Following intense electrical activity, transcription factors of the " Early Growth Response (EGR) " family such as the *Egr1* mRNA and protein increase within 1-2 h, but changes of *Egr3* are seen only after 2-4 h [15]. Moreover, activity at the network level can trigger alterations in gene expression that can affect the firing properties of individual neurons. Thus, in order to unravel the complex events underlying neuronal plasticity at the network level, it is necessary to relate modifications of network electrical properties to concomitant protein and gene expression profile [16,17].

The aim and focus of the investigation described in the present manuscript is to identify different phases of neuronal plasticity and to understand their molecular basis. We combined a detailed analysis of electrical properties of neuronal networks occurring during neuronal plasticity with a transcriptional analysis of the underlying changes of gene expression. We used a multielectrode array (MEA) to monitor the electrical activity from a population of neurons, as MEAs allow stable and long lasting recordings (from hours to entire days). We used dissociated neuronal cultures grown over MEA for 3-5 weeks, because in this preparation it is possible to record extracellular voltage signals which can be reliably ascribed to single spikes of identified neurons. When hippocampal slices or organotypic cultures are grown on MEAs, local field potentials (LFPs) are usually observed and a detailed investigation of neuronal plasticity of a neuronal population at a single spike level is difficult. We analysed neuronal plasticity initiated by a transient treatment (30 minutes) with gabazine, a well known blocker of inhibitory $GABA_A$ receptor, which from now on will be referred to as GabT. Since GabT evokes intense periods of neuronal firing reminiscent of epileptic seizures, the induced neuronal plasticity is related to the neuronal plasticity caused by convulsing agents in models of chemically induced epilepsy [6,18,19] $GABA_A$ receptor antagonists have been widely used to increase neuronal activity in several in vitro hippocampal preparations [6,14] and to study seizure-induced plasticity [18,20]. When neuronal plasticity was induced by standard electrical protocols changes of gene expression measured in the neuronal culture were smaller (in preparation), therefore we used GabT to stimulate neuronal plasticity.

Our investigation of neuronal plasticity following GabT identifies three main phases: an early synchronization (E-Sync) of the spontaneous electrical activity immediately after termination of GabT; a potentiation of the evoked electrical activity (M-LTP) occurring at medium times, i.e. 3-6 hours, after GabT and a late synchronization of the spontaneous electrical activity (L-Sync) 6 to 24 h after GabT. The genomic analysis identified three Clusters of genes: The mRNA of genes in Clusters 1 and 2 is

maximally up-regulated after 1.5 and 3 h after GabT respectively. Many genes of Cluster 1 and 2 are down-regulated 24 h after GabT. Genes in Cluster 3 are up-regulated after 24 h from GabT. These results allow relating different phases of neuronal plasticity to specific molecular events.

Methods

Neuronal culture preparation

Hippocampal neurons dissociated from Wistar rats (P0-P2) were plated on polyorhitine/matrigel pre-coated MEA at a concentration of 8 x 10^5 cells/cm^2 and maintained in a neuron medium as previously described [19]. After 48 h, 5 μM cytosine-*β*-D-arabinofuranoside (Ara-C) was added to the culture medium in order to block glial cell proliferation. Neuronal cultures were kept in an incubator providing a controlled level of CO_2 (5%), temperature (37^{o}C) and moisture (95%).

Electrical recordings and electrode stimulation

Multi electrode array (MEA) recordings were carried out with a MEA60 system (Multi Channel Systems, Reutlingen, Germany). Stimulations and recordings were carried out after 21-35 days *in vitro*. Synchronous network bursting was induced by 30 min. treatment with $GABA_A$ receptor antagonists, such as bicuculline methiodide (50 μM) or gabazine (20 μM). $GABA_A$ antagonists were washed out by changing the medium three times. As bicuculline is known to block also SK K^+ channels [18], experimental results obtained primarily following gabazine treatment (GabT) are described. In some experiments, blockers of the MAPK/ERK pathway such as PD98059 (50 μM) and U0126 (20 μM) or blocker of transcription (Actinomycin D, 8 μM) were used. These drugs were pre-incubated before application of $GABA_A$ antagonists to insure that the MAPK/ERK pathway or transcription was completely blocked. PD98059 and U0126 were pre-incubated for 45 min. and Actinomycin D for 20 min. All of these drugs were washed out together with $GABA_A$ antagonists. In other experiments, diverse K+ channel blockers were added to the culture medium in order to mimic a down-regulation of genes coding for K+ channels following GabT: 4-aminopyridine (4-AP, 100μM) and tetra-etylammonium chloride (TEA, 10mM) which are non-specific K^+ channel blockers; apamin (100nM), a specific blocker of

SK K+ channels; and Heteropodatoxin 2 (HpTx2, 10μM) or arachidonic acid (AA, 40μM) which are specific blockers of the Kv4.2 channel type [38]. Similarly, the inhibitor of HCN1 channel ZD7288 (100μM) was used to mimic a down-regulation of the HCN1 gene following GabT. AA was dissolved in Tocrisolve® and cultures were first treated with Tocrisolve® as negative control. Bicuculline methiodide, TEA and HpTx2 were obtained from Sigma-Aldrich (St. Louis, MO, USA); gabazine, PD98059, U0126, Actinomycin D, 4-AP and arachidonic acid were obtained from Tocris Cookson Ltd (Bristol, UK). In order to avoid saturation, the lowest voltage pulse evoking an electrical response was used and its amplitude varied between 200 and 450 mV depending on the culture. For a given culture, the same amplitude was used before, during and after GabT. The pattern of stimulation consisted of a train of 40 bipolar pulses separated by an inter-pulse interval of 4s and applied to a bar of six neighbouring electrodes.

Data analysis

Acquired data were analyzed using MATLAB (The Mathworks, Inc.) as previously described [19,21]. The *network firing rate* is defined as the sum of all electrodes firing rates (i.e. the number of all spikes recorded in the network in each bin). The average network correlation or *network synchronicity*, was computed by averaging the cross-correlation of individual pairs over all the possible pairs of electrodes as previously described [20]. The total number of spikes as a function of the distance *d* was fitted by the exponential function $Ae^{-d/\lambda}$ from which λ was obtained (inset Fig. 3G).

RNA extraction

The total RNA was extracted using TRIzol reagent (Sigma) according to the manufacturer's instructions followed by a DNase I (Invitrogen, Carlsbad, CA, USA) treatment to remove any genomic DNA contamination. The total RNA was further purified using RNeasy Mini Kit Column (Qiagen, Milan, Italy) and subsequently

quantified by ND-1000 Nanodrop spectrophotometer (Agilent Technologies, Milan, Italy).

DNA microarray analysis

Neuronal cultures grown on MEA were treated for 30 minutes with 50 μM gabazine. Gabazine was removed and RNAs were extracted from cultures 1.5, 3, 6 and 24 h from start of GabT or from untreated cultures. Ten minutes of electrical recording was collected at each time point before harvesting RNAs. At each time point at least 3 biological replicates were collected and Standard Affymetrix protocols were applied for amplification and hybridization. Gene profiling was carried out with the Affymetrix RAT230_2 platform containing 31099 probes, corresponding to 14181 probes with a gene symbol. Low level analysis was performed using an RMA (Robust Multi-array Average) algorithm [22] directly on the scanned images. Because of high dimensionality, we removed probe sets labeled as ambiguous and those without any gene symbol. The variance σ^2 of mean value of expression changes (in $\log_2$ units) relative to untreated controls was computed considering collectively samples collected at 1.5,3, 6 and 24 h after GabT. Genes with a variance σ^2 lower than 0.6 were filtered out. The profiles of the three Clusters evident in Fig.4B were fitted by the curve:

$$x_i = F(t, \theta) = A + \theta_1 t^{\theta_2} \cdot e^{-\theta_3 t} - \theta_4 t$$

where x_i is the log ratio treatment/control of the i-th gene, t is time in hour and A and θ are appropriate parameters which were obtained using a nonlinear curve-fitting procedure. Each cluster was then enriched by considering genes with a time course highly correlated to one of the three profiles.

Quantitative RT-PCR

RNA (250ng) was reverse transcribed using SuperScript II reverse transcriptase and random hexamer (Invitrogen, Milan, Italy). Real-time PCR was performed using iQ SYBR Green supermix (Biorad, Milan, Italy) and the iQ5 LightCycler. Gene specific

primers were designed using Beacon Designer (Premier Biosoft, Palo Alto, CA, USA). The thermal cycling conditions comprised 3 min at 95°C, and 40 cycles of 10 seconds for denaturation at 95°C and 45 sec for annealing and extension at 58°C. The expression level of the target mRNA was normalized to the relative ratio of the expression of *Gapdh* mRNA. The forward primer for *Gapdh* was 5'-CAAGTTCAACGGCACAGTCAAGG-3', reverse primer was 5'-ACATACTCAGCACCAGCATCACC-3'. Fold changes calculations were made between treated and untreated samples at each time point using the $2^{-\Delta\Delta CT}$ method. The forward primer for *Egr1* was 5'-AAGGGGAGCCGAGCGAAC-3', reverse primer was 5'-GAAGAGGTTGGAGGGTTGGTC-3'; forward primer for *Egr2* was 5'-CTGCCTGACAGCCTCTACCC-3', reverse primer was 5'-ATGCCATCTCCAGCCACTCC-3'; forward primer for *Egr3* was 5'-ACTCGGTAGCCCATTACACTCAG-3', reverse primer was 5'-GTAGGTCACGGTCTTGTTGCC-3'; forward primer for *Nr4a1* was 5'-GGTAGTGTGCGAGAAGGATTGC-3', reverse primer was 5'-GGCTGGTTGCTGGTGTTCC-3'; forward primer for *Arc* was 5'-AGACTTCGGCTCCATGACTCAG-3', reverse primer was 5'-GGGACGGTGCTGGTGCTG-3'; forward primer for *Homer1a* was 5'-GTGTCCACAGAAGCCAGAGAGGG-3', reverse primer was 5'-CTTGTAGAGGACCCAGCTTCAGT-3'; forward primer for *Bdnf* was 5'-CGATTAGGTGGCTTCATAGGAGAC-3', reverse primer was 5'-GAAACAGAACGAACAGAAACAGAGG-3'.

Terminal deoxynucleotidyl transferase (TdT)-mediated fluorescein-dUTP nick-end labeling (TUNEL) analysis and immunofluorescence

Hippocampal cultures were fixed with 4% paraformaldehyde in PBS 24 or 48 h after gabazine treatment. TUNEL histochemistry (Roche, Germany) was performed according to manufacturer's instructions. Cultures were then labelled with anti-β tubulin III (TUJ1, Covance, Denver, PA, USA, 1:500) followed by Alexa 594 goat

anti-mouse (Invitrogen, Milan, Italy) and nuclei stained with DAPI (Sigma, Saint Louis, MO, USA) for 10 min, coverslipped with Vectashield mounting medium (Vector, Burlingame, CA, USA).

Results

Cultures of dissociated neonatal rat hippocampal neurons grown over MEAs form functional networks of interacting neurons [21]. We increased synaptic efficacy by exposing hippocampal cultures for 30 min to the $GABA_A$ receptor antagonist gabazine (gabazine treatment, GabT). After GabT, gabazine was washed out and the time course of electrical activity and gene expression was followed. Ten minutes of spontaneous activity was recorded at each time point before harvesting RNAs (see Methods). In another series of experiments, we characterized changes of the evoked activity induced by GabT.

Gabazine treatment induces an early (E-Sync) and a late synchronization (L-Sync)

Spikes were clearly detected from voltage recordings obtained from MEA extracellular electrodes and their frequency was monitored during development of neuronal plasticity (first three rows of Fig. 1A-C). In control conditions, neuronal firing was usually incoherent, but occasional synchronous bursts were observed (see raster plot in Fig. 1B). The global electrical activity was analyzed by computing the network firing rate, i.e. the total number of spikes recorded from all MEA electrodes in a 250 ms bin width (Fig. 1C, see Methods).

(Fig.1 near here)

During GabT the electrical activity became highly synchronous, and the network firing rate exhibited large peaks separated by silent periods (compare raster plots in Fig. 1B). Five minutes after GabT (third column of Fig. 1A-C) the spontaneous activity was more synchronous than in control conditions and very few spikes among burst were detected. These changes were observed for several hours after drug removal (fourth and fifth column of Fig. 1A-C), as previously reported [6]. Changes of the spontaneous activity were quantified by computing three quantities: (i) the network firing rate, computed with a bin width of 250 ms and averaged over 10

minutes; (ii) the average network cross-correlation or network synchronicity (see Methods) and (iii) the occurrence of silent electrical periods determined as the fraction of 100 ms periods with less than a total of 10 spikes. The network firing rate more than doubled during GabT and after its termination remained higher reaching a maximum value at 3-6 h and then slowly returning to control values (Fig. 1D, n=6). During GabT, the network synchronicity increased more than 50% (59.5 ± 13.4 % of control value; Fig. 1E). When gabazine was removed, it slightly decreased and was still 28 ± 24 % higher than what originally observed 3 h after GabT. At later times, however, the network synchronicity increased again and 24 h after GabT it was 51 ± 45 % higher. During GabT, the occurrence of silent periods drastically increased to 244 ± 63 % and remained higher than control value at all time following GabT, being still 65 ± 36 % larger than control values 24 h after GabT (Fig. 1F, n=6).

Thus, after GabT, spontaneous activity between individual bursts quickly recovered affects drastically the fraction of silent periods, and has a weak influence on the network firing rate and network synchronicity.

These results indicate that the network firing rate and network synchronicity had a different time course: the network firing rate reached a maximum value at about 6 h, whereas the network synchronicity showed a biphasic behavior with a minimum value at 5,5 h. This biphasic behavior is consistent with the existence of two components: one component acting at early times (E-Sync) and a later component clearly visible from 6 to 24 h after GabT (L-Synch). This is reminiscent to what is observed for LTP, where an early component (E-LTP) independent of transcription precedes a later component (L-LTP), associated to new transcription and translation [22-25].

E-Sync and L-Sync depend on different signalling pathways

On the one hand, E-LTP depends on the MAPK/ERK pathway and is abolished by selective blocker of this pathway [26, 27]. Moreover, in hippocampal neurons, treatment with bicuculline activates ERK in post-synaptic dendrites within 2 minutes,

which then translocates to the nucleus within 15-30 minutes [28]. On the other hand, L-LTP is selectively blocked by general blocker of transcription [24]. In order to test whether similar mechanisms were could account for the different phases of network synchronization, we then investigated the effect of blockers of the MAPK/ERK pathway, such as PD98059 [26] and U0126 [29], as well as blocker of transcription, such as Actinomycin D [24], on the GabT-induced synchronization. In particular, we looked at the effects of these drugs on the network firing rate, the network synchronicity and the occurrence of silent periods.

The gabazine-induced synchronous bursting was unaffected by treatment with PD98059 (50 μM) or U0126 (20 μM). However, the maintenance of recurrent synchronous bursting after gabazine washout required MAPK/ERK pathway: the network firing rate did not change and remained similar or lower to what observed in untreated cultures (red trace in Fig. 2A, left panel) and the network synchronicity remained lower than the control value (Fig. 2B, left panel). Similarly, the occurrence of silent periods decreased under control value (Fig .2C, left panel): silent periods dropped to 26 ± 19 % 1 h after GabT before returning to the control value after 24 h (Fig. 2C, left panel). On the other hand, when neuronal cultures (n=3) were treated with 8 μM Actinomycin D, the network firing rate remained under the control value at all times after GabT (Fig. 2A, right panel). In contrast, the network synchronicity more than doubled during GabT (223 ± 32%) and remained relatively high up to 3 h after GabT (20 ± 9 % larger than the control value), subsequently returning to the control value (Fig. 2B, right panel). During GabT and in the presence of Actinomycin D, the occurrence of silent periods increased by 237 ± 55 % and 1 and 3 h after GabT it was 79 ± 28 % and 46 ± 32 % larger than in control value, respectively (Fig. 2C, right panel).

(Fig.2 near here)

These results show that in the presence of blockers of the MAPK/ERK pathway, changes of the network firing rate, the network synchronicity and the occurrence of silent periods induced by GabT were abolished. In contrast, when Actinomycin D was added, GabT still evoked a significant increase of the network synchronicity and of the occurrence of silent periods lasting for 1-3 h. However, changes of the network firing rate, the network synchronicity and of the occurrence of silent periods observed 24 h after GabT were abolished. Therefore, E-Sync seems to be mediated by the activity of the MAPK/ERK complex, possibly through the phosphorylation of some target proteins [26,28,30], while L-Sync appears to be mediated by changes of gene expression, as it is eliminated by drugs blocking the transcription.

The evoked response is maximally potentiated 3 hours after GabT

MEA's extracellular electrodes can be used for recording and stimulation. In another series of experiments, we quantified changes of the evoked activity in the cultured hippocampal networks in response to a simple pattern of stimulation (see Methods). 40 brief (200 μs) bipolar pulses were applied to a row of electrodes (black bar in the grid of Fig. 3A) and the propagation of evoked spikes throughout the network was recorded. In order to avoid saturation, the lowest voltage pulse evoking at least one spike was used, before, during and after GabT (Fig. 3). Its amplitude varied between 200 to 450 mV depending of the culture (see Methods). After GabT, the number of evoked spikes increased in almost all trials (Fig. 3B) and at all time points (Fig. 3C).

(Fig.3 near here)

Changes of the evoked response were quantified by computing the total number of evoked spikes in a time window of 100 ms from the stimulus onset, i.e. the network firing rate of the evoked response. The network firing rate of the evoked response significantly increased between 1 and 6 h after GabT (Fig. 3D): the evoked response was maximally potentiated 3 h after GabT and started to decline after 6 h, returning

almost to control level 24 h after GabT. Neuronal plasticity induced by GabT caused evoked spikes to travel through the network in a faster and more reliable way. In some experiments, we could identify a spike produced by the same neuron, and we measured how its latency and jitter changed during neuronal plasticity (Fig. 3E,F). The latency in control conditions from the stimulus was between 6 and 9 ms and was reduced by 2-3 ms after GabT. The standard deviation of the latency (jitter) similarly decreased (blue and red symbols in Fig. 3F). A clear reduction of latency and jitter of evoked spikes were observed in at least 31 identified single neurons (n=5 cultures). We also analyzed how spikes propagated in the network by measuring the space constant λ of the evoked activity (see Methods and inset of Fig. 3G). Collected data from 4 cultures showed that λ increased by about 25 % within 1 h after GabT and remained larger than the control values up to 24 h (Fig. 3G). These results show that GabT – also in the absence of a concomitant strong or tetanic electrical stimulation – potentiated the electrical response propagating in the culture, inducing in this way a form of LTP.

Changes of gene expression

In order to understand the molecular changes underlying the modification of the electrical activity induced by GabT, we investigated changes of gene expression with DNA microarrays and real-time PCR. Gene expression was analysed 1.5, 3, 6 and 24 h after the onset of GabT and the variance of changes relative to the control observed at all these times was computed (see Methods). After GabT, the mean value of expression changes (in $\log_2$ units) relative to untreated controls did not change for the great majority of genes (see Fig. 4A).

(Fig.4 near here)

As the standard deviation σ of changes of housekeeping genes was about 0.25, we filtered out genes with a variance σ^2 lower than 0.6, obtaining 132 genes significantly

modulated (Fig. 4B). Visual inspection of expression changes of these genes (Fig. 4B) indicated three distinct temporal profiles: genes maximally up-regulated 1.5, 3 and 24 h after GabT were grouped in Cluster 1, 2 and 3, respectively. The precise time course of these three profiles was identified (black traces in Fig. 4B-E; see Methods) and the population of the three Clusters was enriched by reanalyzing the data with a lower variance (see Methods) looking for genes whose changes were highly correlated with one of the three profiles. By using this procedure, 25, 318 and 93 genes were present in Clusters 1, 2 and 3, respectively (see Fig. 4C-E). The complete list of identified genes can be found in Supplementary Table 1. Changes of gene expression occurring 1.5 and 3 h after GabT were checked by real-time PCR for some selected genes, namely *Egr1, Egr2, Egr3*, *Nr4a1*, *Bdnf, Homer1a* and *Arc* (Fig. 4F). Genes in Cluster 1 (see Table 1) had a 2-fold up-regulation 1.5 h after gabazine application, returning to the control level or slightly below between 3 and 6 (Fig. 4C). Gene Ontology (GO) analysis indicated that 44% (11/25) of these genes were regulators of transcription, such as members of the Egr [31] and Nr4a families [32]. The identification of genes in Cluster 1 as transcription factors was statistically more significant compared to a similar identification for the other clusters (p value<0.01 Fisher's exact test; see Methods). Five of these transcription factors (*Egr1-3, Nr4a1* and *Junb*) have been shown to play a major role also in LTP. Cluster 1 contained additional genes such as *Arc, Homer1, Ptgs2* and *Dusp5* known to be effector genes in LTP (see Table 2 and references therein).

Several genes in Cluster 2 were maximally up-regulated 3 h after gabazine removal (Fig. 4D) i.e. at the same time of maximal potentiation of the evoked response (Fig. 3D). GO analysis indicated that 28 % of these genes are involved in neuronal electrical transmission and could be grouped in three classes: genes involved in "ion transport" (such as *Kcnd2*, *Cacna2d3*, and *Gria1*), in "signal transduction" (such as *Cck* and *Homer1*), and in "transmission of nerve impulse" (such as *Rab3a Snsap25*, *Syn1* and 2). Of the 435 genes identified, 361 are annotated. To better investigate the functionalities of these genes, we performed an extensive PubMed search to extract

functional information for all these genes. 43 genes belonging to Cluster 1 and 2 are known to be involved in LTP (see Table 2) strongly suggesting that the up-regulation of genes in Cluster 2 mediated the electrophysiological changes described in Figure 3. The list of LTP genes in Table 2 contains many transcription factors and genes encoding for ion channels. Besides these, most of the remaining genes could be categorized as *structural, pre-* and *post-synaptic* based on their biological function. We therefore decided to classify all the other 318 genes in these three groups based on the PubMed search. The results of this search are listed in Table 3. 39 genes have been classified as *structural genes* for their structural role in cellular function and their up-regulation could underlie structural and morphological changes associated to LTP. Analogously the 26 *pre-synaptic* and the 24 *post-synaptic* genes found in our screening and listed in Table 3 could mediate changes of synaptic properties occurring during LTP.

Several genes in Cluster 3 were down-regulated by GabT 3 h after drug removal (like *Abcb1a, Ccnd1, Il1rl1, Tcf19*), and conversely, they were up-regulated at later times (Fig. 4E). 11% of the genes belonging to this cluster were put in the "apoptosis" category by GO and included both pro-apoptotic (such as *Casp4* and *Unc5c*) and pro-survival (such as *Tgfb3* and *Gadd45a*) genes. *Structural genes* were also found in Cluster 3 suggesting their possible involvement in the reinforcement and consolidation of LTP.

The effect of ERK inhibitors on the potentiation of the evoked response

As PD98059 and U0126 blocked changes of the spontaneous activity induced by GabT (Fig. 2), we investigated their effect on the potentiation of the evoked response (Fig. 3). Application of these inhibitors to neuronal cultures decreased the recorded spontaneous activity measured at all extracellular electrode (Fig. 5A). The network firing rate used to describe the global spontaneous activity (see Fig. 2) was almost halved (Fig. 5B) in all tested cultures (n=4), but periods of larger electrical activity could be still observed. In these cultures, inhibitors of the MAPK/ERK were

incubated for 45 minutes before GabT and changes of the network firing rate of the evoked response were analyzed. In the presence of these inhibitors, GabT still potentiated the evoked response, although in a lesser extent (red trace in Fig. 5C), with a time course similar to that observed in the absence of these inhibitors (black trace in Fig. 5C). 3 h after GabT, the number of evoked spikes reached 198 ± 41 % in normal conditions, but increased only by 39 ± 15 % in the presence of PD98059 and U0126. Therefore, inhibition of the MAPK/ERK pathway reduced but not abolished the potentiation of the evoked response caused by GabT.

(Fig.5 near here)

In order to understand the nature of potentiation of the evoked response observed in the presence of inhibitors of the MAPK/ERK pathway, we analyzed with real-time PCR selected genes up-regulated by GabT (Fig. 4). As shown in Figure 5D, the up-regulation induced by GabT of genes of the EGR family, *Nr4a1* and *Arc* was significantly reduced and almost blocked by inhibitors of the MAPK/ERK pathway, but not the up-regulation of *Bdnf* and *Homer1a*.

Several genes coding for K^+ channels are down-regulated 24 hours after GabT

The network firing rate of both the spontaneous (Fig. 1D) and evoked activity (Fig. 3D) returned almost to the control level 24 h after GabT, but not the network synchronicity (Fig. 1E) and the occurrence of silent periods (Fig. 1F) observed during the spontaneous activity. L-LTP is mediated by multiple changes occurring in the pre- and post-synaptic machinery [33] but also involves changes in the density and/or properties of ionic channels present in the dendritic arborization and axon of neurons forming the network [34]. These changes could affect the degree of synchronization of the spontaneous activity. To test this possibility, we investigated in detail changes of genes encoding for subunits and/or ancillary regulatory subunits of Na^+, K^+, Ca^{2+}, HCN ionic channels, as well as GABA and glutamate receptors. The majority of

these genes were not affected by GabT (Fig. 6A-F), but some of them were significantly down-regulated 24 h after GabT (red crosses). Down-regulated genes related to K^+ channels (Fig. 6B) were *Kcnc1, Kcnj6, Kcna4, Kcnn2, Kcnc2, Kcnip3, Ki55.1, Kcnab1, Kcnd2* and *Kcnip4*. Also some genes coding for subunits of Ca^{2+} (*Cacng2, Cacng3, Cacnb4* and *Cacna2d3*; Fig. 6C), Na^+ channels (S*cn1a* and *Scn2a1*; Fig.6*A*) and for glutamate (*Gria1* and *Gria2*; Fig. 6D) and GABA (*Gabrb1, Gabra5, Gabra1, Gabbr2* and *Gabrg2*; Fig. 6E) receptors were down-regulated. The gene coding for HCN1 channels was significantly down-regulated, but not those coding for HCN2-4 channels, in agreement with the larger expression of HCN1 channels in rat hippocampus [35]. As the degree of correlated activity of neuronal networks can also depend on the amount of electrical coupling among neurons, we looked for possible changes of genes expressing connexins, i.e. the ionic channels mediating electrical coupling. No significant changes of genes coding for connexins were found.

(Fig.6 near here)

None of the Ca^{2+} and Na^+ channels or GABA receptors genes found here has been reported to be involved in neuronal plasticity. K^+ channels encoded by the *Kcna4, Kcnn2, Kcnab1,* and *Kcnd2* genes (see references in Table 2) are known to be involved in neuronal plasticity and HCN1 down-regulation has been observed following seizure like events [35,36]. These observations suggest that a down-regulation of HCN1 and K^+ channels could contribute to L-Sync. In order to test this possibility, we pharmacologically blocked HCN1 and K^+ channels. We first analyzed the effect of unspecific K^+ channels blockers, such as 4-aminopyridine (4-AP) and TEA. In the presence of 100 μM 4-AP, synchronous bursts appeared (Fig. 6G) and ρ increased by 304 ± 156 % (Fig. 6J, *t*-test, $p<0.05$, n=4). In the presence of 10 mM TEA, the network firing became more synchronous (Fig. 6H) and ρ almost doubled (Fig. 6J; 195 ± 67 % of the control value, n=3). Synchronization induced by TEA

treatment was transient and in fact, after 10 minutes or so, the value of ρ substantially decreased (data not shown). We also tested the effect of arachidonic acid, a known blocker of the A-current [37] and in the presence of 40 μM of this drug the spontaneous firing was slightly more synchronous (data not shown). Addition of 100 μM of ZD7288, a known blocker of HCN channels, also induced a large and clear synchronization of the electrical spontaneous activity (Fig. 6I,J; 202 ± 59 % of the control value, n=3). Taken together, these data indicate that a down-regulation of genes coding for HCN and K^+ channels could contribute to L-Sync.

Integrity of neuronal cultures after gabazine exposure

The presence of genes linked to apoptosis in Cluster 3, raises the possibility of permanent damage induced in the neuronal culture by GabT. Indeed, bursts of electrical activity caused by GabT are expected to release large amounts of glutamate in synapses, possibly causing spillover reaching extra-synaptic NMDA receptors, known to trigger neuronal death [38]. Thus, we checked the integrity of neuronal cultures in several ways. Tunel assays (Fig. 7A,B) did not show a significant increase in apoptotic nuclei after GabT. In fact we counted 9.2 ± 3.3 % of apoptotic nuclei (positive for tunel: green nuclei in left panel of Fig. 7A) in control conditions, 9.5 ± 5.0 % and 6.7 ± 2.3 % 24 and 48 h after GabT (Fig. 7B), respectively.

(Fig.7 near here)

GABA in the mature hippocampus hyperpolarizes neurons, but can have a depolarizing effect in the immature hippocampus [39] or following insults such as trauma, ischemia or seizures [40]. As GabT caused electrical bursts reminiscent of epileptic seizures, we verified that GabT did not modify the hyperpolarizing effect of the activation of GABA receptors. Addition of 30 μM GABA before GabT blocked almost completely the spontaneous activity by silencing the great majority of the MEA's electrodes and switching to a tonic mode of firing (Fig. 7C), consistently with

the activation of inhibitory synaptic pathways. When the same amount of GABA was added 24 h following GabT, the spontaneous activity was similarly blocked (Fig. 7D). We also verified that subsequent GabT 24 or 48 h after the first GabT had the same effect (Fig. 7E): the network cross-correlation ρ more than doubled for the three consecutive GabTs. These results show that a transient exposure to blockers of inhibitory GABAergic synaptic pathways initiate neuronal plasticity without causing significant damage to neuronal cultures and changes of the hyperpolarizing effect of GABA.

Discussion

The present work identifies several sequential steps underlying neuronal plasticity induced by a transient gabazine treatment. Immediately after termination of GabT, the spontaneous electrical activity becomes more synchronous (E-Sync) than in control conditions. Following GabT, ERK proteins are phosphorylated and activated within less than 5 minutes [28]. E-Sync is blocked by inhibitors of the MAPK/ERK pathway but is not affected by inhibitors of gene transcription (Fig. 2), suggesting that post-translational modifications, like phosphorylation, participate in maintains this phase. Late synchronization however is blocked by both inhibitors demonstrating a major role of MAPK/ERK signalling pathway in neuronal plasticity and showing the requirement of new gene transcription for synchronicity consolidation. Some tens of genes (Cluster 1) primarily composed by transcription factors such as members of the *Egr*, and *Nr4a* families, are maximally up-regulated 1.5 h after GabT. Another cluster of genes (Cluster 2) is maximally up-regulated about 3 h after GabT and many of these genes are known to be involved in LTP. At the same time or slightly later the evoked and spontaneous electrical activity are strongly potentiated (Figure 1 and 3). At 24 h after GabT, the spontaneous electrical activity was more synchronous (L-Sync), in addition a down-regulation of genes coding for several K^+ channels occurred at the same time point. A third group of genes (Cluster 3) involved in cellular homeostasis is up-regulated 24 h after GabT. From these results it is possible to relate specific events occurring during neuronal plasticity to changes of expression of specific gene clusters.

E-Sync of spontaneous activity

As shown in Figure 2, E-Sync is not blocked by Actinomycin D but by inhibitors of the MAPK/ERK pathways. Therefore E-Sync is likely to be dependent on post-translational modification controlled by the MAPK/ERK pathway. In this regard, E-Sync is very similar to a component of LTP, referred as Early LTP, which is not

blocked by inhibitors of gene expression [24,25,26]. Local protein synthesis and regulation of ionic channels, such as phosphorylation of the Kv4.2 channel by ERK [30] PKA or CaMKII are likely mechanisms.

Potentiation of evoked activity

Potentiation of the spontaneous and evoked electrical activity (Fig. 1 and 3) and up-regulation of genes in Cluster 2 have a very similar time course suggesting of a causal relationship between gene activation and electrical potentiation. Potentiation of the evoked activity was reduced, but not eliminated by inhibitors of the MAPK/ ERK pathway (Fig. 5). Therefore potentiation of the evoked response is mediated by several pathways likely to be working in unison. Many genes belonging to Cluster 1 and 2 are well known players in LTP (see Table 2) such as *Bdnf* and its receptor TrkB [41] (referred to as *Ntrk2* in Table 2), *Arc* [42], *Egr1* [43] and *Homer1* [44]. We hypothesize that the large majority of genes of Clusters 1 and 2 underlie induction of LTP and that their activation orchestrates neuronal plasticity. The latter most likely depends on the activation of hundreds - rather than tens or thousands - of genes, in agreement with our findings. In fact, of the 361 annotated genes in our clusters from the PubMed search, we found that one third is, or could be, involved in changes of synaptic strength related to LTP. 43 genes have already been implicated in LTP (Table 2), 39 genes have been classified as *Structural genes* for their structural role in cellular function and their up-regulation could underlie structural and morphological changes associated to LTP. Analogously the 26 *Pre-synaptic* and the 24 *Post-synaptic* genes found in our screening and listed in Table 3 could mediate changes of synaptic properties occurring during LTP.

Structural genes

Among structural genes in Cluster 1 and 2 there are elements that control properties of the cytoskeleton and the dynamics of microtubules and neurofilaments like *Arc, Homer1, Mapt, or Stmn3* or the formation of new dendritic arborisation like *Dscam*

or Nxph1. Many genes of the cadherin family (*Cdh*) controlling cell to cell adhesion are also member of these categories. The gene *Dscam* (Down Syndrome Cell Adhesion Molecule) plays a major role in axon guiding and development of neuronal circuits [45,46] and is well known to be involved in neuronal plasticity. *Nrxn3* (Neurexin) in conjunction with neuroligin is thought to play a major role in the formation of new synapses and in particular in adhesion complex [47] and therefore besides being structural they can be also classified as pre-post synaptic. *Structural Genes* were also found in Cluster 3 and they could be involved in the reinforcement and consolidation of LTP.

Pre- and post-synaptic genes

Several pre-synaptic genes such as synapsin I [48], syntaxin1A [49], *Snap25* [50] code for proteins involved in vesicle release from pre-synaptic terminals, and their up-regulation could be associated to an increase of vesicle release during synaptic transmission.

Among the post-synaptic genes there are elements associated to Post Synaptic Density complex like *Cnksr2 and Opcml*; to the regulation and local trafficking of post-synaptic glutamate ionic channels like *Nsf or Ptpn5* and to the regulation of post-synaptic spines like *Slc12a5* and therefore could be involved in the reinforcement of the synaptic strength. As shown in Figure 6, many genes coding for ionic channels and their accessory proteins belong to Cluster 2. Their up-regulation closely follows the time course of potentiation of the evoked response, suggesting that they also could participate to the regulation and orchestration of LTP.

For these reasons, we propose that genes found in this screening could represent a template – to be verified – for genes involved in neuronal plasticity in several other preparations.

L-Synch of spontaneous activity

L-Sync could be in part mediated by a down-regulation of K^+ and HCN channels and in fact, blockers of K^+ channels with a wide spectrum of action, such as TEA and 4-AP, increase the degree of synchronization of the spontaneous activity (Fig. 6). Blockage of HCN1 channels by changing dendritic excitability modulates LTP [51] and contributes to neuronal plasticity by prolonging the entry of Ca^{2+} in distal dendrites [52]. Synchronous bursts induced by blockage of K^+ channels are more frequent and less regular and therefore the down-regulation of K^+ channels can be one of the several mechanisms underlying neuronal plasticity. In addition, network synchronization was not observed or was rather small when specific K^+ channels blockers (Apamin for *Kcnn2*, Heteropodatoxin 2 and arachidonic acid for *Kcnd2*) were used (data not shown), indicating that a fine tuning and a precise regulation of several ionic channels (Fig. 6) underlie L-Sync.

Genes of Cluster 3

Genes belonging to Cluster 3 are up-regulated 24 h after GabT and some of them (5/93) are also up-regulated in mouse hippocampal cultures 2-4 h after addition of glutamate or bicuculline [14]. Several genes from Cluster 3 are associated to apoptosis, with pro-apoptotic (such as *Casp4* and *Unc5c*) and pro-survival (such as *Tgfb3* and *Gadd45a*) genes. The homeostatic mechanisms present in neuronal cultures – both in the cytoplasm and at the network level – minimize the number of apoptotic neurons (Fig. 7) and provide a way to safely return to control conditions 24 h after GabT.

Comparison with previous investigations

Several previous investigations have identified hundreds of genes up-regulated by standard electrical protocols inducing LTP [53] or chemically induced seizures using convulsant agents such as bicuculline and glutamate [14]. These investigations were conducted in the mouse hippocampus [14,53] and in rat hippocampus and cerebral

cortex [54]. Zhang and colleagues increased electrical activity either by stimulating synaptic NMDA receptors by using bicuculline or extra-synaptic NMDA receptors by adding glutamate to the medium in mouse dissociated hippocampal neurons [14]. The present investigation used GabT to elevate the global electrical firing. In all these investigations an elevated global firing initiates the transcription of several genes associated to metabolic and structural components and synaptic functions.

A parallel analysis of genes up-regulated in these experiments shows a significant number of commonly regulated genes. 13 (out of 25) genes in Cluster1 and also some genes in Cluster 2 (like *Pnoc*, *Rgs2* and *Ntrk2*) of the present investigation are also up-regulated in mouse hippocampal cultures following a permanent stimulation of synaptic NMDA receptors with bicuculline [14]. Similarly, 16 genes (*Bdnf, Ptgs2, Homer1, Tac2, Egr1,2,4, Arc, Nrp1, TrkB, Vegf, Vgf, JunB, Nr4a3, cFos,* and *Syn2*) regulated by increasing the electrical activity with electroconvulsive seizures *in vivo* were also up-regulated in our system. Moreover, 5 LTP genes (*Egr2, Fos, Homer1, Nrgn,* and *Rab3a*) found in our investigation and listed in Table 2 were also up-regulated by a tetanic stimulation of the perforant path, a well known protocol for LTP induction in the hippocampus [54]. Therefore, despite experimental differences, these investigations identify several genes commonly up-regulated in many forms of LTP.

Conclusion

By combining MEA and DNA microarrays, we were able to identify distinct events in neuronal plasticity initiated by GabT of hippocampal neuronal cultures: (i) within 5-10 minutes the MAPK/ERK pathways are activated and likely underlie E-Sync via phosphorylation of several target proteins; (ii) a cluster of genes (Cluster 1), primarily composed by transcription factors such as members of the EGR and Nr4a families, is stimulated reaching its maximal up-regulated 1.5 h after GabT; (iii) some hundred genes many of which known to be involved in LTP (Cluster 2) are successively stimulated and reach their maximal expression about 3 h after GabT. These genes could underlie M-LTP observed at similar times after GabT; (iv) several genes coding for K^+ channels and the HCN1 channels are down-regulated at later times from 6-24 hours after GabT. Down-regulation of these genes can be one of the several mechanisms responsible for L-Sync; (v) a late up-regulation occurring 24 h after GabT of several genes (Cluster 3) involved in cellular homeostasis. These results allow relating changes of electrical properties occurring during neuronal plasticity to specific underlying molecular events. In the near future we will extend our analysis to organotypic hippocampal slices and we will analyze changes of gene expression when neuronal plasticity is stimulated with conventional electrical protocols for inducing LTP.

Figure Legends

Figure 1. Synchronization of the spontaneous electrical activity induced by GabT. The spontaneous electrical activity of hippocampal cultures grown on MEAs for three weeks was recorded for 10 min before the addition (control) and during treatment with gabazine (50 μM for 30min, GabT). ***A***, Representative traces from three individual extracellular electrodes showing the presence of synchronized bursts of electrical activity during GabT and at different time points following gabazine washout. ***B***, Raster plots of the activity of all 60 MEA electrodes. Each horizontal line represents the activity of a single electrode. Synchronous bursts are represented by black vertical lines. Spikes between synchronous bursts are drastically reduced during GabT and after the drug washout. ***C***, Network firing rate (NFR) expressed as the total number of spikes recorded from all the MEA electrodes in bins of 250 ms. The scale bar on the left is similar for all conditions except during GabT. Data from a single experiment shown in ***(A-C)***. ***D***, Time course of the average NFR. ***E***, Time course of the average network synchronicity. The degree of network synchronization was estimated by averaging the network cross-correlation ρ over all electrode pairs (see Methods). ***F***, Time course of the fraction of silent periods, defined as the fraction of frames containing ten or less spikes, showing the reduction of the number of individual spikes during and after GabT. Bin size was 250 ms. n = 5 cultures for ***(D, E F)***. Values were normalized relative to control values. Error bars are mean ± s.e.m.

Figure 2. Effects of MAPK inhibitors and Actinomycin D on early and late gabazine-induced synchronization ***A***, Left, Average NFR time course in the presence of the MAPK cascade inhibitors PD98059 and U0126 (red trace). Data for PD98059 (50 μM; n = 3) and U0126 (20 μM; n = 3) were pooled together as they affected similarly network properties. The NFR fluctuates around the baseline after GabT and

is not potentiated unlike in control conditions (black trace). U0126 and PD98059 were preincubated 20 and 45 minutes before GabT, respectively, and washed out with gabazine. Right, Actinomycin D decreases slightly the NFR. ***B***, E-Sync and L-Sync depend on different signaling pathways. Left, network synchronicity is abolished in the presence of PD98059 or U0126. Right, in the presence of Actinomycin D, L-Sync but not E-sync is blocked, indicating that L-Sync depends on gene transcription. ***C***, Time course of the fraction of silent periods containing ten or less spikes. Left, blockers of the MAPK pathway reduces the fraction of silent periods following GabT, i.e. the number of individual spikes increase in the network. Right, in presence of Actinomycin D, the fraction of silent periods is smaller than control value after tens of hours. Bin size was 250ms. Values were normalized relative to control values.

Figure 3. Potentiation of the evoked response induced by GabT. ***A***, Examples of the evoked activity's time course for a single trial for three representative electrodes located at 0.5, 1 and 2 mm distance (see *inset*) from the stimulating electrode respectively (black bar in *inset*). The number of evoked spikes increases following the GabT. Hippocampal cultures were stimulated with the lowest intensity (200-450 mV) evoking a response. 40 pulses (trials) with an inter-pulse interval 4s were used. Inset, graphical representation of the MEA grid. Each square represents an electrode. Distance between electrodes is 500 μm. Black bar corresponds to the stimulated electrodes and grey numbered squares to the electrodes whose activity is shown in ***(A)***. ***B***, Raster plots of the spikes evoked in one electrode at each time point analyzed. Each horizontal line represents the response to one trial recorded up to 250 ms after the stimulus onset. ***C***, Time course of the NFR. The total number of evoked spikes was counted in 10 ms bins, following electrical stimulation. The increase of evoked spike is especially pronounced in the first 100 ms following stimulation. Data from a single experiment shown in ***(A-C)***. ***D***, Average time course of the NFR (n=5

cultures). The NFR was normalized relative to control values. Bin size was 250 ms. ***E***, Ten overlapping spike traces in control conditions (black traces) and 3h after gabazine washout (red traces) of an individual electrode showing the decrease of the latency of the first evoked spike. Artifacts have been truncated for clarity. ***F***, Time course of the latency (blue traces) and jitter (red traces) of the first spike for three neurons showing that the latency and jitter decrease after GabT. Each symbol corresponds to a different neuron. ***G***, Time course of the activity propagation constant (λ, see Methods) showing the increase of the activity spread following GabT. Inset, the number of spikes in a 100 ms time window was counted and averaged, for electrodes located at 0.5, 1 and 2 mm from the stimulated bar of electrodes, and fitted with an exponential function $Ae^{-d/\lambda}$ (grey line). Colours as in ***(E)***.

Figure 4. Gene expression profile revealed by DNA microarrays. ***A***, Time course of all the probe sets unequivocally hybridized. ***B***, Time course the 132 probe sets in **A** whose variance is bigger than 0.6 over the entire time course. ***C-E***, Time course of three gene clusters identified in ***(B)***. The clusters were identified using the K-means method between the specific time profiles (blue traces in ***B***) and the entire probe set shown in ***(A)***. ***F***, Changes of gene expression occurring 1.5 h and 3 h after GabT measured by Real-Time PCR for Egr1, Nr4a1, Arc, Homer1a and Bdnf. See also Table 1 for a list of genes up-regulated 1.5h after gabazine washout in cluster 1 and Table 2 for a list of genes known to be involved in neuronal plasticity and belonging to Cluster 1 and 2.

Figure 5. Effect of inhibitors of the MAPK pathway. ***A***, Representative traces from two individual extracellular electrodes in control conditions (left) and in presence of 50 μM PD98059 (right). ***B***, Corresponding network firing rate computed with a bin width of 25 ms, in normal conditions (left) and in presence of 50 μM PD98059 (right) showing a depression of the spontaneous electrical activity by PD98059.

Dotted line indicates zero spike. ***C***, The evoked activity is still potentiated when the MAPK pathway was blocked before GabT (see Results). Dashed line corresponds to potentiation of the evoked activity without blocking the MAPK pathway before GabT. Data for PD98059 (50 μM; n = 3) and U0126 (20 μM; n = 3) were pooled together as they affected similarly network properties. ***D***, Changes of gene expression occurring 1.5 h after GabT measured by Real-Time PCR for Egr1, Egr2, Egr3, Nr4a1, Bdnf, Homer1a and Arc in presence of gabazine and PD98059 (gray bars) relative to normalized expression in presence of gabazine alone (black bar).

Figure 6. Ionic channels expression and K^+ channel blockers induced-synchronization. ***A-F***, Time course of the ionic channels and receptors channels expression induced by GabT. Red bars correspond to the mean. Horizontal blue bars correspond to the first and third quartile. Red crosses represent deviation from the mean. ***G-I***, Effects of K^+ channels blockers on the network synchronization. Three representative electrodes showing the synchronous bursting induced by 100 μM 4-aminopyridine (4-AP**,** ***G***), 10 mM tetra-etylammonium (TEA**,** ***H***) and 100 μM ZD7288 (***I***), respectively. Bottom panels show the average network firing rate computed with a bin width of 100ms. Dashed lines correspond to zero spike. Note the absence of individual spikes in the intra-burst intervals in ***(H)***. ***J***, Summary of the effect of diverse K^+ and HCN channel blockers on the average network correlation coefficient ρ (see Methods).

Figure 7. Gabazine treatment does not interfere with the cell culture integrity. ***A***, Staining of hippocampal cells in control conditions with different markers. Nuclei positive to TUNEL assay (green, left panel). Neurons expressing type III tubulin recognized by TUJ1 antibody (red, middle panel); total nuclei stained with DAPI (blue, right panel). Scale bar 20 μm. ***B***, Merge pictures of the three markers shown in ***(A)***, in control conditions (left), 24 h (middle) and 48 h (right) after gabazine

treatment demonstrating the absence of apoptosis by this treatment. Scale bar as in ***(A)***. ***C***, Modification of the network activity by GABA. Top panels, The NFR and bursting activity in control conditions (left) are drastically reduced in the presence of 30 μM GABA (right). Bottom panels, raster plots. ***D***, Similar to ***C*** but 24h after gabazine washout. The same reduction of bursting activity by GABA is observed for cultures treated with gabazine. ***E***, Time course of the network synchronicity following repeated GabT. GBZ 1, 2 and 3 correspond to the first, second and third GabT, respectively.

Table 1: List of genes present in Cluster 1, i.e. maximally up-regulated at 1.5h after gabazine wash-out.

Table 2: List of genes present in Cluster 1 and 2 known to be involved in LTP.

Table 3: List of genes involved in structural, pre- and post-synaptic processes.

References

1. Goelet, P., Castellucci, V.F., Schacher, S. and Kandel, E.R. **The long and the short of long-term memory--a molecular framework**. *Nature* 1986 322: 419-22.

2. Malenka, R.C. and Nicoll, R.A. **Long-term potentiation – A decade of Progress ?** *Science* 1999 285: 1871-76.

3. Bliss, T.V. and Lomo, T. **Long-lasting potentiation of synaptic transmission in the dentate area of the anaesthetized rabbit following stimulation of the perforant path**. *J Physiol* 1973 232: 331-56.

4. Jensen, M.S. and Yaari, Y. **Role of intrinsic burst firing, potassium accumulation, and electrical coupling in the elevated potassium model of hippocampal epilepsy**. *J Neurophysiol* 1997 77: 1224-33.

5. Otmakhov, N., Khibnik, L., Otmakhova, N., Carpenter, S., Riahi, S., Asrican, B. and Lisman, J. **Forskolin-induced LTP in the CA1 region of the hippocampus is NMDA receptor dependent**. *J Neurophysiol* 2004 91: 1955-62.

6. Arnold, F.J., Hofman, F., Bengston, C.P., Wittmann, M., Vanhoutte, P. and Bading, H. **Microelectrode array recordings of cultured hippocampal networks reveal a simple model for transcription and protein synthesis-dependent plasticity**. *J Physiol* 2005 564: 3-19.

7. Westbrook, G.L. and Lothman, E.W. **Cellular and synaptic basis of kainic acid-induced hippocampal epileptiform activity**. *Brain Res* 1983 273: 97-109.

8. Carlisle, H.J. and Kennedy, M.B. **Spine architecture and synaptic plasticity**. *Trends Neurosci* 2005 28: 182-7.

9. Lau, C.G. and Zukin, R.S. **NMDA receptor trafficking in synaptic plasticity and neuropsychiatric disorders**. *Nat Rev Neurosci* 2007 8: 413-26.

10. Groc, L. and Choquet, D. **AMPA and NMDA glutamate receptors trafficking: multiple roads for reaching and leaving the synapse**. *Cell Tissue Res* 2007 326: 423-38.

11. Martin, S.J., Grimwood, P.D. and Morris, R.G. **Synaptic plasticity and memory: an evaluation of the hypothesis**. *Annu Rev Neurosci* 2000 23: 649-711.

12. Rao, V.R., Pintchovski, S.A., Chin, J., Peebles, C.L., Mitra, S. and Finkbeiner, S. **AMPA receptors regulate transcription of the plasticity-related immediate-early gene Arc**. *Nat Neurosci* 2006 9: 887-95.

13. Bading, H., Gintly, D.D. and Greenberg, M.E. **Regulation of gene expression in hippocampal neurons by distinct calcium signaling pathways**. *Science* 1993 260: 181-6.

14. Zhang, S.J., Steijaert, M.N., Lau, D., Schütz, G., Delucinge-Vivier, C., Descombes, P. and Bading, H. **Decoding NMDA receptor signaling: identification of genomic programs specifying neuronal survival and death**. *Neuron* 2007 53: 549-62.

15. O'Donovan, K.J., Tourtellotte, W.G., Millbrandt, J. and Baraban, J.M. **The EGR family of transcription-regulatory factors: progress at the interface of molecular and systems neuroscience**. *Trends Neurosci* 1999 22: 167-73.

16. Martin, K.C. and Zukin, R.S. **RNA trafficking and local protein synthesis: an overview**. *J Neurosci* 2006 26: 7131-34.

17. Tzingounis, A.V. and Nicoll, R.A. A**rc/Arg3.1 : linking gene expression to synaptic plasticity and memory**. *Neuron* 2006 52: 403-7.

18. Schwartzkroin, P.A. and Prince D.A. **Penicillin-induced epileptiform activity in the hippocampal in vitro preparation**. *Ann Neurol* 1977 1: 463-9.

19. Schneiderman, J.H., Sterling, C.A. and Luo, R. **Hippocampal plasticity following epileptiform bursting produced by $GABA_A$ antagonists**. *Neuroscience* 1994 2:259-73.

20. Coulter, D.A. and DeLorenzo, R.J. **Basic mechanisms of status epilepticus**. *Adv Neurol* 1999 79: 725-33.

21. Ruaro, M.E., Bonifazi, P. and Torre, V. **Towards the neurocomputer: image processing and pattern recognition with neuronal cultures**. *IEEE Trans Biomed Eng* 2005 52: 371-83.

22. Lynch, M.A. **Long-term potentiation and memory**. *Physiol Rev* 2004 84: 87-136.

23. Malenka, R.C. and Bear, M.F. **LTP and LTD: an embarrassment of riches**. *Neuron* 2004 44: 5-21.

24. Raymond, C.R. and Redman, S.J. **Spatial segregation of neuronal calcium signals encodes different forms of LTP in rat hippocampus**. *J Physiol* 2006 570: 97-111.

25. Raymond, C.R. **LTP forms 1, 2 and 3: different mechanisms for the "long" in long-term potentiation**. *Trends Neurosci* 2007 30: 167-75.

26. Sweatt, J.D. **The neuronal MAP kinase cascade: a biochemical signal integration system subserving synaptic plasticity and memory**. *J Neurochem* 2001 76: 1-10.

27. Thomas, G.M. and Huganir, R.L. **MAPK cascade signalling and synaptic plasticity**. *Nat Rev Neurosci* 2004 5: 173-83.

28. Wiegert, J.S., Bengston, C.P. and Bading, H. **Diffusion and not active transport underlies and limits ERK1/2 synapse-to-nucleus signaling in hippocampal neurons**. *J Biol Chem* 2007 282: 29621-33.

29. Favata, M.F., Horiuchi, K.Y., Manos, E.J., Daulerio, A.J., Stradley, D.A., Feeser, W.S., Van Dyk, D.E., Pitts, W.J., Earl, R.A., Hobbs, F., Copeland, R.A., Magolda, R.L., Scherle, P.A. and Trzaskos, J.M. **Identification of a novel inhibitor of mitogen-activated protein kinase kinase**. *J Biol Chem* 1998 273: 18623-32.

30. Schrader, L.A., Birnbaum, S.G., Nadin, B.M., Ren, Y., Bui, D., Anderson, A.E. and Sweatt, J.D. **ERK/MAPK regulates the Kv4.2 potassium channel by direct phosphorylation of the pore-forming subunit**. *Am J Physiol Cell Physiol* 2006 290: C852-61.

31. Hughes, P. and Dragunow, M. **Induction of immediate-early genes and the control of neurotransmitter-regulated gene expression within the nervous system**. *Pharmacol Rev* 1995 47: 133-78.

32. Giguere, V. **Orphan nuclear receptors: from gene to function**. *Endocr Rev* 1999 20: 689–725.

33. Lisman, J. **Long-term potentiation: outstanding questions and attempted synthesis**. *Phil Trans R Soc Lond B* 2003 358: 829-42.

34. Frick, A., Magee, J. and Johnston, D. **LTP is accompanied by an enhanced local excitability of pyramidal neuron dendrites**. *Nat Neurosci* 2004 7: 126-35.

35. Richichi, C., Brewster, A.L., Bender, R.A., Simeone, T.A., Zha, Q., Yin, H.Z., Weiss, J.H. and Baram, T.Z. **Mechanisms of seizure-induced 'transcriptional channelopathy' of hyperpolarization-activated cyclic nucleotide gated (HCN) channels**. *Neurobiol Dis* 2008 29: 297-305.

36. Shah, M.M., Anderson, A.E., Leung, V., Lin, X. and Johnston, D. **Seizure-induced plasticity of h channels in entorhinal cortical layer III pyramidal neurons.** *Neuron* 2004 44: 495-508.

37. Villarroel, A. **Suppression of neuronal potassium A-current by arachidonic acid.** *FEBS Lett* 1993 335: 184-8.

38. Hardingham, G.E., Fukunaga, Y. and Bading, H. **Extrasynaptic NMDARs oppose synaptic NMDARs by triggering CREB shut-off and cell death pathways**. *Nat Neurosci* 2002 5: 405-14.

39. Ben-Ari, Y., Cherubini, E., Corradetti, R. and Gaiarsa, J.L. **Giant synaptic potentials in immature rat CA3 hippocampal neurones**. *J Physiol* 1989 416: 303-25.

40. Galanopoulou, A.S. **Developmental patterns in the regulation of chloride homeostasis and GABA(A) receptor signaling by seizures**. *Epilepsia* 2007 48: 14-8.

41. Barco, A., Patterson, S., Alarcon, J.M., Gromova, P., Mata-Roig, M., Morozov, A. and Kandel, E.R. **Gene expression profiling of facilitated L-LTP in VP16-CREB mice reveals that BDNF is critical for the maintenance of LTP and its synaptic capture**. *Neuron* 2005 48: 123-37.

42. Messaoudi, E., Kanhema, T., Soulé, J., Tiron, A., Dagyte, G., da Silva, B. and Bramham, C.R. **Sustained Arc/Arg3.1 synthesis controls long-term potentiation consolidation through regulation of local actin polymerization in the dentate gyrus in vivo**. *J Neurosci* 2007 27: 10445-55.

43. Davis, S., Bozon, B. and Laroche, S. **How necessary is the activation of the immediate early gene zif268 in synaptic plasticity and learning?** *Behav Brain Res* 2003 142: 17-30.

44. Hernandez, P.J., Schlitz, C.A. and Kelley, A.E. **Dynamic shifts in corticostriatal expression patterns of the immediate early genes Homer 1a and Zif268 during early and late phases of instrumental training.** *Learn Mem* 2005 13: 599-608.

45. Yamagata, M. and Sanes, J.R. **Dscam and Sidekick proteins direct lamina-specific synaptic connections in vertebrate retina**. *Nature* 2008 451: 465-9.

46. Fuerts, P.G., Koizumi, A., Masland, R.H. and Burgess, R.W. **Neurite arborisation and mosaic spacing in the mouse retina requires DSCAM**. *Nature* 2008 451: 470-4.

47. Fabrichny, I.P., Leone, P., Sulzenbacher, G., Comoletti, D., Miller, M.T., Taylor, P., Bourne, Y. and Marchot, P. **Structural analysis of the synaptic protein neuroligin and its beta-neurexin complex: determinants for folding and cell adhesion**. *Neuron* 2007 56: 979-91.

48. James, A.B., Conway, A.M., Thiel, G. and Morris, B.J. **Egr-1 modulation of synapsin I expression: permissive effect of forskolin via cAMP**. *Cell Signal* 2004 16: 1355-62.

49. Yamakawa, T., Saith, S.**,** Li, Y.**,** Gao, X.**,** Gaisano, H.Y. and Tsushima, R.G. **Interaction of syntaxin 1A with the N-terminus of Kv4.2 modulates channel surface expression and gating**. *Biochemistry* 2007 46: 10942-9.

50. Bailey, J.A. and Lahiri, D.K. **Neuronal differentiation is accompanied by increased levels of SNAP-25 protein in fetal rat primary cortical neurons: implications in neuronal plasticity and Alzheimer's disease**. *Ann NY Acad Sci* 2006 1086: 54-65.

51. Narayanan, R. and Johnston, D. **Long-term potentiation in rat hippocampal neurons is accomplished by spatially widespread changes in intrinsic oscillatory dynamics and excitability**. *Neuron* 2007 56: 1061-75.

52. Tsay, D., Dudman, J.T. and Siegelbaum, S.A. **HCN1 channels constrain synaptically evoked Ca^{2+} spikes in distal dendrites of CA1 pyramidal neurons**. *Neuron* 2007 56: 1076-89.

53. Park, C.S., Gong, R., Stuart, J. and Tang, S.J. **Molecular network and chromosomal clustering of genes involved in synaptic plasticity in the hippocampus**. *J Biol Chem* 2006 281: 30195-211.

54. Altar, C.A., Laeng, P., Jurata, L.W., Brockman, J.A., Lemire, A., Bullard, J., Bukhman, Y.V., Young, T.A., Charles, V. and Palfreyman, M.G. **Electroconvulsive seizures regulate gene expression of distinct neurotrophic signaling pathways**. *J Neurosci* 2004 24: 2667-77.

Author's contribution

FB performed and analyzed MEA experiments and prepared results for publication. SP performed and analyzed the molecular biology experiments, made parts of the MEA experiments, interpreted and prepared results for publication. MER participated in the design of the experiments and interpreted and prepared results for publication. DB and CA carried out statistical analysis of the microarrays data. GP contributed in some molecular biology experiments. DA performed TUNEL assays. VT headed the project, and participated in its design and coordination and drafts the manuscript. FB, SP, MER and VT wrote the manuscript. All authors read and approved the final manuscript.

Acknowledgements

We thank M. Lough for critical reading of the manuscript, Prof. E. Cherubini for helpful comments on a previous version of this manuscript, H. Bading for useful discussion. This work was supported by the grant from CIPE (GRAND FVG), by the FP6 grant NEURO (12788) from the European Community and by the FIRB grant RBLA03AF28 007 from the Italian Ministry of Research (MIUR).

TABLE 1 Genes belonging to Cluster 1 and up-regulated at 90 minutes after gabazine wash-out

Gene Symbol	Gene Name	TF*	LTP	Reference
Arc	Activity regulated cytoskeletal-associated protein		+	Rodriguez JJ et al. (2005) Eur. J. Neurosci. 21:2384
Arf4l_pred.	ADP-ribosylation factor-like 4D			
Dusp5	Dual specificity phosphatase 5		+	Hevroni D et al. (1998) J. Mol. Neurosci.10:75
Egr1	Early growth response 1	+	+	M. W. Jones et al.(2001) Nat. Neurosci. 4: 289
Egr2	Early growth response 2	+	+	Williams J et al. (1995) Mol. Brain Res. 28: 87
Egr3	Early growth response 3	+	+	Li L et al. (2007) Mol. Cell. Neurosci. 35:76
Egr4	Early growth response 4	+		
Gem_pred.	GTP binding protein (expressed in skeletal muscle)			
Homer1	Homer homolog 1 (Drosophila)		+	Kato A et al. (2003) Mol. Brain Res. 118: 33
Jmjd3_pred.	Jumonji domain containing 3			
Junb	Jun-B oncogene	+	+	Abraham WC et al. (1991) Mol Neurobiol. 5:297
Klf2_predicted	Kruppel-like factor 2	+		
Klf7_predicted	Kruppel-like factor 7	+		
LOC684871				
LOC686523				
Mmp12	Matrix metallopeptidase 12			
Nfil3	Nuclear factor, interleukin 3 regulated	+		
Nr4a1	Nuclear receptor subfamily 4, group A, member1	+	+	Dragunow M. et al. (1996) Mol. Brain Res.36:349
Nr4a2	Nuclear receptor subfamily 4, group A, member2	+		
Nr4a3	Nuclear receptor subfamily 4, group A, membe 3	+		
Ptgs2	Prostaglandin-endoperoxide synthase 2		+	Slanina KA et al. (2005) Neuropharmacol. 49:660
RGD1306880_pred.				
Rgs4	Regulator of G-protein signaling 4			
Serpinb2	Serpin peptidase inhibitor, clade B member2			
Tfpi2	Tissue factor pathway inhibitor 2			

* TF Transcription factor

TABLE 2 Genes involved in LTP in cluster 1 and 2

	Gene Symbol	Gene Name	Cluster 1	Cluster 2	Reference
S	Arc	Activity regulated cytoskeletal-associated protein	+		Rodriguez JJ et al. 2005 Eur. J. Neurosci. 21:2384
p	Bdnf	Brain derived neurotrophic factor		+	Ying S-W et al. (2002) J. Neurosci. 22:1532
P	Camk2a	Calcium/calmodulin-dependent protein kinase II, □		+	Wang H et al. (2004) Nat. Neurosci. 7:635
-	Cck	Cholecystokinin		+	Balschun D et al (1994) Neuropeptides 26:421
p	Cplx2	Complexin 2		+	Gibson HE (2005) Eur J Neurosci.22:1701
-	Dusp5	Dual specificity phosphatase 5	+		Hevroni D et al. (1998) J. Mol. Neurosci.10:75
T	Egr1	Early growth response 1	+		M. W. Jones et al.(2001) Nat. Neurosci. 4: 289
T	Egr2	Early growth response 2	+		Williams J et al. (1995) Mol. Brain Res. 28: 87
T	Egr3	Early growth response 3	+		Li L et al (2007) Mol. Cell. Neurosci. 35:76
T	Fos	FBJ murine osteosarcoma viral oncogene homolog		+	Dragunow M et al. (1989) Neurosci Lett. 101:274
C	Gria1	Glutamate receptor, ionotropic, AMPA1 (alpha 1)		+	Mead AN et al (2003a) J. Neurosci. 23:1041
C	Gria2	Glutamate receptor, ionotropic, AMPA1 (alpha 2)		+	Mead & Stephens (2003b) J Neurosci. 23:9500
-	Grp	Gastrin releasing peptide		+	Shumyatsky GP et al. (2002) Cell 111: 905
S	Homer1	Homer homolog 1 (Drosophila)	+	+	Kato A et al. (2003) Mol. Brain Res. 118: 33
T	Junb	Jun-B oncogene	+		Abraham WC et al (1991) Mol Neurobiol. 5:297
C	Kcna4	Potassium voltage-gated channel, shaker-related, 4		+	Meiri N et al (1998)Proc Natl Acad Sci U S A. 95:15037
C	Kcnab1	Potassium voltage-gated channel shaker-related,□ 1		+	Murphy GG et al (2004) Curr Biol 14:1907
C	Kcnd2	Potassium voltage-gated channel, Shal-related, 2		+	Chen X et al (2006) J Neurosci 26:12143
C	Kcnn2	Potassium calcium-activated channel subfamily N, 2		+	Kramar EA et al. (2004) J. Neurosci. 24:5151
p	L1cam	L1 cell adhesion molecule		+	Itoh K et al(2005) Mol CellNeurosci. 29:245
p	Nptx1	Neuronal pentraxin 1		+	Ring et al. (2006) J. Neurobiol. 66:361
T	Nr4a1	Nuclear receptor subfamily 4, group A, member 1	+		Dragunow M. et al. (1996) Mol. Brain Res.36:349
P	Nrgn	Neurogranin		+	Kuo-Ping Huang et al. (2004) J. Neurosci. 24:10660
-	Nsg1	Neuron specific gene family member 1		+	Ernfors et al.(2003)TRENDS in Neuroscience 26: 171
P	Ntrk2	Neurotrophic tyrosine kinase, receptor, type 2 (TrkB)		+	Gooney M. et al (2001) J. Neurochem. 77: 1198
P	Ntrk3	Neurotrophic tyrosine kinase, receptor, type 3 (TrkC)		+	Bramham CR (1996) J. Comp. Neurol. 368:371
-	Pnoc	Prepronociceptin		+	Ring et al. (2006) J. Neurobiol. 66:361
-	Prkar1b	Proteinkinase,cAMPdependent regulatory, type1, beta		+	Hensch TK et al (1998) J.Neurosci. 18:2108
-	Prkcc	Protein kinase C, gamma		+	Gärtner A (2006) J. Neurosci. 26:3496
P	Ptgs2	Prostaglandin-endoperoxide synthase 2 (Cox2)	+		Slanina KA et al., (2005) Neuropharmacol. 49:660
p	Rab3a	RAB3A, member RAS oncogene family		+	Castillo PE et al. (1997) Nature 388: 590
-	Reln	Reelin		+	Weeber et al. (2002) J.Biol. Chem. 277:39944
p	Rgs2	Regulator of G-protein signaling 2		+	Ingi T et al (1998) J. Neurosci. 19:7179
-	Rnf39	Ring finger protein 39		+	Matsuo R et al. (2001) BBRC 288: 479
-	Ryr2	Ryanodine receptor 2		+	Welsby P. et al. (2006) Eur. J. Neurosci. 24: 3109
P	Shank1	SH3 and multiple ankyrin repeat domain 1		+	Hung AY et al (2008) J.Neurosci. 28:1697
p	Snap25	Synaptosomal-associated protein 25		+	Roberts LA et al (1998) Neuroreport 9:33
p	Stx1a	Syntaxin 1A (brain)		+	Fujiwara et al. (2006) J. Neurosci. 26:5767
p	Stx1b2	Syntaxin 1B2		+	Helme-Guizon et al. (1998) Eur. J. Neurosci. 10:2231
p	Syn1	Synapsin I		+	Sato K et al. 2000 Brain Res. 872:219
p	Syn2	Synapsin II		+	Spillane et al. (1995) Neuropharmacol 34:1573
p	Syp	Synaptophysin		+	Janz R. et al.(1999) Neuron 24: 687
-	Vsnl1	Visinin-like 1		+	Brackmann M.et al. (2004) BBRC 322: 1073

* S= Structural p=presynaptic P=postsynaptic T= transcription factor C= channel

TABLE 3 List of genes involved in structural, pre- and post-synaptic processes

Gene Name	Gene Symbol	Cluster
Presynaptic		
ATPase, Ca++ transporting, plasma membrane 2	Atp2b2	2
ATPase, H+ transporting, V1 subunit G isoform 2	Atp6v1g2	2
Complexin 1	Cplx1	2
Dynamin 1	Dnm1	2
EF hand calcium binding protein 2	Efcbp2 o NECAB2	2
Kinesin family member 1A	Kif1a	2
Protein kinase C and casein kinase substrate in neurons 1	Pacsin1 o syndapin I	2
Protein tyrosine phosphatase, receptor type, f polypeptide, interacting protein (liprin), α3	Ppfia3	2
Regulator of G-protein signaling 4	Rgs4	2
Regulator of G-protein signaling 7	Rgs7	2
Solute carrier family 17 (Na-dependent inorganic phosphate cotransporter), member 6	Slc17a6	2
Solute carrier family 17 (Na-dependent inorganic phosphate cotransporter), member 7	Slc17a7	2
Solute carrier family 32 (GABA vesicular transporter), member 1	Slc32a1	2
Solute carrier family 6 (neurotransmitter transporter, GABA), member 1	Slc6a1 o GAT1	2
Somatostatin	Sst	2
Spectrin beta 3	Spnb3	2
Synaptic vesicle glycoprotein 2a	Sv2a	2
Synaptogyrin 3 (predicted)	Syngr3_predicted	2
Synaptoporin	Synpr	2
Synaptotagmin I	Syt1	2
Synaptotagmin XIII	Syt13	2
Synaptotagmin-like 2 (predicted)	Sytl2_predicted	3
Synuclein, alpha	Snca	2
Synuclein, beta	Sncb	2
Vesicle-associated membrane protein 1	Vamp1	2
Vesicular membrane protein p24 (predicted)	Vmp_predicted	2
Postsynaptic		
Calcium binding protein 1	Cabp1	2
Calcium/calmodulin-dependent protein kinase II, alpha	Camk2a	2
Connector enhancer of kinase suppressor of Ras 2	Cnksr2	2
Dendrin	Ddn	2
Dipeptidylpeptidase 10	Dpp10	2
Discs, large homolog 2 (Drosophila)	Dlgh2	2
Dopamine receptor D1 interacting protein	Drd1ip	2
G protein-coupled receptor 85	Gpr85	2
Glycine receptor, alpha 2 subunit	Glra2	2
Guanine nucleotide binding protein, gamma 2	Gng2	2
Inositol 1,4,5-trisphosphate 3-kinase A	Itpka	2
Junctophilin 3 (predicted)	Jph3_predicted	2
Kinesin family member C2	KIFC2	2
Leucine rich repeat and fibronectin type III domain containing 5 (predicted)	Lrfn5_predicted	2
Lin-7 homolog b (C. elegans)	Lin7b o MALS	2
N-ethylmaleimide sensitive fusion protein	Nsf	2
Opioid binding protein/cell adhesion molecule-like	Opcml o OBCAM	2

Protein kinase C, epsilon	Prkce	2
Protein tyrosine phosphatase, non-receptor type 5	Ptpn5 o STEP	2
Protein tyrosine phosphatase, receptor type, R	Ptprr	2
Rap guanine nucleotide exchange factor (GEF) 4	Rapgef4	2
Solute carrier family 12, (potassium-chloride transporter) member 5	Slc12a5 o KCC2	2
Somatostatin receptor 1	Sstr1	2
Somatostatin receptor 2	Sstr2	2
Structural		
Cadherin 10	Cdh10	2
Cadherin 11	Cdh11	2
Calcium/calmodulin-dependent protein kinase II, beta	Camk2b	2
Doublecortin	Dcx	2
Down syndrome cell adhesion molecule	Dscam	2
Fibulin 2	Fbln2	3
Integrin alpha 1	Itga1	3
Lysyl oxidase	Lox	3
Microtubule-associated protein tau	Mapt	2
Neurexin 3	Nrxn3	2
Neurexophilin 1	Nxph1	2
Neurofilament, heavy polypeptide	Nefh	2
Neurofilament, light polypeptide	Nefl	2
Neurotrimin	Hnt	2
Nexilin	Nexn	3
Nidogen 2	Nid2	3
Plakophilin 2	Pkp2	3
Plasticity related gene 1	Prg1	2
Pregnancy upregulated non-ubiquitously expressed CaM kinase	Pnck	2
Procollagen, type I, alpha 2	Col1a2	3
Procollagen, type IV, alpha 1	Col4a1	3
Procollagen, type V, alpha 2	Col5a2	3
Procollagen, type XI, alpha 1	Col11a1	3
Protocadherin 17 (predicted)	Pcdh17_predicted	2
Protocadherin 20 (predicted)	Pcdh20_predicted	2
Protocadherin 8	Pcdh8	2
Rho guanine nucleotide exchange factor 7	Arhgef7	2
Seizure related 6 homolog (mouse)	Sez6	2
SLIT and NTRK-like family, member 1 (predicted)	Slitrk1_predicted	2
Stathmin-like 3	Stmn3 o SCLIP	2
Stathmin-like 4	Stmn4 o RB3	2
T-cell lymphoma invasion and metastasis 1	Tiam1	2
Thrombospondin 1	Thbs1	3
Tissue inhibitor of metalloproteinase 3	Timp3	3
Transgelin	Tagln	3
Tubulin, beta 3	Tubb3	2
Tubulin, beta 4	Tubb4	2
Unc-5 homolog C (C. elegans)	Unc5c	3
Vasoactive intestinal polypeptide	Vip	2

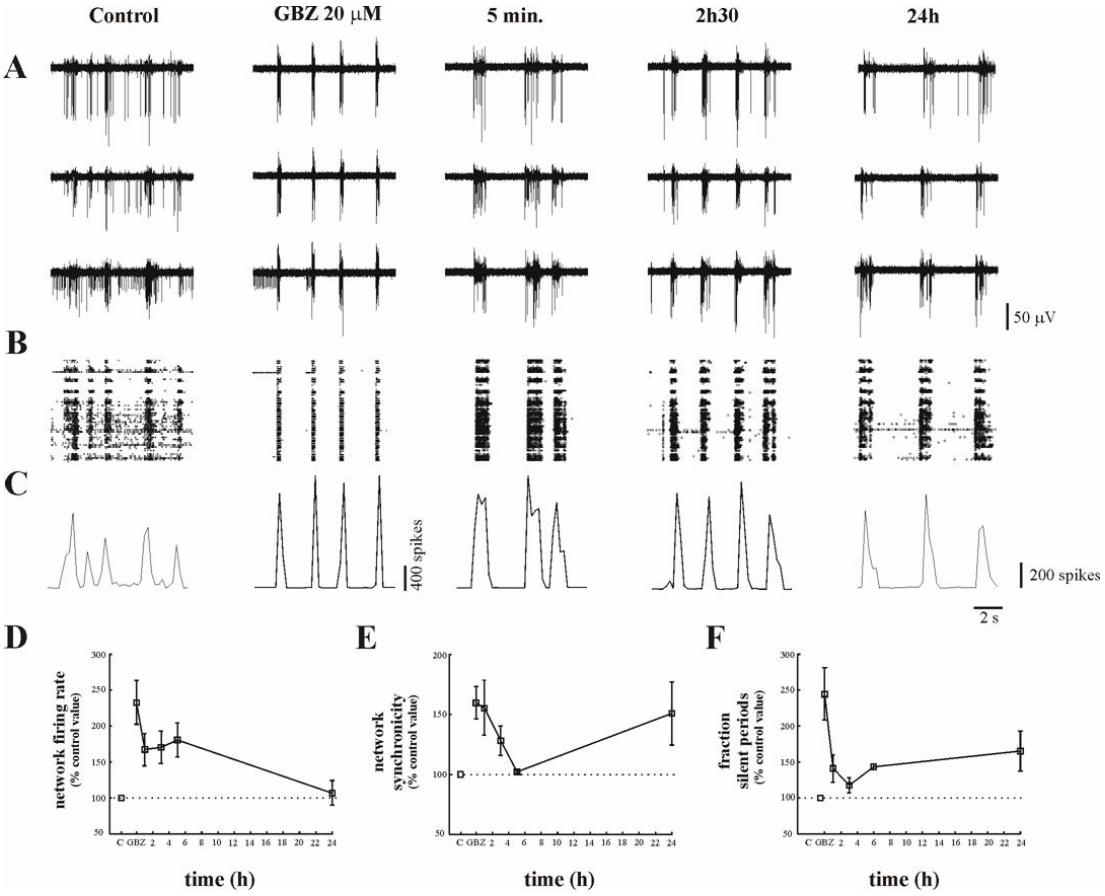
Control
GBZ 20 μM
5 min.
2h30
24h
A
B
C
D
E
F
50 μV
400 spikes
200 spikes
2 s
network firing rate
(% control value)
network
synchronicity
(% control value)
fraction
silent periods
(% control value)
C GBZ 2 4 6 8 10 12 14 16 18 20 22 24
time (h)

Fig.1

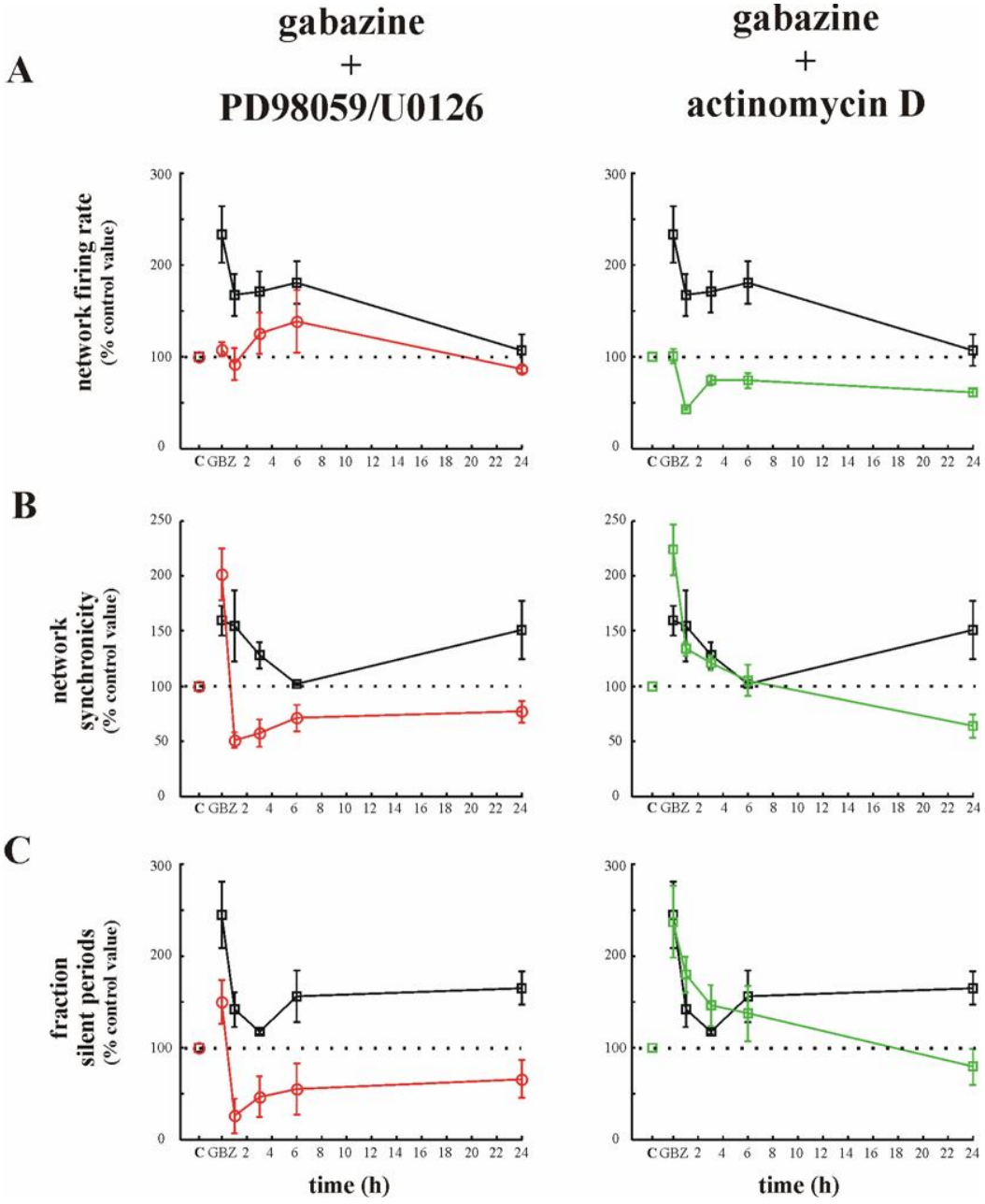
A
gabazine
+
PD98059/U0126
gabazine
+
actinomycin D
network firing rate
(% control value)
B
network
synchronicity
(% control value)
C
fraction
silent periods
(% control value)
C GBZ 2 4 6 8 10 12 14 16 18 20 22 24
time (h)

Fig. 2

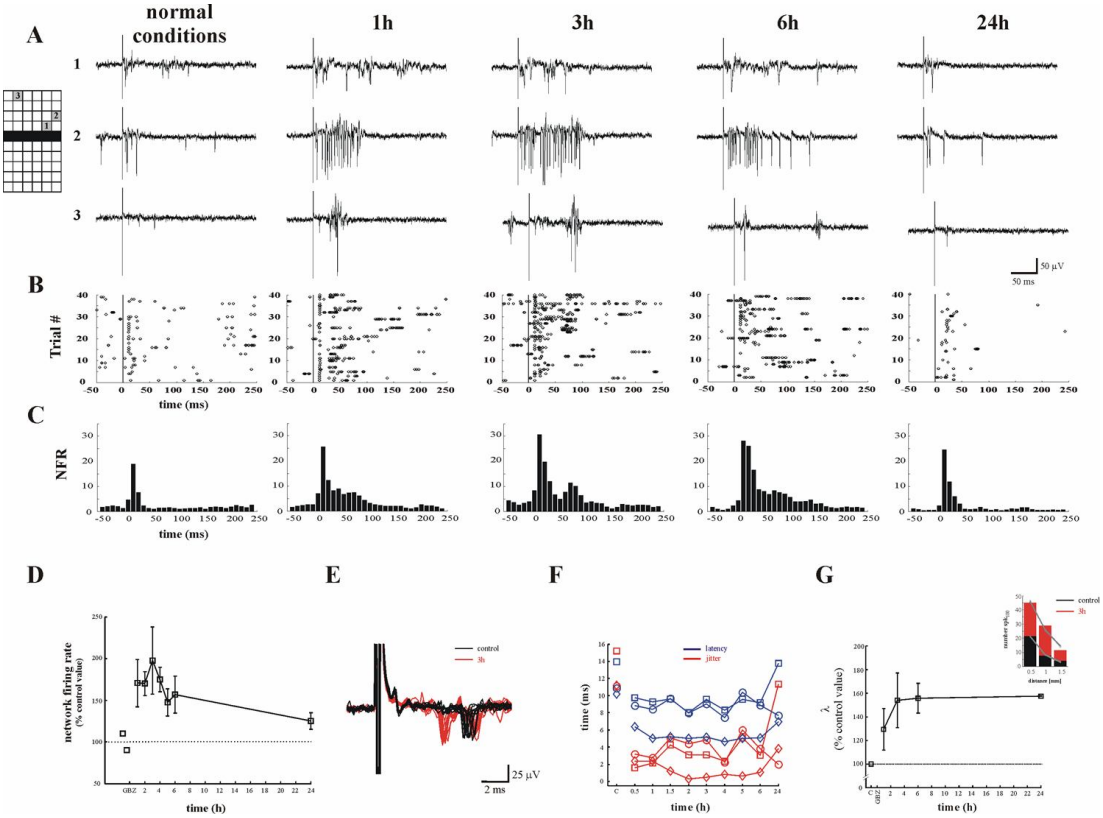
A
normal conditions
1h
3h
6h
24h
1
2
3
50 µV
50 ms
B
Trial #
time (ms)
C
NFR
time (ms)
D
network firing rate (% control value)
time (h)
E
control
3h
25 µV
2 ms
F
latency
jitter
time (ms)
time (h)
G
control
3h
time (h)

Fig.3

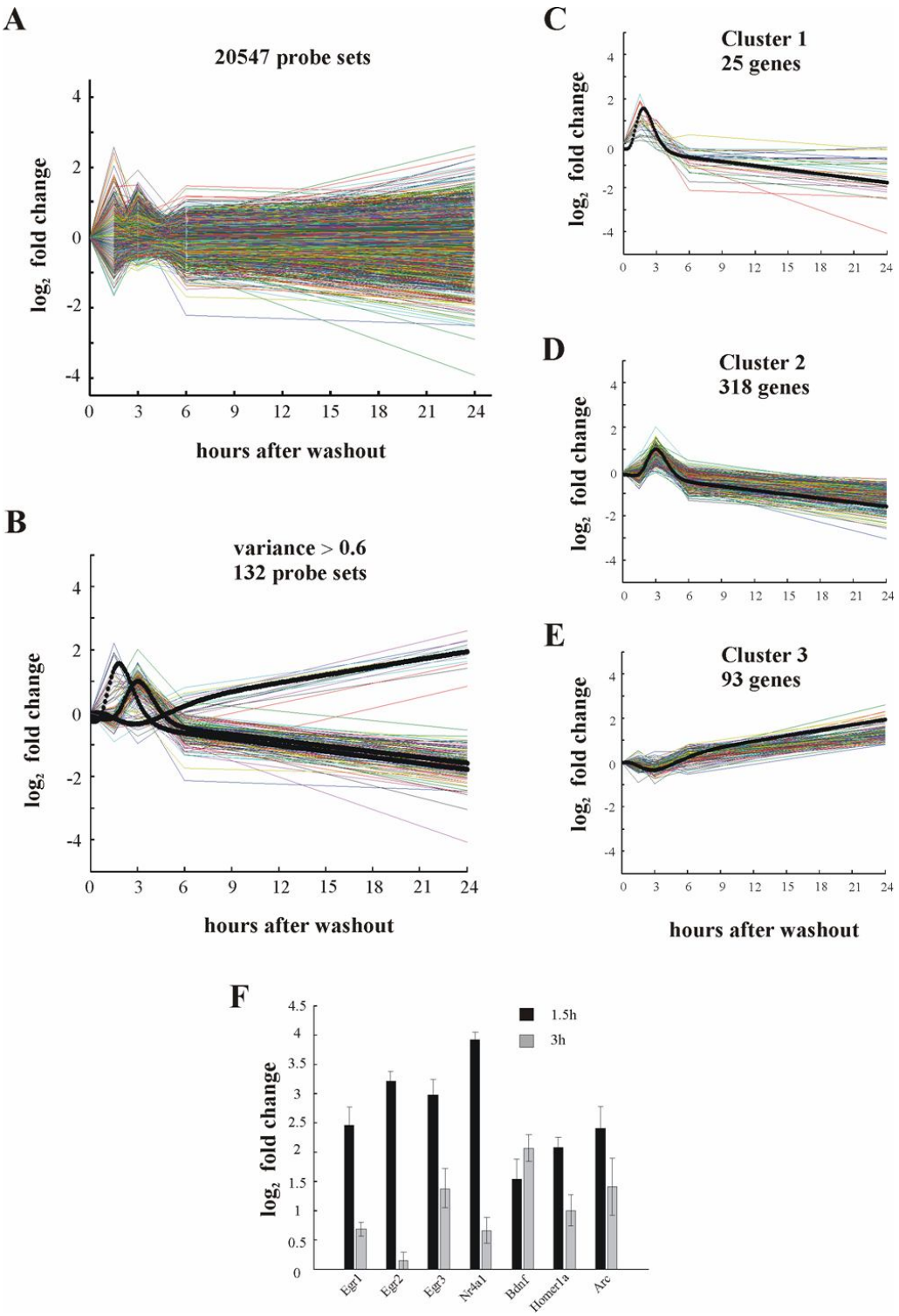
A
20547 probe sets
log2 fold change
hours after washout
B
variance > 0.6
132 probe sets
log2 fold change
hours after washout
C
Cluster 1
25 genes
log2 fold change
D
Cluster 2
318 genes
log2 fold change
E
Cluster 3
93 genes
log2 fold change
hours after washout
F
1.5h
3h
log2 fold change
Egr1
Egr2
Egr3
Nr4a1
Bdnf
Homer1a
Arc

Fig.4

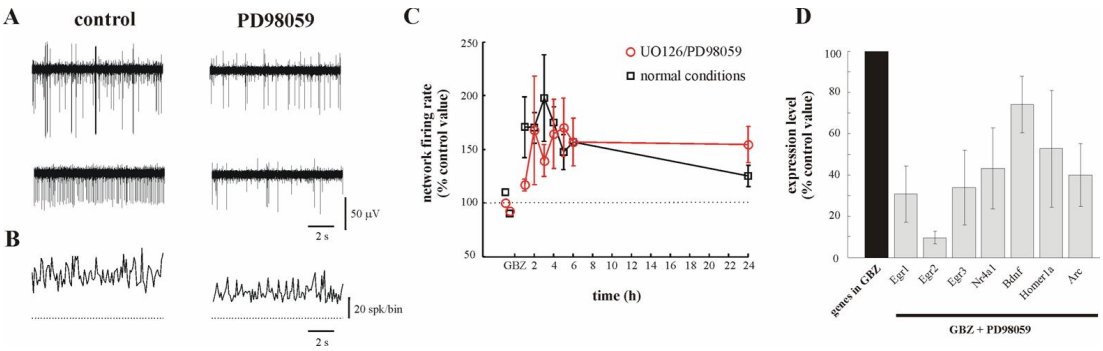
A
control
PD98059
50 µV
2 s
B
20 spk/bin
2 s
C
UO126/PD98059
normal conditions
network firing rate
(% control value)
GBZ 2 4 6 8 10 12 14 16 18 20 22 24
time (h)
D
expression level
(% control value)
genes in GBZ
Egr1
Egr2
Egr3
Nr4a1
Bdnf
Homer1a
Arc
GBZ + PD98059

Fig.5

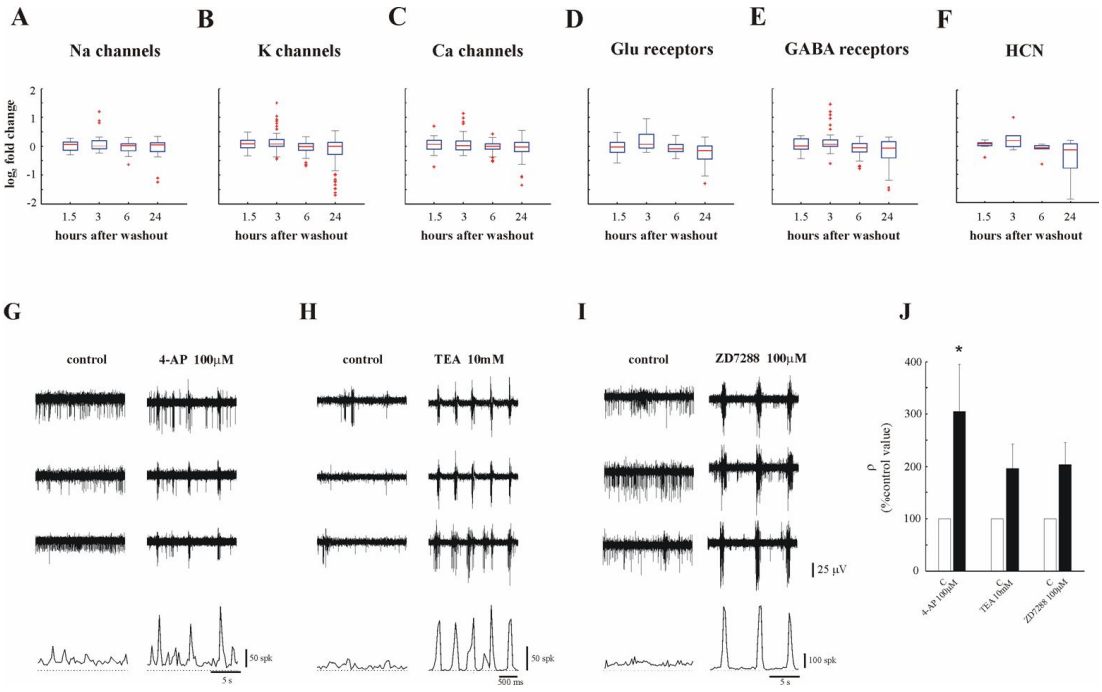
A
Na channels
B
K channels
C
Ca channels
D
Glu receptors
E
GABA receptors
F
HCN
log fold change
hours after washout
G
control
4-AP 100µM
50 spk
5 s
H
control
TEA 10mM
50 spk
500 ms
I
control
ZD7288 100µM
25 µV
100 spk
5 s
J
ρ
(%control value)
*
C
4-AP 100µM
C
TEA 10mM
C
ZD7288 100µM

Fig.6

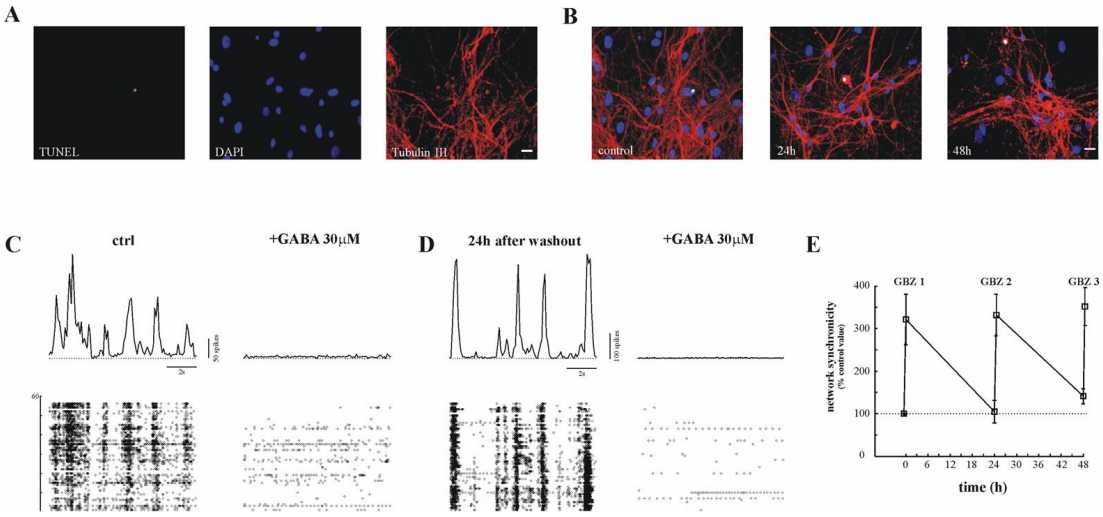
A
TUNEL
DAPI
Tubulin IH
B
control
24h
48h
C
ctrl
+GABA 30μM
50 spikes
2s
60
D
24h after washout
+GABA 30μM
100 spikes
2s
E
GBZ 1
GBZ 2
GBZ 3
network synchronicity
(% control value)
400
300
200
100
0
0 6 12 18 24 30 36 42 48
time (h)

Fig.7

Supplementary Table S1

List of all genes present in clusters 1, 2 and 3

CLUSTER 1			
Affymetrix ID	**GenBank ID**	**Gene Name**	**Gene Symbol**
1387068_at	NM_019361	Activity regulated cytoskeletal-associated protein	Arc
1380383_at	AI030650	ADP-ribosylation factor 4-like (predicted)	Arf4l_predicted
1368124_at	NM_133578	Dual specificity phosphatase 5	Dusp5
1368321_at	NM_012551	Early growth response 1	Egr1
1387306_a_at	NM_053633	Early growth response 2	Egr2
1392791_at	AA964492	Early growth response 3	Egr3
1387442_at	NM_019137	Early growth response 4	Egr4
1382351_at	AI069972	GTP binding protein (gene overexpressed in skeletal muscle) (predicted)	Gem_predicted
1370997_at	AF030088	Homer homolog 1 (Drosophila)	Homer1
1390000_at	BE118720	Jumonji domain containing 3 (predicted)	Jmjd3_predicted
1387788_at	NM_021836	Jun-B oncogene	Junb
1376569_at	BM385790	Kruppel-like factor 2 (lung) (predicted)	Klf2_predicted
1380363_at	BF420490	Kruppel-like factor 7 (ubiquitous) (predicted)	Klf7_predicted
1373403_at	AI230625	Similar to Protein C8orf4 (Thyroid cancer protein 1) (TC-1)	LOC684871
1397460_at	BE119491	Similar to G protein-coupled receptor 158 isoform a	LOC686523
1368530_at	NM_053963	Matrix metallopeptidase 12	Mmp12
1368488_at	NM_053727	Nuclear factor, interleukin 3 regulated	Nfil3
1386935_at	NM_024388	Nuclear receptor subfamily 4, group A, member 1	Nr4a1
1369007_at	L08595	Nuclear receptor subfamily 4, group A, member 2	Nr4a2
1369067_at	NM_031628	Nuclear receptor subfamily 4, group A, member 3	Nr4a3
1368527_at	U03389	Prostaglandin-endoperoxide synthase 2	Ptgs2
1397241_at	BE101570	Similar to hypothetical protein MGC47816 (predicted)	RGD1306880_predicted
1368506_at	U27767	Regulator of G-protein signaling 4	Rgs4
1368487_at	NM_021696	Serine (or cysteine) proteinase inhibitor, clade B, member 2	Serpinb2
1377340_at	AI179507	Tissue factor pathway inhibitor 2	Tfpi2

CLUSTER 2			
Affymetrix ID	**GenBank ID**	**Gene Name**	**Gene Symbol**
1384869_at	AW531594	Abhydrolase domain containing 7 (predicted)	Abhd7_predicted
1370206_at	BM386997	Amiloride-sensitive cation channel 4, pituitary	Accn4
1382608_at	BI281712	Actin-like 6B (predicted)	Actl6b_predicted
1370638_at	AF069525	Ankyrin 3, epithelial	Ank3
1385910_at	AW533307	Rho guanine nucleotide exchange factor 7	Arhgef7
1376198_at	BI303342	Adipocyte-specific adhesion molecule	Asam
1393141_at	BF285419	Aspartate-beta-hydroxylase (predicted)	Asph_predicted
1383340_at	BG671011	Ataxia, cerebellar, Cayman type (caytaxin) (predicted)	Atcay_predicted
1368701_at	NM_012506	ATPase, Na+/K+ transporting, alpha 3 polypeptide	Atp1a3
1368698_at	J03754	ATPase, Ca++ transporting, plasma membrane 2	Atp2b2

1388037_at	J05087	ATPase, Ca++ transporting, plasma membrane 3	Atp2b3
1377722_at	BE100072	ATPase, H+ transporting, V1 subunit G isoform 2	Atp6v1g2
1369755_at	AF106624	Beta-1,3-glucuronyltransferase 2 (glucuronosyltransferase S)	B3gat2
1383010_at	AW531880	B-cell CLL/lymphoma 11A (zinc finger protein)	Bcl11a
1391948_at	BM390227	B-cell leukemia/lymphoma 11B (predicted)	Bcl11b_predicted
1368677_at	NM_012513	Brain derived neurotrophic factor	Bdnf
1388802_at	AI579422	Brain expressed X-linked 1	Bex1
1381995_at	AW530502	Bruno-like 4, RNA binding protein (Drosophila) (predicted)	Brunol4_predicted
1376707_at	AW918311	C1q and tumor necrosis factor related protein 4 (predicted)	C1qtnf4_predicted
1386922_at	AI408948	Carbonic anhydrase 2	Ca2
1369886_a_at	AJ315761	Calcium binding protein 1	Cabp1
1390358_at	BF405996	Calcium channel, voltage-dependent, alpha 2/delta 3 subunit	Cacna2d3
1382898_at	BG376849	Calcium channel, voltage-dependent, beta 4 subunit	Cacnb4
1368759_at	NM_053351	Calcium channel, voltage-dependent, gamma subunit 2	Cacng2
1370757_at	AF361340	Calcium channel, voltage-dependent, gamma subunit 3	Cacng3
1387133_at	NM_053988	Calbindin 2	Calb2
1391229_at	BG381458	Calcium/calmodulin-dependent protein kinase I gamma	Camk1g
1388187_at	BM384558	Calcium/calmodulin-dependent protein kinase II, alpha	Camk2a
1398251_a_at	NM_021739	Calcium/calmodulin-dependent protein kinase II, beta	Camk2b
1368845_at	NM_024000	CaM kinase-like vesicle-associated	Camkv
1370438_at	AF037071	C-terminal PDZ domain ligand of neuronal nitric oxide synthase	Capon
1385519_at	BE105678	CBFA2T1 identified gene homolog (human) (predicted)	Cbfa2t1_predicted
1387032_at	NM_012829	Cholecystokinin	Cck
1369670_at	NM_031518	Cd200 antigen	Cd200
1391127_at	BF400818	Cell division cycle 42 homolog (S. cerevisiae)	Cdc42
1380317_at	BF402765	Cadherin 10	Cdh10
1391146_at	BE111632	Cadherin 11	Cdh11
1369425_at	NM_138889	Cadherin 13	Cdh13
1368887_at	NM_019161	Cadherin 22	Cdh22
1387194_at	U51013	Centaurin, alpha 1	Centa1
1397549_at	AW526039	Centaurin, gamma 1	Centg1
1373256_at	BM391119	Chromodomain helicase DNA binding protein 3	Chd3
1387235_at	NM_021655	Chromogranin A	Chga
1368034_at	NM_012526	Chromogranin B	Chgb
1368287_at	NM_032083	Chimerin (chimaerin) 1	Chn1
1387462_at	NM_012527	Cholinergic receptor, muscarinic 3	Chrm3
1395429_at	BF281401	Cholinergic receptor, nicotinic, alpha polypeptide 7	Chrna7
1394334_at	BF545197	Carbohydrate (N-acetylgalactosamine 4-0) sulfotransferase 8 (predicted)	Chst8_predicted
1390566_a_at	BI301453	Creatine kinase, mitochondrial 1, ubiquitous	Ckmt1
1372492_at	AI412937	Claudin 10 (predicted)	Cldn10_predicted
1369731_at	AF102854	Connector enhancer of kinase suppressor of Ras 2	Cnksr2
1369964_at	NM_130411	Coronin, actin binding protein 1A	Coro1a
1368648_at	NM_053472	Cytochrome c oxidase subunit IV isoform 2	Cox4i2
1398357_at	BI281575	Complexin 1	Cplx1
1368584_a_at	NM_053878	Complexin 2	Cplx2
1384780_at	BF402747	Copine IV (predicted)	Cpne4_predicted
1368381_at	NM_134401	Cartilage acidic protein 1	Crtac1

1368059_at	NM_053955	Crystallin, mu	Crym
1368200_at	NM_134455	Chemokine (C-X3-C motif) ligand 1	Cx3cl1
1369408_at	NM_080482	Deleted in bladder cancer chromosome region candidate 1 (human)	Dbccr1
1374966_at	BE109057	Doublecortin	Dcx
1388177_at	X96589	Dendrin	Ddn
1387265_at	NM_013126	Diacylglycerol kinase, gamma	Dgkg
1375433_at	AI412473	Dispatched homolog 2 (Drosophila) (predicted)	Disp2_predicted
1375139_at	BF406295	Discs, large homolog 2 (Drosophila)	Dlgh2
1392064_at	BF400590	Distal-less homeobox 1	Dlx1
1377125_at	AW523481	DnaJ (Hsp40) homolog, subfamily C, member 6 (predicted)	Dnajc6_predicted
1368292_at	NM_080689	Dynamin 1	Dnm1
1393299_at	BF567794	Dipeptidylpeptidase 10	Dpp10
1376345_at	BG381734	Dopamine receptor D1 interacting protein	Drd1ip
1368699_at	NM_133587	Down syndrome cell adhesion molecule	Dscam
1391246_at	BF390318	Dystrobrevin alpha (predicted)	Dtna_predicted
1387025_at	NM_019234	Dynein cytoplasmic 1 intermediate chain 1	Dync1i1
1367799_at	NM_012660	Eukaryotic translation elongation factor 1 alpha 2	Eef1a2
1368443_at	NM_133415	EF hand calcium binding protein 2	Efcbp2
1383078_at	BG381007	Ephrin B3 (predicted)	Efnb3_predicted
1383736_at	AI145457	ELAV (embryonic lethal, abnormal vision, Drosophila)-like 2 (Hu antigen B)	Elavl2
1368114_at	NM_053428	Fibroblast growth factor 13	Fgf13
1375043_at	BF415939	FBJ murine osteosarcoma viral oncogene homolog	Fos
1387383_at	NM_031802	Gamma-aminobutyric acid (GABA) B receptor 2	Gabbr2
1380828_at	AI145413	Gamma-aminobutyric acid A receptor, alpha 1	Gabra1
1371057_at	AW520967	Gamma-aminobutyric acid (GABA-A) receptor, subunit alpha 5	Gabra5
1369904_at	NM_012956	Gamma-aminobutyric acid (GABA-A) receptor, subunit beta 1	Gabrb1
1391653_at	BE120391	Gamma-aminobutyric acid A receptor, gamma 2	Gabrg2
1396238_at	AI763990	UDP-N-acetyl-alpha-D-galactosamine:polypeptide N-acetylgalactosaminyltransferase 14	Galnt14
1387696_a_at	X61159	Glycine receptor, alpha 2 subunit	Glra2
1367633_at	BI296610	Glutamate-ammonia ligase (glutamine synthase)	Glul
1387906_a_at	AF107845	GNAS complex locus	Gnas
1386660_at	BF565021	Guanine nucleotide binding protein, gamma 2	Gng2
1368272_at	D00252	Glutamate oxaloacetate transaminase 1	Got1
1368786_a_at	NM_030831	G-protein coupled receptor 12	Gpcr12
1384004_at	AI030360	G protein-coupled receptor 158 (predicted)	Gpr158_predicted
1382319_at	BM389005	G protein-coupled receptor 68 (predicted)	Gpr68_predicted
1368299_at	NM_080411	G protein-coupled receptor 83	Gpr83
1387666_at	AF203907	G protein-coupled receptor 85	Gpr85
1375050_at	BI294558	G protein-regulated inducer of neurite outgrowth 1 (predicted)	Gprin1_predicted
1371013_at	BG376217	Glutamate receptor, ionotropic, AMPA1 (alpha 1)	Gria1
1394578_at	BI299761	Glutamate receptor, ionotropic, AMPA2	Gria2
1368572_a_at	NM_017010	Glutamate receptor, ionotropic, N-methyl D-aspartate 1	Grin1
1368306_at	U08259	Glutamate receptor, ionotropic, NMDA2C	Grin2c
1387286_at	NM_017011	Glutamate receptor, metabotropic 1	Grm1
1388189_at	AW522430	Glutamate receptor, metabotropic 3	Grm3
1368611_at	NM_133570	Gastrin releasing peptide	Grp

1369097_s_at	NM_012769	Guanylate cyclase 1, soluble, beta 3	Gucy1b3
1379920_at	BG671844	Hyperpolarization-activated cyclic nucleotide-gated potassium channel 1	Hcn1
1374105_at	H31665	Hypoxia induced gene 1	Hig1
1368255_at	NM_017354	Neurotrimin	Hnt
1370454_at	AB003726	Homer homolog 1 (Drosophila)	Homer1
1375765_at	BI296503	Hippocalcin-like 4	Hpcal4
1386953_at	NM_017080	Hydroxysteroid 11-beta dehydrogenase 1	Hsd11b1
1373480_at	BG670210	Heat shock 70kDa protein 12A (predicted)	Hspa12a_predicted
1387226_at	NM_019128	Internexin, alpha	Inexa
1391036_at	BG376106	IQ motif and Sec7 domain 3	Iqsec3
1387291_at	NM_017351	Inter-alpha trypsin inhibitor, heavy chain 3	Itih3
1368462_at	NM_031045	Inositol 1,4,5-trisphosphate 3-kinase A	Itpka
1385562_at	AI059487	Jjunctophilin 3 (predicted)	Jph3_predicted
1369043_at	NM_012971	Potassium voltage-gated channel, shaker-related subfamily, member 4	Kcna4
1378738_at	BE097574	Potassium voltage-gated channel, shaker-related subfamily, beta member 1	Kcnab1
1368524_at	NM_012856	Potassium voltage gated channel, Shaw-related subfamily, member 1	Kcnc1
1370439_a_at	M34052	Potassium voltage gated channel, Shaw-related subfamily, member 2	Kcnc2
1379863_at	AW528891	Potassium voltage gated channel, Shal-related family, member 2	Kcnd2
1373987_at	AI410448	Kv channel-interacting protein 2	Kcnip2
1383220_at	BE114231	Kv channel interacting protein 4	Kcnip4
1373991_at	AI411366	Potassium inwardly-rectifying channel, subfamily J, member 16	Kcnj16
1369035_a_at	AB073753	Potassium inwardly-rectifying channel, subfamily J, member 6	Kcnj6
1370111_at	NM_019314	Potassium intermediate/small conductance calcium-activated channel, subfamily N, member 2	Kcnn2
1392785_at	AA800908	Potassium channel tetramerisation domain containing 12 (predicted)	Kctd12_predicted
1397505_at	BE115743	Kinesin family member 1A	Kif1a
1380172_at	BE104278	Kinesin family member 5C (predicted)	Kif5c_predicted
1378197_at	AW433953	Kinesin family member C2	KIFC2
1369213_at	NM_017345	L1 cell adhesion molecule	L1cam
1386023_at	AI229354	Leucine-rich repeat LGI family, member 1	Lgi1
1370078_at	NM_021758	Lin-7 homolog b (C. elegans)	Lin7b
1382207_at	BE097085	Similar to Cerebellin-2 precursor (Cerebellin-like protein)	LOC288979
1383571_at	BF411217	Hypothetical protein LOC303515	LOC303515
1377615_at	AI112395	Similar to hypothetical protein	LOC304280
1391513_at	BE110237	Similar to hypothetical protein FLJ20331	LOC310946
1383422_at	AW252401	Hypothetical LOC362564	LOC362564
1380866_at	AA817746	Similar to adenylate kinase 5 isoform 1	LOC365985
1378904_at	AW529244	Similar to solute carrier family 7, member 14	LOC499587
1385950_at	AI454926	Hypothetical protein LOC500102	LOC500102
1391030_at	AW524694	Similar to calmodulin-binding transcription activator 1	LOC500591
1398659_at	AW528611	Similar to crossveinless 2 CG15671-PA	LOC501231
1378857_at	AI716196	Similar to transcription elongation factor A (SII)-like 5	LOC678833
1381132_at	AI501937	Similar to TAFA2 protein	LOC680647
1373648_at	AI102627	Similar to Protein C6orf142 homolog	LOC681849
1376736_at	BG375419	Hypothetical protein LOC683263	LOC683263
1396388_at	AW522161	Similar to Potassium channel tetramerisation domain-containing protein 4	LOC684884
1396381_at	BE097451	Hypothetical protein LOC684957	LOC684957

1378064_at	AI144892	Hypothetical protein LOC689106	LOC689106
1386119_at	BE110033	Hypothetical protein LOC689147	LOC689147
1398405_at	BI289917	Similar to septin 6	LOC691335
1384942_at	AA818417	Leucine rich repeat and fibronectin type III domain containing 5 (predicted)	Lrfn5_predicted
1368964_at	NM_030856	Leucine rich repeat protein 3, neuronal	Lrrn3
1387947_at	U56241	V-maf musculoaponeurotic fibrosarcoma oncogene family, protein B (avian)	Mafb
1368137_at	NM_017212	Microtubule-associated protein tau	Mapt
1387834_at	NM_021859	Megakaryocyte-associated tyrosine kinase	Matk
1389605_at	AI101952	Multiple coiled-coil GABABR1-binding protein	MGC125215
1376106_at	AI010157	Similar to hypothetical protein MGC33926	MGC94782
1370831_at	AY081195	Monoglyceride lipase	Mgll
1388300_at	AA892234	Microsomal glutathione S-transferase 3 (predicted)	Mgst3_predicted
1378430_at	AI555053	Monooxygenase, DBH-like 1	Moxd1
1370535_at	U48809	Myelin transcription factor 1-like	Myt1l
1372953_at	AI101330	Neurocalcin delta	Ncald
1367956_at	NM_053543	Neurochondrin	Ncdn
1370815_at	AF031879	Neurofilament, heavy polypeptide	Nefh
1370058_at	NM_031783	Neurofilament, light polypeptide	Nefl
1370016_at	NM_031070	Nel-like 2 homolog (chicken)	Nell2
1370977_at	X66022	Neuronal d4 domain family member	Neud4
1387288_at	NM_019218	Neurogenic differentiation 1	Neurod1
1369999_a_at	NM_053601	Neuronatin	Nnat
1370517_at	U18772	Neuronal pentraxin 1	Nptx1
1376362_at	BG380575	Neuronal pentraxin receptor	Nptxr
1370211_at	BE106940	Neurogranin	Nrgn
1370570_at	AF016296	Neuropilin 1	Nrp1
1368261_at	NM_053817	Neurexin 3	Nrxn3
1369689_at	AF142097	N-ethylmaleimide sensitive fusion protein	Nsf
1387817_at	NM_024128	Neuron specific gene family member 1	Nsg1
1368972_at	NM_012731	Neurotrophic tyrosine kinase, receptor, type 2	Ntrk2
1368939_a_at	L14447	Neurotrophic tyrosine kinase, receptor, type 3	Ntrk3
1368688_at	NM_022695	Neurotensin receptor 2	Ntsr2
1369079_at	NM_012994	Neurexophilin 1	Nxph1
1368993_at	NM_020088	Odd Oz/ten-m homolog 2 (Drosophila)	Odz2
1387927_a_at	U03415	Olfactomedin 1	Olfm1
1369417_a_at	NM_053848	Opioid binding protein/cell adhesion molecule-like	Opcml
1368958_at	NM_017294	Protein kinase C and casein kinase substrate in neurons 1	Pacsin1
1395792_at	AI549034	Poly(rC) binding protein 2	Pcbp2
1384509_s_at	BF558981	Protocadherin 17 (predicted)	Pcdh17_predicted
1391208_at	BG379836	Protocadherin 20 (predicted)	Pcdh20_predicted
1368956_at	NM_022868	Protocadherin 8	Pcdh8
1368089_at	NM_031079	Phosphodiesterase 2A, cGMP-stimulated	Pde2a
1389597_at	BI293445	PiggyBac transposable element derived 5 (predicted)	Pgbd5_predicted
1374862_at	AI764464	Phytanoyl-CoA hydroxylase interacting protein	Phyhip
1387281_a_at	D86556	Pregnancy upregulated non-ubiquitously expressed CaM kinase	Pnck
1368369_at	NM_013007	Prepronociceptin	Pnoc
1370432_at	M72711	POU domain, class 3, transcription factor 1	Pou3f1

1382821_at	AA998957	Protein tyrosine phosphatase, receptor type, f polypeptide (PTPRF), interacting protein (liprin), alpha 3	Ppfia3
1379374_at	AW526088	Plasticity related gene 1	Prg1
1372382_at	AW527165	Protein kinase, AMP-activated, gamma 2 non-catalytic subunit	Prkag2
1389463_at	BG375376	Protein kinase, cAMP dependent regulatory, type I, beta	Prkar1b
1369089_at	NM_012628	Protein kinase C, gamma	Prkcc
1374593_at	AA799421	Protein kinase C, epsilon	Prkce
1368421_at	NM_019253	Protein tyrosine phosphatase, non-receptor type 5	Ptpn5
1371086_at	BE096879	Protein tyrosine phosphatase, receptor type, F	Ptprf
1368358_a_at	NM_053594	Protein tyrosine phosphatase, receptor type, R	Ptprr
1368674_at	NM_022268	Liver glycogen phosphorylase	Pygl
1369004_at	NM_133580	RAB26, member RAS oncogene family	Rab26
1369816_at	NM_013018	RAB3A, member RAS oncogene family	Rab3a
1383826_at	AA924620	Rab40b, member RAS oncogene family (predicted)	Rab40b_predicted
1388632_at	BG665929	RAB6B, member RAS oncogene family (predicted)	Rab6b_predicted
1373631_at	BF284067	RAP1, GTPase activating protein 1	Rap1ga1
1371081_at	U78517	Rap guanine nucleotide exchange factor (GEF) 4	Rapgef4
1373666_at	AI102560	Rap guanine nucleotide exchange factor (GEF) 5	Rapgef5
1370372_at	AF134409	RASD family, member 2	Rasd2
1393081_at	AI145237	RasGEF domain family, member 1A (predicted)	Rasgef1a_predicted
1369093_at	NM_080394	Reelin	Reln
1370989_at	AI639318	Ret proto-oncogene	Ret
1392315_at	BE107351	REV1-like (S. cerevisiae) (predicted)	Rev1l_predicted
1384289_at	BI281651	Similar to RIKEN cDNA 4631403P03	RGD1305276
1373414_at	BG380515	Similar to Brain specific membrane-anchored protein precursor	RGD1305557
1383706_at	BF409331	Similar to RIKEN cDNA 2900011O08	RGD1305733
1380852_at	AI112346	Hypothetical LOC294883	RGD1305844
1390167_at	BI286834	Similar to hypothetical protein FLJ30373 (predicted)	RGD1306256_predicted
1380228_at	BG672066	Similar to hypothetical protein MGC47816 (predicted)	RGD1306880_predicted
1385744_at	BF389238	Similar to KIAA1679 protein (predicted)	RGD1306938_predicted
1383887_at	AA924984	Similar to Protein C20orf103 precursor	RGD1306991
1374176_at	AI408727	Similar to DNA segment, Chr 4, Brigham & Womens Genetics 0951 expressed	RGD1308059
1376654_at	AW521378	Similar to RIKEN cDNA B130016O10 gene (predicted)	RGD1308448_predicted
1393733_at	BF402788	Similar to hypothetical protein FLJ20300 (predicted)	RGD1309567_predicted
1379894_at	AI501165	Similar to 3632451O06Rik protein (predicted)	RGD1310110_predicted
1393841_at	AA859317	Similar to hypothetical protein FLJ31810 (predicted)	RGD1310773_predicted
1376328_at	BI278776	Similar to putative protein (5S487) (predicted)	RGD1310819_predicted
1383794_at	AI575277	Similar to RIKEN cDNA A930038C07 (predicted)	RGD1311080_predicted
1390865_at	AW524822	Similar to Ca2+-dependent activator for secretion protein 2 (predicted)	RGD1559440_predicted
1383800_at	AW523537	Similar to expressed sequence AW121567 (predicted)	RGD1559498_predicted
1376901_a_at	AA964675	Similar to Hypothetical protein 6330514E13 (predicted)	RGD1559693_predicted
1376460_at	BI286710	Similar to ataxin 2-binding protein 1 isoform 2 (predicted)	RGD1560070_predicted
1391308_at	AI101675	Similar to vacuolar protein sorting 13C protein (predicted)	RGD1560364_predicted
1373985_at	BI282311	Similar to KIAA1183 protein (predicted)	RGD1560435_predicted
1393408_at	BF567707	Similar to NEX-1 (predicted)	RGD1562793_predicted
1396206_at	BG665525	Similar to Docking protein 5 (Downstream of tyrosine kinase 5) (Protein dok-5) (predicted)	RGD1562846_predicted

1376459_at	AW533060	Similar to AP2 associated kinase 1 (predicted)	RGD1563580_predicted
1375305_at	BI282028	RGD1563912 (predicted)	RGD1563912_predicted
1389086_at	BF408444	Similar to RIKEN cDNA E430021N18 (predicted)	RGD1564043_predicted
1380901_at	AW527298	Similar to synaptotagmin XIV-related protein Strep14 (predicted)	RGD1564654_predicted
1379460_at	BF387898	Similar to RIKEN cDNA 3110007P09 (predicted)	RGD1564957_predicted
1388705_at	BI282694	Similar to selenoprotein SelM (predicted)	RGD1565037_predicted
1374785_at	BG380471	Similar to CD69 antigen (p60, early T-cell activation antigen) (predicted)	RGD1565373_predicted
1379564_at	AW528486	Similar to cajalin 2 isoform a (predicted)	RGD1565556_predicted
1383704_at	BF410844	Similar to actin-related protein 3-beta (predicted)	RGD1565759_predicted
1392003_at	AA943753	Similar to KIAA0316 protein (predicted)	RGD1566031_predicted
1381462_at	BI294541	Similar to mKIAA1940 protein (predicted)	RGD1566130_predicted
1389937_at	BF404834	Similar to Neuropilin- and tolloid-like protein 1 (predicted)	RGD1566269_predicted
1384202_at	BI287326	Similar to Tescalcin (predicted)	RGD1566317_predicted
1377008_at	BI296868	Similar to GTL2, imprinted maternally expressed untranslated (predicted)	RGD1566401_predicted
1368144_at	AF321837	Regulator of G-protein signaling 2	Rgs2
1368505_at	NM_017214	Regulator of G-protein signaling 4	Rgs4
1368373_at	NM_019343	Regulator of G-protein signaling 7	Rgs7
1395991_at	BE107556	RIM binding protein 2	Rimbp2
1368662_at	NM_134374	Ring finger protein 39	Rnf39
1376110_at	AI009623	Ribonuclease P 25 subunit (human)	Rpp25
1372690_at	AI137471	Reticulon 4 receptor-like 1	Rtn4rl1
1382088_at	AI548753	Ryanodine receptor 2, cardiac	Ryr2
1369210_at	NM_030875	Sodium channel, voltage-gated, type I, alpha	Scn1a
1369662_at	NM_012647	Sodium channel, voltage-gated, type 2, alpha 1 polypeptide	Scn2a1
1368256_at	NM_053779	Serine (or cysteine) peptidase inhibitor, clade I, member 1	Serpini1
1391032_at	AI112194	Seizure related 6 homolog (mouse)	Sez6
1374825_at	BG380338	Seizure related 6 homolog (mouse)-like 2 (predicted)	Sez6l2_predicted
1370419_a_at	AF230520	SH3-domain kinase binding protein 1	Sh3kbp1
1396040_at	BE108568	SH3 and multiple ankyrin repeat domains 1	Shank1
1370069_at	NM_134363	Solute carrier family 12, (potassium-chloride transporter) member 5	Slc12a5
1368564_at	NM_053427	Solute carrier family 17 (sodium-dependent inorganic phosphate cotransporter), member 6	Slc17a6
1368986_at	NM_053859	Solute carrier family 17 (sodium-dependent inorganic phosphate cotransporter), member 7	Slc17a7
1383444_at	AA964069	Solute carrier family 24 (sodium/potassium/calcium exchanger), member 2	Slc24a2
1387380_at	NM_031782	Solute carrier family 32 (GABA vesicular transporter), member 1	Slc32a1
1373326_at	AI716512	Solute carrier family 4, sodium bicarbonate transporter-like, member 10	Slc4a10
1368170_at	NM_024371	Solute carrier family 6 (neurotransmitter transporter, GABA), member 1	Slc6a1
1391019_at	BF285698	SLIT and NTRK-like family, member 1 (predicted)	Slitrk1_predicted
1368991_at	NM_053605	Sphingomyelin phosphodiesterase 3, neutral	Smpd3
1387073_at	NM_030991	Synaptosomal-associated protein 25	Snap25
1367977_at	NM_019169	Synuclein, alpha	Snca
1369924_at	NM_080777	Synuclein, beta	Sncb
1389752_at	BE109861	Sortilin-related VPS10 domain containing receptor 3 (predicted)	Sorcs3_predicted
1367812_at	NM_019167	Spectrin beta 3	Spnb3
1394252_at	BG668764	Sparc/osteonectin, cwcv and kazal-like domains proteoglycan 3 (predicted)	Spock3_predicted
1367762_at	NM_012659	Somatostatin	Sst

1369770_at	NM_012719	Somatostatin receptor 1	Sstr1
1368782_at	NM_019348	Somatostatin receptor 2	Sstr2
1368157_at	NM_024346	Stathmin-like 3	Stmn3
1370315_a_at	AF026530	Stathmin-like 4	Stmn4
1387360_at	BI290256	Syntaxin 1A (brain)	Stx1a
1368352_at	NM_012700	Syntaxin 1B2	Stx1b2
1368562_at	NM_031641	Sulfotransferase family 4A, member 1	Sult4a1
1368682_at	NM_057210	Synaptic vesicle glycoprotein 2a	Sv2a
1369251_a_at	NM_019133	Synapsin I	Syn1
1369482_a_at	NM_019159	Synapsin II	Syn2
1390209_at	BE097982	Synaptogyrin 3 (predicted)	Syngr3_predicted
1368865_at	BG666364	Synaptoporin	Synpr
1368276_at	NM_012664	Synaptophysin	Syp
1373896_at	AA943569	Synaptotagmin I	Syt1
1374427_at	AI144986	Synaptotagmin XIII	Syt13
1369309_a_at	BG671061	Tachykinin 1	Tac1
1387138_at	NM_019162	Tachykinin 2	Tac2
1370150_a_at	NM_012703	Thyroid hormone responsive protein	Thrsp
1369651_at	NM_012673	Thymus cell antigen 1, theta	Thy1
1374257_at	BM389265	T-cell lymphoma invasion and metastasis 1	Tiam1
1387850_at	NM_023020	Ttransmembrane protein with EGF-like and two follistatin-like domains 1	Tmeff1
1397227_at	BE120895	Transmembrane protein 35	Tmem35
1376721_at	BF400666	Triple functional domain (PTPRF interacting)	Trio
1371618_s_at	AI229029	Tubulin, beta 3	Tubb3
1384927_at	AI230430	Tubulin, beta 4	Tubb4
1397612_at	BF391002	Ubiquitin protein ligase E3A (predicted)	Ube3a_predicted
1395054_at	BF416262	Ubiquitin specific protease 29 (predicted)	Usp29_predicted
1373510_at	BF281373	Vesicle-associated membrane protein 1	Vamp1
1377146_at	AI412212	Vasoactive intestinal polypeptide	Vip
1376893_at	AI406821	Vesicular membrane protein p24 (predicted)	Vmp_predicted
1368853_at	NM_012686	Visinin-like 1	Vsnl1

CLUSTER 3

Affymetrix ID	GenBank ID	Gene Name	Gene Symbol
1384603_at	AI602131	ATP-binding cassette, sub-family A (ABC1), member 4 (predicted)	Abca4_predicted
1370464_at	AF286167	ATP-binding cassette, sub-family B (MDR/TAP), member 1A	Abcb1a
1394483_at	AW535310	A disintegrin-like and metallopeptidase (reprolysin type) with thrombospondin type 1 motif, 5 (aggrecanase-2)	Adamts5
1367974_at	NM_012823	Annexin A3	Anxa3
1372601_at	BM391471	Activating transcription factor 5	Atf5
1398431_at	BI294910	Carbonic anhydrase 8	Car8
1387818_at	NM_053736	Caspase 4, apoptosis-related cysteine peptidase	Casp4
1379935_at	BF419899	Chemokine (C-C motif) ligand 7	Ccl7
1379582_a_at	AA998516	Cyclin A2	Ccna2
1371150_at	X75207	Cyclin D1	Ccnd1
1374139_at	BG671589	Cerebellar degeneration-related 2	Cdr2

1376193_at	AA819658	Kohjirin	Chrdl1
1384068_at	BI295150	Cytoskeleton associated protein 2 (predicted)	Ckap2_predicted
1377765_at	AA848723	Chloride intracellular channel 4	Clic4
1384211_at	BM388456	Procollagen, type XI, alpha 1	Col11a1
1387854_at	BI282748	Procollagen, type I, alpha 2	Col1a2
1373245_at	BE111752	Procollagen, type IV, alpha 1	Col4a1
1370895_at	AI179399	Procollagen, type V, alpha 2	Col5a2
1370269_at	X00469	Cytochrome P450, family 1, subfamily a, polypeptide 1	Cyp1a1
1368990_at	NM_012940	Cytochrome P450, family 1, subfamily b, polypeptide 1	Cyp1b1
1369590_a_at	NM_024134	DNA-damage inducible transcript 3	Ddit3
1389533_at	AA944398	Fibulin 2	Fbln2
1374726_at	AI411941	Fibronectin type III domain containing 1	Fndc1
1371331_at	BG665037	Follistatin-like 1	Fstl1
1379440_at	AW144239	Follistatin-like 3	Fstl3
1368947_at	NM_024127	Growth arrest and DNA-damage-inducible 45 alpha	Gadd45a
1372273_at	AA944212	Glycophorin C (Gerbich blood group)	Gypc
1387273_at	NM_013037	Interleukin 1 receptor-like 1	Il1rl1
1376845_at	AA819034	Putative ISG12(b) protein	Isg12(b)
1387144_at	NM_030994	Integrin alpha 1	Itga1
1372870_at	BM391302	KDEL (Lys-Asp-Glu-Leu) endoplasmic reticulum protein retention receptor 3 (predicted)	Kdelr3_predicted
1372478_at	AI137605	Similar to chemokine-like factor super family 7	LOC501065
1378094_at	BM389654	Similar to pleckstrin homology-like domain, family B, member 2	LOC685611
1384231_at	BE108276	Similar to Shc SH2-domain binding protein 1	LOC687121
1368171_at	NM_017061	Lysyl oxidase	Lox
1372006_at	BM391274	Lysyl oxidase-like 2 (predicted)	Loxl2_predicted
1388102_at	U66322	Leukotriene B4 12-hydroxydehydrogenase	Ltb4dh
1367912_at	NM_021587	Latent transforming growth factor beta binding protein 1	Ltbp1
1368448_at	NM_021586	Latent transforming growth factor beta binding protein 2	Ltbp2
1390585_at	AI169829	Mannan-binding lectin serine peptidase 1	Masp1
1376055_at	AA859768	Minichromosome maintenance deficient 5, cell division cycle 46 (S. cerevisiae) (predicted)	Mcm5_predicted
1371074_a_at	U17565	Minichromosome maintenance deficient 6 (MIS5 homolog, S. pombe) (S. cerevisiae)	Mcm6
1374775_at	AI714002	Antigen identified by monoclonal antibody Ki-67 (predicted)	Mki67_predicted
1370854_at	AA799423	Nexilin	Nexn
1372559_at	AI103527	Ng23 protein	Ng23
1387454_at	NM_022242	Niban protein	Niban
1388618_at	BM389302	Nidogen 2	Nid2
1371052_at	AA859752	Noggin	Nog
1388340_at	BF281153	NS5A (hepatitis C virus) transactivated protein 9	Ns5atp9
1368547_at	NM_130402	Osteoclast inhibitory lectin	Ocil
1393129_at	AI711403	Procollagen-proline, 2-oxoglutarate 4-dioxygenase (proline 4-hydroxylase), alpha polypeptide III	P4ha3
1367949_at	NM_017139	Proenkephalin 1	Penk1
1385182_at	BG371843	Plakophilin 1 (predicted)	Pkp1_predicted
1388539_at	BE113268	Plakophilin 2	Pkp2
1384558_at	BI276313	Placenta-specific 9 (predicted)	Plac9_predicted

1393982_at	AI070935	Polymerase (DNA directed), epsilon 2 (p59 subunit) (predicted)	Pole2_predicted
1372729_at	AI137406	Protein C receptor, endothelial	Procr
1368259_at	NM_017043	Prostaglandin-endoperoxide synthase 1	Ptgs1
1374284_at	AI227769	Ras association (RalGDS/AF-6) domain family 4	Rassf4
1389107_at	AI008974	Similar to KIAA1749 protein (predicted)	RGD1304623_predicted
1380243_at	BE098614	Similar to CG14803-PA (predicted)	RGD1304693_predicted
1373447_at	BF281350	Similar to HN1-like protein	RGD1305117
1393451_at	BI295149	Similar to RIKEN cDNA 2610510J17	RGD1310953
1371970_at	AA799328	Similar to expressed sequence AW413625 (predicted)	RGD1560913_predicted
1374805_at	AW251849	Similar to hypothetical protein MGC5528 (predicted)	RGD1561749_predicted
1376231_at	BF389244	Similar to Hypothetical UPF0080 protein KIAA0186 (predicted)	RGD1562246_predicted
1375857_at	AW917760	Similar to Myoferlin (Fer-1 like protein 3) (predicted)	RGD1564216_predicted
1373250_at	AI229404	Similar to Anillin (predicted)	RGD1566097_predicted
1377967_at	AI112987	Retroviral integration site 2 (predicted)	Ris2_predicted
1389408_at	BG379338	Ribonucleotide reductase M2	Rrm2
1368519_at	NM_012620	Serine (or cysteine) peptidase inhibitor, clade E, member 1	Serpine1
1388569_at	AI179984	Serine (or cysteine) peptidase inhibitor, clade F, member 1	Serpinf1
1387134_at	NM_053687	Schlafen 3	Slfn3
1393041_at	AW535052	SMC2 structural maintenance of chromosomes 2-like 1 (yeast) (predicted)	Smc2l1_predicted
1373026_at	BI303598	Spindle pole body component 24 homolog (S. cerevisiae) (predicted)	Spbc24_predicted
1390107_at	BG670294	Synaptotagmin-like 2 (predicted)	Sytl2_predicted
1367570_at	NM_031549	Transgelin	Tagln
1389555_at	BM387190	Transcription factor 19	Tcf19
1367859_at	NM_013174	Transforming growth factor, beta 3	Tgfb3
1375951_at	AA818521	Thrombomodulin	Thbd
1374529_at	AI406660	Thrombospondin 1	Thbs1
1372926_at	AI009159	Tissue inhibitor of metalloproteinase 3 (Sorsby fundus dystrophy, pseudoinflammatory)	Timp3
1373401_at	AI176034	Tenascin C	Tnc
1379331_at	AA965084	Tenascin N (predicted)	Tnn_predicted
1368838_at	NM_012678	Tropomyosin 4	Tpm4
1368912_at	M12138	Thyrotropin releasing hormone	Trh
1370694_at	AB020967	Tribbles homolog 3 (Drosophila)	Trib3
1372639_at	AA800245	Tripartite motif-containing 54	Trim54
1379448_at	BE110883	Ttk protein kinase (predicted)	Ttk_predicted
1384506_at	H33706	Unc-5 homolog C (C. elegans)	Unc5c
1368463_at	NM_053653	Vascular endothelial growth factor C	Vegfc
1368359_a_at	NM_030997	VGF nerve growth factor inducible	Vgf
1369484_at	NM_031590	WNT1 inducible signaling pathway protein 2	Wisp2

3.2

Calcium control of gene regulation in rat hippocampal neuronal cultures

*__Pegoraro S__, *Pinato G, Ruaro ME, Torre V

* These authors equally contributed to this work and their names are in alphabetical order

Submitted to the Journal of Cellular Physiology

Calcium control of gene regulation in rat hippocampal neuronal cultures

Silvia Pegoraro[1‡], Giulietta Pinato[1‡], Maria Elisabetta Ruaro[1] and Vincent Torre[1,2,]*

[1]International School for Advanced Studies, Trieste, Italy
[2]IIT Italian Institute of Technology

[‡] These authors equally contributed to this work and their names are in alphabetical order

Corresponding author: Vincent Torre
Scuola Superiore di Studi Avanzati (SISSA)
Area Science Park, Edificio Q1
SS 14 Km 163.5
34012 Basovizza, Trieste, Italy
Phone: +39-040-3756513
Fax: +39-040-3756502
Email: torre@sissa.it

Running title: Calcium and gene activation

Keywords:
- **Gene profiling**
- **Neuronal plasticity**
- **Voltage gated calcium channels**
- **NMDA receptors**
- **Microarray**

Number of figures: 11
Number of tables: 2
Grant information:
Contract grant sponsor: European Community; Contract grant number: 012788 (FP6-STREP, NEST).

Contract grant sponsor: Friuli Venezia Giulia; Contract grant number: GRAND FVG Grant
Contract grant sponsor: Italian Government; Contract grant number: FIRB grant D.M.31/03/05

Abstract:

Blockage of GABA-A receptors in hippocampal neuronal cultures by gabazine treatment (GabT) triggers synchronous bursts of spikes initiating neuronal plasticity partly mediated by changes of gene expression. By using specific blockers, we have investigated which sources of Ca^{2+} entry primarily control changes of gene expression. Intracellular Ca^{2+} transients were monitored with Ca^{2+} imaging while recording electrical activity with patch clamp microelectrodes. Concomitant transcription profiles were obtained using Affymetrix oligonucleotide microarray. Blockage of NMDA receptors with 2-amino-5-phosphonovaleric acid (APV) did not reduce significantly somatic Ca^{2+} transients, which, on the contrary, were reduced by selective blockage of L, N and P/Q types voltage gated calcium channels (VGCCs). Therefore, we investigated changes of gene expression in the presence of blockers of NMDA receptors and L, N and P/Q VGCCs. Our results show that: i - among genes upregulated by GabT, there are genes selectively dependent on NMDA activation, genes selectively dependent on L-type VGCCs and genes dependent on the activation of both channels; ii - NMDA receptors play a major role in inducing gene transcription 1.5 hours after GabT, whereas L-type VGCCs become more important 3 hours after GabT; iii - blockage of N and P/Q VGCCs has an effect similar but not identical to blockage of L-type VGCCs.

Introduction

Activity-dependent plasticity is a fundamental property of the nervous system and is at the basis of the formation and consolidation of memory and learning (Bliss and Collingridge, 1993). Neuronal plasticity has a complex phenomenology resulting from multiple biological mechanisms. Local protein trafficking is responsible for rapidly decaying forms of plasticity while gene transcription dependent mechanisms account for more persistent changes (Goelet et al., 1986; Schuman, 1997; Malenka and Nicoll, 1999; Martin et al., 2000; Rao et al., 2006; Raymond, 2007). Neuronal plasticity is initiated by events occurring across the plasma membrane activating signal transduction pathways in the cytoplasm and reaching the nucleus, in which calcium (Ca^{2+}) ions play a major role (Cavazzini et al., 2005). Ca^{2+} entry into the cytoplasm can initiate gene transcription (Bading et al., 1993) through the mitogen-activated protein kinases (MAPKs) cascade and/or the activation of Ca^{2+}/calmodulin-dependent protein kinases (CaMKs) (Dolmetsch et al., 2001).

A very useful model of neuronal plasticity is provided by neuronal cultures where it is possible to study in details how changes of electrical activity initiate neuronal plasticity. It has been shown that periods of intense synchronous electrical activity modify both neuronal firing properties and synaptic efficiency (Abegg et al., 2004; Arnold et al., 2005; Debanne et al., 2006; Remy and Spruston, 2007). Large bursts of spontaneous synchronous spikes can be induced by blockage of GABA-A receptors with application of gabazine or bicuculline (Traub et al., 1993; Arnold et al., 2005). Ca^{2+} ions enter into the cytoplasm mainly through opening of ligand- and voltage-gated Ca^{2+} channels (VGCCs) and by release from internal stores. All neuronal classes of VGCCs have been found and described in hippocampal neurons (Eliot and Johnston, 1994; Avery and Johnston, 1996; Vinet and Sik, 2006; Bloodgood and Sabatini, 2007).

The purpose of the present manuscript is to determine which source of Ca^{2+} entry into cytoplasm controls changes of gene expression initiated by gabazine treatment

(GabT). We have analyzed the contribution of Ca^{2+} entry through NMDA receptors and different types of VGCCs. Changes of gene expression were determined using Affymetrix oligonucleotide microarray in the presence or absence of blockers of NMDA receptors and L, N and P/Q -type VGCCs. Our results show that calcium transients reaching the soma were amplified and conveyed by the activation of L, N and P/Q type Ca^{2+} channels and that blockage of NMDA receptors did not affect significantly Ca^{2+} transients in the soma during GabT, but profoundly reduced changes of gene expression observed 1.5 h after GabT. Changes of gene expression measured 3 h after GabT became more sensitive to blockage of L-type and of N and P/Q type VGCCs. Therefore changes of gene expression induced by GabT depend - in a complex and time related way - on Ca^{2+} entry through NMDA receptors and different types of VGCCs.

Methods

Neuronal culture preparation

Hippocampal neurons from Wistar rats (P0-P2) were prepared as previously described (Ruaro et al., 2005). Cells were plated on polyorhitine/matrigel pre-coated coverslips (Ruaro et al., 2005) at a concentration of 8 x 10^5 cells/cm^2 and maintained in Minimal Essential Medium with Earle's salts (Invitrogen, Carlsbad, CA) supplemented with 5% fetal calf serum, 0.5% D-glucose, 14 mM Hepes, 0.1 mg/ml apo-transferrin, 30 μg/ml insulin, 0.1 μg/ml D-biotin, 1 mM Vit. B12, and 2μg/ml gentamycin. After 48 hours 5 μM cytosine-*β*-D-arabinofuranoside (Ara-C) was added to the culture medium, in order to block glial cell proliferation. Half of the medium was changed twice a week. Neuronal cultures were kept in an incubator providing a controlled level of CO_2 (5%), temperature (37°C) and moisture (95%). In order to induce synchronous electrical activity initiating neuronal plasticity, cultures were treated for 30 min with 20 μM of gabazine (GabT), a specific GABA-A receptor antagonist (Uchida et al., 1996).

Electrophysiological recordings

Dissociated hippocampal neuronal cultures were transferred to a recording chamber, perfused in Ringer's solution (in mM:145 NaCl, 3 KCl, 1.5 CaCl2, 1 MgCl2, 10 Glucose, 10 Hepes, adjusted to pH 7.4 with NaOH) and visualized with an upright microscope (Olympus BX50WI) with differential interference contrast (DIC) optics. Patch-clamp recordings were performed with an Axoclamp 2-B amplifier (Axon Instruments, Foster City, CA). Experiments were performed at 37° C. Electrodes were pulled (Narishige, Japan) and filled with an intracellular solution containing in mM: 120 K-gluconate, 10 Na-gluconate, 10 Hepes, 10 Na-phosphocreatine, 4 MgATP, 4 NaCl, 2 Na2ATP and 0.3 Na3GTP (adjusted to pH 7.4 with KOH): in these conditions the electrode resistance was 10-15 MΩ. The data were digitized at 20 kHz (Digidata 1200, Axon Instruments) and analyzed using pClamp9 software

(Axon Instruments). Values of membrane potentials were not corrected for the effects of liquid junction potential during seal formation.

Imaging

Calcium imaging experiments were performed using water immersion optics (40x/0.80 NA) a mirror unit (U-MSWB: exciter filter BP 420-480 nm, barrier BA >515 nm and dichroic mirror 500 nm) and a halogen lamp (Olympus, Japan) for illumination. The fluorescence emitted light was collected with a fast CCD camera (Neuro CCD-SM, RedShirtImaging). Images were taken at 40 Hz with a spatial resolution of 80x80 pixels. Experiments were analyzed with Neuroplex Software, Igor (Wavemetrics, Lake Oswego, OR) and Matlab (Mathworks, Natick, MA). Cultures were loaded with cell permeant calcium dye Oregon Green 488 BAPTA1-AM, (Molecular Probes O-6807). 4mM stock solution of this calcium dye was prepared in Pluronic F-127 20% solution in DMSO (Molecular Probes P3000MP). Cultures were incubated with a final concentration of 1.5 μM of the calcium dye for 30 min. After incubation the cultures were washed and then transferred under the microscope for imaging. In order to load single cells for electrophysiology and simultaneous calcium imaging 150 μM Oregon Green 488 BAPTA1, cell impermeant (Molecular Probes O-6806) was included in the patch pipette solution. A period of at least 20 min after reaching the whole cell configuration was necessary to reach a good fluorescent signal from the dendrites. Calcium imaging data are expressed as DF/F values. The collected fluorescence F(t) was first dark frame subtracted to minimize the noise, then it was averaged over the regions of interest (ROIs). F0, the baseline fluorescence, was calculated as the time average of the fluorescence during the absence of any signal for each ROI. Finally (DF/F)(t) = (F(t)-F0)/F0 was calculated.

Pharmacology

The following chemicals were used: 2-amino-5-phosphonovalerate (APV, Sigma-Aldrich, St Louis, MO), gabazine (SR95531, Tocris, Bristol, UK), ω-conotoxin MVIIC (Tocris), kurtoxin (Sigma-Aldrich), SNX-482 (Sigma-Aldrich), different dihydropyridines (nimodipine, nifedipine, nitrendipine, Tocris). After completion of the measurements, chemicals were washed out by 3 medium replacements, and the original extracellular medium was restored.

RNA extraction andoligonucleotide microarray analysis

Cultures were incubated with APV or other blockers of VGCCs for 10 minutes before gabazine addition. In all these experiments the amplitude of somatic Ca^{2+} transients was monitored by loading cultures with the membrane permeable calcium dye Oregon Green 488-BAPTA-1-AM and by measuring the optical signals. After 30 minutes, gabazine was removed, but not the tested blocker. mRNA was harvested from these cultures either 1.5 or 3 hours after GabT. The total RNA was extracted using TRIzol reagent (Sigma) according to the manufacturer's instructions followed by a DNase I (Invitrogen) treatment to remove any genomic DNA contamination. The total RNA was further purified using RNeasy Mini Kit Column (Qiagen, Valencia, CA) and subsequently quantified by ND-1000 Nanodrop spectrophotometer (Agilent Technologies, Palo Alto, CA). At each time point, 3 biological replicates were collected and Standard Affymetrix protocols were applied for amplification and hybridization. Gene profiling was carried out with the Affymetrix RAT230_2 GeneChip containing 31099 probes, corresponding to 14181 probes with a gene symbol. Low level analysis was performed using an RMA (Robust Multi-array Average) algorithm (Irizarry et al., 2003) directly on the scanned images. Because of the high dimensionality we removed those probe sets labeled as ambiguous and those without any gene symbol. In each replica (R_i i=1-3) four cultures were considered: an untreated culture (C_i), a culture treated with gabazine (G_i), a culture treated with gabazine and APV ($GAPV_i$), a culture treated with

gabazine and nifedipine ($GNif_i$). Data were analyzed by considering changes of gene expression in each replica against its own untreated control, i.e. G_i/C_i , $GAPV_i/C_i$ and $GNif_i/C_i$.

Quantitative RT-PCR

RNA (250ng) was reverse-transcribed using SuperScript II reverse transcriptase and random hexamer (Invitrogen). qRT-PCR was performed using iQ SYBR Green supermix (Bio-Rad, Munich, Germany) and the iQ5 LightCycler (Bio-Rad). Gene specific primers were designed using Beacon Designer (Premier Biosoft, Palo Alto, CA). The thermal cycling conditions comprised 3 min at 95°C, and 40 cycles of 10 s for denaturation at 95°C and 45 s for annealing and extension at 58°C. The expression level of the target mRNA was normalized to the relative ratio of the expression of Gapdh mRNA. The forwarded primer for *Gapdh* was -CAAGTTCAACGGCACAGTCAAGG-3', reverse primer was 5'-ACATACTCAGCACCAGCATCACC-3'. Fold changes calculations were made between treated and untreated samples at each time point using the $2^{-\Delta\Delta CT}$ method. The forward primer for *Egr2* was 5'-CTGCCTGACAGCCTCTACCC-3', the reverse primer was 5'-ATGCCATCTCCAGCCACTCC-3'; the forward primer for *Nr4a1* was 5'-GGTAGTGTGCGAGAAGGATTGC-3', the reverse primer was 5'-GGCTGGTTGCTGGTGTTCC-3'; the forward primer for *Arc* was 5'-AGACTTCGGCTCCATGACTCAG-3', the reverse primer was 5'-GGGACGGTGCTGGTGCTG-3'; the forward primer for *Homer1a* was 5'-GTGTCCACAGAAGCCAGAGAGGG-3', the reverse primer was 5'-CTTGTAGAGGACCCAGCTTCAGT-3'; the forward primer for *Bdnf* was 5'-CGATTAGGTGGCTTCATAGGAGAC-3', the reverse primer was 5'-GAAACAGAACGAACAGAAACAGAGG-3'; the forward primer for *Nr4a3* was 5'-TCGGGATGGTGAAGGAAGTTGTG-3', the reverse primer was 5'-GTTGTAGTGGGCTCTTTGGTTTGG-3'.

Results

After pharmacological blockage of GABA-A receptors, spontaneous bursts of synchronous spikes appear in dissociated neuronal cultures from rat hippocampus (Arnold et al., 2005; Mazzoni et al., 2007). Even a small number of these bursts can initiate neuronal plasticity (Debanne et al., 2006; Remy and Spruston, 2007). Gabazine exposure lasting 5-15 minutes (Arnold et al., 2005), triggers significant changes of gene expression (Zhang et al., 2007, Broccard, personal comunication). In order to link specific sources of calcium influx to changes of gene expression, we have tested the effect of VGCC blockers and NMDA receptor antagonists on Ca^{2+} entry during bursts and concomitant changes of gene expression. Changes of intracellular Ca^{2+} were analyzed by imaging neuronal cultures stained with the membrane permeable calcium dye Oregon Green 488-BAPTA-1-AM and/or by imaging single neurons loaded with the cell impermeable calcium dye Oregon Green 488-BAPTA-1. The fluorescence F emitted by these dyes is an indicator of the intracellular Ca^{2+} and changes of F (DF) report Ca^{2+} transients, quantified by the relative fluorescence change DF/F. By using membrane permeable dyes, Ca^{2+} transients occurring in the soma of several dozen of neurons were simultaneously measured. By imaging single neurons, changes of intracellular Ca^{2+} could be measured both in the soma and in the dendrites and compared with the intracellular electrical activity recorded with a patch pipette. Changes of gene expression were measured with DNA microarray (Affymetrix RAT230_2 GeneChip) and with qRT-PCR from the same neuronal cultures where Ca^{2+} transients were recorded.

Calcium signals from hippocampal neurons

When neuronal cultures were stained with the membrane permeable Ca^{2+} dye, the soma of several dozens of neurons could be visualized simultaneously (fig.1A). In control conditions, spontaneously occurring Ca^{2+} transients were observed in the soma (fig.1B). These Ca^{2+} transients usually occurred randomly in different neurons,

but a partial synchronization was observed in some cultures (15/107). The average amplitude DF/F of spontaneous Ca^{2+} events in control conditions was 0.069 ± 0.035 (range: 0.006-0.24, number of cells: 100, from 6 representative cultures). Addition of 20 μM gabazine to the extracellular medium caused the appearance of large Ca^{2+} transients occurring synchronously in the stained neurons (fig.1C). These Ca^{2+} transients had an average amplitude of 0.33 ± 0.15 (range: 0.10-0.68) which lasted for some seconds (average half height duration: 3.26 ± 1.48 s, range: 0.85-8.6 s) and occurred almost periodically (average frequency: 0.075 ± 0.053 Hz range: 0.02-0.16 Hz). These Ca^{2+} transients were associated to burst of spikes caused by a prolonged depolarization of the membrane potential, as shown from the simultaneous intracellular recordings reported in fig.4-7, and persisted for several hours after termination of GabT.

(Fig.1 near here)

In order to dissect the origin of these Ca^{2+} transients (fig.1C), the action of specific blockers of VGCCs and NMDA receptors was tested (fig.1D). Optical signals from the soma of several tens of neurons were averaged, so to obtain an estimate of the effect of different blockers averaged over several tens of neurons (fig.1D bottom traces).

Blockers of L-type VGCCs significantly reduced somatic Ca^{2+} transients: nifedipine (20 μM, fig.1D first column) reduced the amplitude of DF/F by 69 ± 23 % from its control value (data from 77 cells, from 5 cultures, fig.2A). Nifedipine increased significantly also the burst frequency from 0.05 ± 0.03 Hz to 0.13 ± 0.05 Hz, probably by interfering with mechanisms controlling synaptic release (Hirasawa and Pittman, 2003; Piriz et al., 2003). Therefore the effect of two other dihydropiridines - nitrendipine and nimodipine - known to block L-type VGCCs without interfering with synaptic release were tested. Nitrendipine and nimodipine decreased somatic

Ca^{2+} transients by 87 ±10 % (data from 45 cells, from three cultures) and 40 ± 9 % (data from 38 cells, from three cultures) respectively. Nitrendipine reduced the burst frequency from 0.14 to 0.08 Hz, while nimodipine did not modify the burst occurrence. The differences in affinity that may exist between the drugs, the distribution of the channels (pre- and post-synaptic) and the side effects of some of the drugs could be explain the heterogeneity of our results. Blockers of T and R-type VGCCs were also tested. 100 μM $NiCl_2$ (fig.1D, second column), known to block T-type and some R-type VGCCs (Tottene et al., 1996; Huguenard, 1996; Pinato and Midtgaard, 2003; Metz et al., 2005) reduced by 21 ± 12 % (data from 71 cells taken from 6 cultures, fig.2B) the amplitude of Ca^{2+} transients and increased the burst rate from 0.10 ± 0.04 Hz to 0.15 ± 0.02 Hz. 300 nM of kurtoxin, a blocker of T-type VGGC (Sidach and Mintz, 2002) reduced by 20 ± 9 % the amplitude of Ca^{2+} transients and increased the burst rate from 0.08 to 0.26 Hz (data from 10 cells taken from one culture, data not shown). 500 nM SNX-482, a selective antagonist of recombinant Cav2.3 (Newcomb et al., 1998), which inhibits some native R-type channels (Totenne et al., 2000) reduced by 13 ± 9 % (data from 30 cells taken from two cultures) the amplitude of Ca^{2+} transients (fig.1D, third column) without affecting the burst occurrence. The blocker of N and P/Q types Ca^{2+} channels, ω-conotoxinMVIIC (Losonczy and Magee, 2006) reduced the amplitude of calcium transients by 44 ± 25 % (data from 43 cells, from 4 cultures, fig.1D fourth column and fig.2C) from the control value without affecting the burst frequency.

The effect of blockage of NMDA receptors with APV was rather variable (Fig.2E). We analyzed the effect of APV in 18 neuronal cultures by monitoring Ca^{2+} transients with membrane permeable (10 cultures) and impermeable (8 cultures) Ca^{2+} dye. In 4 of these cultures, 20 μM APV completely blocked both synchronous bursts and Ca^{2+} transients. In 2 of these cultures the number of neurons present in 1 mm^2 was counted and the average density of neurons was 500-700 cells/mm^2, i.e. 2-3 times less than in

our usual cultures (1500-2000 cells/mm^2, Bonifazi et al., 2005). Results obtained in these sparse neuronal cultures were not included in the statistical analysis shown in Fig.2. In the 8 cultures treated with the cell permeable Ca^{2+} dye APV decreased the duration of the late phase of synchronous bursts as previously reported by Traub and colleagues (1993). APV decreased the half-duration of somatic Ca^{2+} transients by 46 ± 17% of control ($P<0.01$, data from 132 cells 8 cultures), but did not significantly affect either their amplitude ($P>0.4$, fig.2D) or the burst frequency ($P>0.1$). As shown by the distribution of fractional blockage in Fig.2D, in many neurons the amplitude of the peak of somatic Ca^{2+} transients was not significantly affected by the presence of APV, but the positive and negative tails in the histogram indicate the existence of two small populations where the amplitude of Ca^{2+} transients was either reduced (left panel of Fig.2E) or increased (middle and right panels of Fig.2E). Simultaneous electrical and optical recordings (see Fig.2E) showed that a reduction of the amplitude of peak Ca^{2+} transients correlated with a reduction in the number of spikes occurring during the burst, whereas a rise in the instantaneous firing rate during the early phase of the burst caused an increase of peak Ca^{2+} transients. The variability of the effect of APV was caused by the combination of neuronal diversity and differences in the degree of connectivity of the cultures under investigation.

In order to elucidate whether these results could be due to an insufficient blockage of NMDA receptors, the effect of increasing APV concentration up to 500 μM was then tested (Hardingham et al., 2001). Ca^{2+} transients in the soma persisted in the presence of 50, 100 and 500 μM APV and the concomitant presence of large synchronous bursts of electrical activity was verified by simultaneously monitoring electrophysiological signals and Ca^{2+} transients. In the presence of 500 μM APV, however, Ca^{2+} transients became less frequent.

(Fig.2 near here)

These results were obtained with the calcium dye Oregon Green 488-BAPTA-1 which has a K_D for Ca^{2+} ions of 170 nM. Given the high affinity of this dye for Ca^{2+}, i.e. a low value of K_D, in the presence of a massive increase of cytosolic Ca^{2+} induced by gabazine exposure, the dye could become saturated and as a consequence the measurements would not reveal a decrease in Ca^{2+} entry. In order to exclude this possibility, the experiments were repeated with the calcium dye Oregon green 488-BAPTA-2 (OGB-2-AM) which has a higher K_D value of 580 nM. Fig. 3 shows the effect of nifedipine (fig.3A) and APV (fig.3B) on DF/F obtained with the dye OGB-2-AM. When cultures were stained with this dye the signal to noise ratio was low and in order to detect an appreciable optical signal it was necessary to average the fluorescence from many cells. Nifedipine reduced DF/F by 22 ± 8 % (48 cells, 3 cultures), while APV had no significant effect (P>0.2) (52 cells, 3 cultures).

(Fig.3 near here)

Somatic calcium transients during spikes evoked by current injection

When the membrane permeable Ca^{2+} dye is used, the entire neuronal culture is stained, and therefore it is possible to measure the simultaneous Ca^{2+} transients from the soma of several neurons. However, but it is not possible to reliably resolve optical signals originating from dendrites and to make a precise correlation between fluorescence measurements and electrical recordings. Single cell imaging obtained by staining single neurons with cell impermeable Ca^{2+} dye during patch clamp recordings allows to compare the time course of Ca^{2+} transients in different compartments of the cells with changes of membrane voltage recorded from the soma. In particular, with this technique it is possible to measure the contribution of different VGCCs by stimulating the cell to fire a fixed number of spikes with a current step - before and after the application of a given pharmacological blocker (fig.4) - and by recording simultaneous Ca^{2+} transients in these two conditions. In fact, since VGCCs are known to be implicated in exocytosis (Gasparini et al., 2001;

Carbone et al., 2006), the decreased somatic Ca^{2+} transients associated to bursts observed in previous experiments (fig. 1D) could be caused also by a reduction of the underlying electrical activity following a decrease of synaptic efficacy.

(Fig.4 near here)

As shown in fig.4, nifedipine (A), $NiCl_2$ (B) and ω-conotoxinMVIIC (C) reduced somatic Ca^{2+} transients by 43± 26 % (3 neurons), 56± 30 % (3 neurons) and 43± 19 % (2 neurons) respectively. Complete blockage of Ca^{2+} transients in the soma was observed by perfusing the neuronal culture with $NiCl_2$, blocking T and R -type VGCCs and $CdCl_2$ blocking L, N and P/Q types VGCCs (fig. 4D). However this treatment did not influence the ability of the neurons to fire spikes.

Calcium transients in the soma and dendrites

Patch clamp voltage recordings during GabT (black trace in figs. 2A and 5A) showed that bursts had a complex structure, composed of several spikes with different height and duration often superimposed on a plateau potential lasting for some seconds. During these bursts, large Ca^{2+} transients were recorded in the soma (see red traces in fig. 5A). Several types of VGCCs as well as other intrinsic conductances are activated during these depolarizations, as observed both in hippocampal and cortical neurons (Straub et al., 1990; Timofeev et al., 2004; Schiller, 2004). Ca^{2+} transients in dendrites (see green trace in fig.5A) could be as large as those recorded in the soma, but usually had a shorter duration, reflecting different mechanisms of intracellular Ca^{2+} control, i.e. extrusion, compartmentalization and buffering in the periphery with respect to the somatic compartment (Markram et al., 1995). In several neurons, optical signals had a larger amplitude in dendrites (green trace in fig. 5A) where the peak was reached in about 100 ms whereas somatic Ca^{2+} peak occurred with a delay of 200-400 ms (red trace in fig.5A) and could be detected for several seconds when Ca^{2+} transients in the dendrites had already extinguished. Optical signals associated

to somatic Ca^{2+} transients were less noisy because the larger volume underlying each pixel contributed to an increased signal to noise ratio. It was often possible to detect very clearly step-like fluorescence increase associated to the generation of individual spikes (see red trace in fig5A).

(Fig. 5 near here)

When 20 μM nifedipine was added to the extracellular medium, bursts lasted for a shorter time. A decrease in the peak of Ca^{2+} was observed in the soma, while in dendrites the peak reached almost the same value as in control but the duration of Ca^{2+} transients was shorter both in the dendrites and in the soma (fig.5 A and C). Ionic currents implicated in this complex pattern of activity were not investigated in details, but our experiments show that the activation of L-type VGCCs plays a major role during the long lasting potentials underlying GabT induced bursts. Moreover, as shown by the color coded map of Ca^{2+} transients (fig.5B and D), nifedipine reduced more powerfully Ca^{2+} transients in the soma than in the dendrites, showing that activation of L-type VGCCs has a major role in the accumulation of calcium in the soma.

(Fig.6 near here)

We then investigated the effect of blockage of N and P/Q types VGCCs on Ca^{2+} transients in different cellular compartments (fig.6). In the presence of 1 μM ω-conotoxinMVIIC, the amplitude of Ca^{2+} transients in the dendrites was not significantly affected (compare the initial component of green traces in fig.6A and C) whereas somatic Ca^{2+} transients decreased at a much larger extent (compare red traces in fig.6A and C). The differential effect of ω-conotoxinMVIIC on somatic and dendritic Ca^{2+} transients is also evident in the color images of fig.6 B and D. Treatment with ω-conotoxinMVIIC did not alter significantly the long lasting

depolarization underlying the bursts, as it was observed in the presence of nifedipine, suggesting that N and P/Q -type VGCCs, did not play a major role in sustaining bursts (fig.5 A and C).

As shown above (fig.1D), experiments with cell permeable Ca^{2+} dye, demonstrated that NMDA receptors did not contribute significantly to Ca^{2+} transients in the soma during bursts. Since NMDA receptors are normally activated in the dendrites during glutamatergic transmission (Kovalchuk et al., 2000), the contribution of calcium through NMDA receptors was investigated in distal compartments. Fig.7 illustrates an experiment in which NMDA receptors were blocked by the addition of 20 μM APV to the extracellular medium. Electrophysiological recordings (fig.7 A and C, black traces) show that APV reduced the excitatory events present in the late part of the bursts, but either the somatic or the dendritic Ca^{2+} transients did not reduce them.

(Fig.7 near here)

Changes of gene expression induced by gabazine and regulation by Ca^{2+} entry through NMDA receptors and L-type VGCCs

The analysis presented in the previous sections showed that the contribution to somatic Ca^{2+} transients during gabazine was predominantly due to L, N and P/Q -type VGCCs, and, to a minor extent, to Ca^{2+} entry through NMDA receptors. NMDA receptors and L-type VGCCs are key elements in activity dependent changes of gene expression in neurons (Deisseroth et al., 2003; Xiang et al., 2007). In order to elucidate the role of changes of cytosolic Ca^{2+} in the communication between synapse and nucleus in our model (Zhang et al., 2007, Broccard, personal comunication), we compared the effect of blockers of NMDA receptors and of L-type VGCCs on a transcriptional profile after GabT by microarray analyses.

In order to check whether the network activity was preserved after the pharmacological treatments, in all the microarray experiments the amplitude of

somatic Ca^{2+} transients was monitored by imaging the cultures loaded with the membrane permeable calcium dye Oregon Green 488-BAPTA-1-AM (fig.8 A-C). Changes of gene expression were assessed at 1.5 and 3 hours after GabT, using Affymetrix GeneChip Rat Expression 230 2.0, that allows the simultaneous detection of 31099 probes set. Changes of gene expression were analyzed in three replicas. In each replica four cultures derived from the same neonatal rats were considered: an untreated culture (C_i), a culture treated with gabazine (G_i), a culture treated with gabazine and APV ($GAPV_i$) and a culture treated with gabazine and nifedipine ($GNif_i$). Changes of gene expression were evaluated comparing each replica against its own untreated control. Genes with ratio value greater than 1.5 were considered as up-regulated, while genes with ratio value lower than 1.5 were considered as down-regulated. The number of up-regulated genes 1.5 hours after GabT in the three replicas were 1070, 685 and 710 and those down-regulated were 1355, 331 and 360 respectively. 3 hours after GabT the number of up-regulated genes were 451, 351 and 571 and those down-regulated were 394, 231 and 154 in the three replicas respectively.

(Fig.8 near here)

Genes up and down-regulated in the three replicas were - to some extent - different and therefore, for further analysis, only those genes that were up-regulated in at least two replicas were considered: on the basis of this criterion, genes up-regulated and down-regulated 1.5 hours after GabT were reduced to 83 and 20 respectively and 3 hours after GabT to 68 and 48 respectively. The expression profile of these genes was then analyzed when the stimulation with gabazine was done in the presence of APV or nifedipine, to evaluate the contribution of the NMDA receptors and L-type VGCCs to their regulation (fig.8 D-G). With this criterion the genes regulated by gabazine were classified in four groups. The first group represented the genes up-regulated (or down-regulated) by GabT in the presence of nifedipine but not in the

presence of APV. These genes were presumably controlled primarily by activation of NMDA receptors (GenesNMDA, indicated in white in the pie charts of fig.8). The second group included genes which were up-regulated (or down-regulated) by GabT and in the presence of APV but not in the presence of nifedipine, therefore presumably controlled by Ca^{2+} entry through L-type VGCCs (GenesL, indicated in black in the pie charts of fig.8). The third group of genes was composed of those up-regulated (or down-regulated) genes either in the presence of blockers of NMDA receptors or of L-type VGCCs. This group of genes could be activated by NMDA receptors or by L-type VGCCs or by a different pathway (GenesNMDAorL indicated in pale grey in the pie charts of fig.8). The fourth and final group of genes was composed of those genes up-regulated by gabazine, but neither in the presence of APV nor in nifedipine (GenesNMDAandL indicated in dark grey in the pie charts of fig.8). The regulation of these genes needs Ca^{2+} entry through both NMDA receptors and L-type VGCCs.

Among the 83 up-regulated genes taken 1.5 hours after GabT, 71 (85%) were blocked by APV. Of these genes 45 (54%) were controlled only by NMDA receptor, since they remained up-regulated in the presence of nifedipine. At this time point, up-regulation of genes was poorly dependent on blockage of L-type VGCCs. In fact 28 (33%) genes were dependent on Ca^{2+} entry through L-type VGCCs, but only 2 of these genes (2.4%) were blocked selectively by nifedipine. A different behavior, however, was observed at longer time intervals: 3 hours after GabT 36 over 68 genes up-regulated by gabazine (53%), were blocked by APV, and 41 (60.5%) by nifedipine. In particular the up-regulation of 22 (32.4%) genes was blocked only by APV and 27 (40%) genes only by nifedipine. So 3 hours after GabT the proportion of genes blocked specifically by nifedipine increased from 2.4% to 40% and that of genes controlled only by NMDA slightly decreased from 54% to 32.4%. At both time points there was a considerable proportion of up-regulated genes that were blocked both by APV and by nifedipine, 31% and 20.4% at 1.5 and 3 hours after GabT

respectively. There were also genes whose up-regulation was affected neither by APV nor by nifedipine at 1.5 (12%) and 3 (7.5%) hours after GabT. Therefore, the regulation of the majority of the genes induced by GabT was controlled by Ca^{2+} entry through NMDA receptors and L-type VGCCs. Moreover, NMDA receptors activation is a key event for the up-regulation of genes induced by gabazine after 1.5 hours, whereas, 3 hours after GabT also Ca^{2+} entry through L-type VGCCs becomes significant.

Our results show that NMDA receptors and L-type VGCCs play a less specific role for the down-regulation with respect to up-regulation of genes. In fact, after 1.5 and 3 hours down-regulated GenesNMDA were respectively 20% and 12.5% compared to 54% and 32.4% of up-regulated GenesNMDA. After 3 hours, down-regulated GenesL were 4.2% compared to 40% of up-regulated GenesL.

(Table 1 near here)

As shown in Table 1, at 1.5 hours after, GabT 45/83 genes represented the group defined GenesNMDA. Several transcription factors, such as *Egr4, Fosl2, Nr4a1, Nr4a3, Klf4* and *Klf5* belong to this group, as well as the two effector genes *Homer1* and *Arc*. The group of GenesNMDAandL included 23 genes, among which we found synapsin II (*Syn2*) and the beta 4 subunit of voltage dependent Ca^{2+} channels (*Cacnb4*), two genes involved in synaptic function. *Serpinb2, Errfi1, Bdnf* and the transcription factors *Nr4a2* and *Egr2* belonged to the group called GenesNMDAorL. Only two genes, with an unknown function, were classified as GenesL.

(Table 2 near here)

Seventeen genes were up-regulated after GabT after 1.5 and 3 hours. Among these genes *Dusp1, Arc, Arf4l_predicted, Egr4, Homer1 (Ania-3), Nr4a1* and *Ptgs2* were classified as GenesNMDA at both time points. In contrast, *Egr2, Nr4a2* and

Homer1a were classified as GenesNMDAandL after 1.5 hours and GenesNMDA after 3 hours. These results suggest possible modifications in the signalling pathway responsible for the regulation of *Egr2, Nr4a2* and *Homer1a* between 1.5 and 3 hours.

The gene expression analysis shown in fig.8 and reported in Table 1 and 2 was obtained from neuronal cultures loaded with the membrane permeable Ca^{2+} dye, which - to some extent - acts also as a Ca^{2+} buffer. Therefore, we verified whether the presence of the dye could affected the results of our experiments on gene expression. Fig.9 compares the mRNA level of *Nr4a1* measured with qRT-PCR in cultures loaded with Ca^{2+} dye Oregon Green 488-BAPTA-1-AM (black bars) with that in unloaded cultures (white bars). The presence of the Ca^{2+} dye does not alter significantly (ANOVA $p>0.5$) either up-regulation induced by GabT or that observed during the simultaneous exposure to APV or nifedipine. The same results were obtained with all the other genes tested with qRT-PCR (data not shown).

(Fig.9 near here)

The up-regulation of a group of selected genes 1.5 hours after GabT, and the effect of APV and nifedipine on their induction was also verified with qRT-PCR (fig.10 A-B). These genes, *Arc, Bdnf, Homer1a, Nr4a1, Nr4a3* and *Egr2,* were selected because of their known involvement in synaptic plasticity. From microarray analysis *Nr4a1, Nr4a3* and *Arc* resulted to belong to the group GenesNMDA, while *Bdnf, Homer1a* and *Egr2* to the group GenesNMDAorL. As shown in fig.10 A, 20 μM APV reduced the up-regulation of *Nr4a1, Nr4a3* (t test $p<0.05$) and *Arc* by at least 50% of the induction in gabazine alone, in contrast, nifedipine did not alter their regulation. For *Nr4a1* and *Arc*, qRT-PCR detected a slight up-regulation in the cultures treated with APV in respect to the control that was not observed with microarray. This difference can be ascribed to the sensitivities of the two techniques used to assay gene expression changes. In fact, it is known that microarray experiments underestimate

the fold-changes in gene expression compared to qRT-PCR (Irizarry et al., 2003). However, for these genes, qRT-PCR confirmed the same trend obtained in microarray experiments. From the results obtained during Affymetrix experiments the up-regulation of *Bdnf, Egr2* and *Homer1a* was not affected by either APV or nifedipine, and with qRT-PCR we confirm these results. As shown in fig.10 B there were not significant differences (t test $p>0.05$) between the up-regulation after GabT with or without the addiction of APV or nifedipine.

(Fig. 10 near here)

Comparison of the effect of blockage of N and P/Q-type VGCCs and L-type VGCCs on changes of gene expression induced by Gabazine

As shown in figs 1 and 2, blockage of L-type VGCCs with nifedipine and of N and P/Q type VGCCs channels with ω-conotoxinMVIIC significantly reduce the amplitude of somatic Ca^{2+} transients. If the intracellular signal relevant for the Ca^{2+}-dependent gene transcription is the elevation of the concentration of the somatic free Ca^{2+}, then blockage of L-type VGCCs and of N and P/Q type VGCCs should have similar effects on gene transcription. In contrast, if activation of L-type VGCCs is necessary, because of their association with specific signalling pathways (Dolmetsch et al., 2001) blockage of N and P/Q type VGCCs will not affect significantly gene transcription changes. Therefore, in order to discriminate between these two possible mechanisms, we compared the effect of nifedipine and ω-conotoxinMVIIC on up-regulation of genes observed 3h after GabT, when Ca^{2+} entry through L-type VGCCs becomes more relevant (see previous section). In order to minimize experimental variability, we compared the pattern of gene up-regulation in replicas obtained from neuronal cultures derived from hippocampal neurons obtained from the same rats.

(Fig. 11 near here)

As shown in fig.11A, 65% of genes whose up-regulation was blocked by nifedipine, was also blocked by ω-conotoxinMVIIC. Similarly, 75% of genes whose up-regulation was not blocked by nifedipine, was not blocked by ω-conotoxinMVIIC (fig.11B). Therefore blockage of N and P/Q VGCCs and of L-type VGCCs have similar – but not identical - effects on gene expression induced by GabT.

Discussion

Blockage of GABA-A inhibitory receptors by GabT causes the appearance of synchronous bursts of spikes (Arnold et al., 2005) associated to large Ca^{2+} transients both in the soma and in the dendrites (fig.1, 3, 5-7). GabT in hippocampal cultures (Zhang et al., 2007) initiates also concomitant changes of gene expression, becoming prominent 1-3 hours after GabT. The present manuscript analyzes the origin of the large somatic Ca^{2+} transients and their contribution to changes of gene expression. Somatic Ca^{2+} transients were significantly reduced by blockers of L, N and P/Q -type VGCCs. As shown in figs.1-3 and 7, blockage of NMDA receptors did not modify significantly somatic Ca^{2+} transients. Blockage of NMDA receptors, in contrast, drastically reduced changes of gene expression initiated by GabT. Blockage of L, N and P/Q -type VGCCs significantly decreased Ca^{2+} transients measured in the soma but did not modify in similar way changes of gene expression 1.5 hours after GabT. Blockage of these VGCCs, however, had a more pronounced role on gene expression 3 hours after GabT.

Somatic Ca^{2+} transients in hippocampal neurons

Somatic Ca^{2+} transients associated to spontaneous bursts were reduced with the application of specific blockers of different types of VGCCs. Nifedipine, nitrendipine and nimodipine reduced the amplitude of somatic Ca^{2+} transients by 64±31 %, 87 ±10 % and 40 ± 9 %. Nifedipine reduced by 43 ±26 % Ca^{2+} transients associated to spikes elicited by passing a depolarizing step of current in the soma. ω-conotoxinMVIIC, a blocker of N and P/Q, reduced somatic Ca^{2+} transients associated to spontaneous bursts by 36±21 % and those associated to directly evoked spikes by 43±19 %. Blockage of T and R-type VGCCs with $NiCl_2$ reduced somatic Ca^{2+} transients associated to bursts by 27±8 %. Blockage of T-type and R-type VGCCs with kurtoxin and SNX-482 respectively reduced somatic Ca^{2+} transients by 20±9 % and 13±9 % respectively. These results demonstrate that all major types of VGCCs

are expressed in hippocampal neurons and that changes of somatic Ca^{2+} are mediated primarily by L, N and P/Q types (Christie et al., 1995).

All major types of VGCCs are present in dendritic arborization of CA1 hippocampal pyramidal neurons (Bloodgood and Sabatini, 2007). However, in spines Ca^{2+} transients are primarily controlled by T and R -type VGCCs and, in their parent dendrites, by T type VGCCs. Electrophysiological investigations have demonstrated the existence of T-type VGCCs in hippocampal rat pyramidal neurons (Eliot and Johnston, 1994; Magee and Johnston, 1995; Kavalali et al., 1997) with an increase of their density in distal dendrites. Immunohistochemical studies of the distribution of different isoforms of alpha subunits constituting VGCCs in rat hippocampal neurons have also shown that T and R-types are prominently expressed in the dendrites while L, N and P/Q -types are mainly expressed in the soma or proximal dendrites (Westenbroek et al., 1990; Westenbroek et al., 1992; Vinet and Sik, 2006; McKay et al., 2006). These results suggest that during spontaneous bursts of spikes, Ca^{2+} transients are initiated in spines by the activation of NMDA, and are locally amplified by T and R type VGCCs. Ca^{2+} transients are then conveyed to the soma by the activation of other VGCCs such as L, N and P/Q types VGCCs.

Ca^{2+} dependent changes of gene expression induced by GabT

Somatic Ca^{2+} transients were modified by APV in a variable way: in many neuronal cultures (figs. 1-3 and 7) and in those used for the genomic assays (fig.8), APV did not reduce the amplitude of somatic Ca^{2+}. As shown in fig.8, 9 and 10, APV significantly reduced changes of gene expression 1.5 hours after GabT and also at some extent 3 hours after GabT (fig.8). Several genes, such as Nr4a3 and Homer1a are not up-regulated by GabT in the presence of APV either after 1.5 or 3 hours. However, as shown in fig.8, many genes are up-regulated and down-regulated in a significant way by GabT also in the presence of APV. Therefore, activation of NMDA receptors is not the only pathway by which GabT influences gene expression and different sources of increase of intracellular Ca^{2+} concentration are likely to be

contributed. Our results demonstrate that also Ca^{2+} entry through VGCCs, L, N and P/Q types, contributes to GabT-induced gene expression.
The fraction of GenesNMDA - i.e. genes up-regulated by GabT but not in the presence of APV - was 54% (45/83) 1.5 hours after GabT but this proportion decreased to 32 % (22/68) 3 hours after GabT (fig.8). Similarly, at early times (1.5 hours after GabT) the up-regulation of only two genes (2/83) was blocked specifically by nifedipine. A different behavior, however, was observed for longer time intervals: 3 hours after GabT, 40% (27/68) of up-regulated genes were GenesL. These results suggest that at early times NMDA activation is the major route for gene up-regulation but at later times gene up-regulation mediated by Ca^{2+} entry through L-type VGCCs becomes more significant. As shown in Fig.11, blockage of N and P/Q VGCCs has an effect similar to what observed when L-type VGCCs are blocked.

If activation of NMDA receptors and Ca^{2+} entry through L-type, N and P/Q type VGCCs play a major role for gene up-regulation initiated by GabT, a different behavior seems to occur for gene down-regulation. As shown in fig.8, both APV and nifedipine 3 hours after GabT changed the number of down-regulated genes by less than 20%. Therefore, down-regulation seems to be mediated by signaling pathways different - to some extent - from those controlling up-regulation.

It has been assumed that the elevation of mRNA caused by blockage of inhibitory pathways mediated by GABAergic receptors is primarily mediated by Ca^{2+} dependent signaling pathways (Hardingham et al., 2001; Hardingham and Bading, 2002). Entry of Ca^{2+} ions through NMDA receptors and L-type VGCCs is known to activate the MAPK/ERK signaling pathways (Murphy and Blenis, 2006) in which phosphorylated ERK translocates to the nucleus where it activates transcription. Ca^{2+} ions entering through VGCCs activate different signaling pathways mediated by a variety of Ca^{2+}/calmodulin-dependent protein kinases (CaMKs) (Konur and Ghosh,

2005) leading to the activation of the nuclear CREB transcription factor (Wu et al., 2001; Lonze and Ginty, 2002).

Our results show that blockage of NMDA receptors by APV, consistently modifies changes of gene up-regulation, without a concomitant drastic reduction of the amplitude of somatic Ca^{2+} transients. On the other hand, blockage of L, N and P/Q – type VGCCs also modifies changes of gene expression with concomitant reduction of somatic Ca^{2+} influx. In the first case, Ca^{2+} entering through the NMDA receptors is supposed to act as a second messenger in confined regions at the neuronal periphery, by activating locally signaling pathways and modifying gene transcription (CaMKII, ERK). During neuronal firing, membrane potential repetitively depolarizes, opening VGCCs that cause influx of Ca^{2+} both in the dendrites and in the soma. Ca^{2+} transients in the dendrites and the soma have very specific buffering properties so that the kinetics of Ca^{2+} signaling varies in distinct neuronal compartments. Indeed, somatic Ca^{2+} transients are characterized by a slower decay kinetics that makes them integrators of the global neuronal activity. Moreover the slower kinetics of Ca^{2+} transients could be suitable for Ca^{2+} ions to permeate the nuclear pores (Eder and Bading, 2007). Nuclear Ca^{2+} activates the nuclear CaMKIV with consequent induction of CREB dependent transcription, or can directly bind to the transcriptional repressor DREAM.

Given the ubiquitous role of Ca^{2+} in cell physiology and homeostasis, it is not surprising to see complex interactions between the activation of NMDA receptors and Ca^{2+} ions. It is also possible that NMDA activation modifies intracellular Ca^{2+} stores and that the level of nuclear Ca^{2+} is the result of entry and uptake of this ion occurring through a variety of channels and pumps present in the plasma membrane and in the intracellular compartments.

Acknowledgements

We thank M. Lough for critical reading of the manuscript. This work was supported by the EU projects: NEURO Contract n. 012788 (FP6-STREP, NEST). In addition we need to acknowledge the financial support of a FIRB grant D.M.31/03/05 from the Italian Government and of the GRAND Grant from CIPE/FVG by the Friuli Venezia Giulia region.

Literature Cited

Abegg MH, Savic N, Ehrengruber MU, McKinney RA, and Gahwiler BH. 2004. Epileptiform activity in rat hippocampus strengthens excitatory synapses. J Physiol 554:439-448.

Arnold FJ, Hofmann F, Bengtson CP, Wittmann M, Vanhoutte P, and Bading H. 2005. Microelectrode array recordings of cultured hippocampal networks reveal a simple model for transcription and protein synthesis-dependent plasticity. J Physiol 564:3-19.

Avery RB and Johnston D. 1996. Multiple channel types contribute to the low-voltage-activated calcium current in hippocampal CA3 pyramidal neurons. J Neurosci 16:5567-5582.

Bading H, Ginty DD, and Greenberg ME. 1993. Regulation of gene expression in hippocampal neurons by distinct calcium signaling pathways. Science 260:181-186.

Bliss TV and Collingridge GL. 1993. A synaptic model of memory: long-term potentiation in the hippocampus. Nature 361:31-39.

Bloodgood BL and Sabatini BL. 2007. Ca^{2+} signaling in dendritic spines. Curr Opin Neurobiol 17:345-351.

Bonifazi P, Ruaro ME, and Torre V. 2005. Statistical properties of information processing in neuronal networks. Eur J Neurosci 22:2953-2964.

Carbone E, Marcantoni A, Giancippoli A, Guido D, and Carabelli V. 2006. T-type channels-secretion coupling: evidence for a fast low-threshold exocytosis. Pflugers Arch 453:373-383.

Cavazzini M, Bliss T, and Emptage N. 2005. Ca^{2+} and synaptic plasticity. Cell Calcium 38:355-367.

Christie BR, Eliot LS, Ito K, Miyakawa H, and Johnston D. 1995. Different Ca^{2+} channels in soma and dendrites of hippocampal pyramidal neurons mediate spike-induced Ca^{2+} influx. J Neurophysiol 73:2553-2557.

Debanne D, Thompson SM, and Gahwiler BH. 2006. A brief period of epileptiform activity strengthens excitatory synapses in the rat hippocampus in vitro. Epilepsia 47:247-256.

Deisseroth K, Mermelstein PG, Xia H, and Tsien RW. 2003. Signaling from synapse to nucleus: the logic behind the mechanisms. Curr Opin Neurobiol 13:354-365.

Dolmetsch RE, Pajvani U, Fife K, Spotts JM, and Greenberg ME. 2001. Signaling to the nucleus by an L-type calcium channel-calmodulin complex through the MAP kinase pathway. Science 294:333-339.

Eder A and Bading H. 2007. Calcium signals can freely cross the nuclear envelope in hippocampal neurons: somatic calcium increases generate nuclear calcium transients. BMC Neurosci 8:57.

Eliot LS and Johnston D. 1994. Multiple components of calcium current in acutely dissociated dentate gyrus granule neurons. J Neurophysiol 72:762-777.

Gasparini S, Kasyanov AM, Pietrobon D, Voronin LL, and Cherubini E. 2001. Presynaptic R-type calcium channels contribute to fast excitatory synaptic transmission in the rat hippocampus. J Neurosci 21:8715-8721.

Goelet P, Castellucci VF, Schacher S, and Kandel ER. 1986. The long and the short of long-term memory--a molecular framework. Nature 322:419-422.

Hardingham GE, Arnold FJ, and Bading H. 2001. Nuclear calcium signaling controls CREB-mediated gene expression triggered by synaptic activity. Nat Neurosci 4:261-267.

Hardingham GE and Bading H. 2002. Coupling of extrasynaptic NMDA receptors to a CREB shut-off pathway is developmentally regulated. Biochim Biophys Acta 1600:148-153.

Hirasawa M and Pittman QJ. 2003. Nifedipine facilitates neurotransmitter release independently of calcium channels. Proc Natl Acad Sci U S A 100:6139-6144.

Huguenard JR. 1996. Low-threshold calcium currents in central nervous system neurons. Annu Rev Physiol 58:329-348.

Irizarry RA, Bolstad BM, Collin F, Cope LM, Hobbs B, and Speed TP. 2003. Summaries of Affymetrix GeneChip probe level data. Nucleic Acids Res 31:e15.

Kavalali ET, Zhuo M, Bito H, and Tsien RW. 1997. Dendritic Ca^{2+} channels characterized by recordings from isolated hippocampal dendritic segments. Neuron 18:651-663.

Konur S and Ghosh A. 2005. Calcium signaling and the control of dendritic development. Neuron 46:401-405.

Kovalchuk Y, Eilers J, Lisman J, and Konnerth A. 2000. NMDA receptor-mediated subthreshold Ca^{2+} signals in spines of hippocampal neurons. J Neurosci 20:1791-1799.

Lonze BE and Ginty DD. 2002. Function and regulation of CREB family transcription factors in the nervous system. Neuron 35:605-623.

Losonczy A and Magee JC. 2006. Integrative properties of radial oblique dendrites in hippocampal CA1 pyramidal neurons. Neuron 50:291-307.

Magee JC and Johnston D. 1995. Characterization of single voltage-gated Na^{+} and Ca^{2+} channels in apical dendrites of rat CA1 pyramidal neurons. J Physiol 487 (Pt 1):67-90.

Malenka RC and Nicoll RA. 1999. Long-term potentiation--a decade of progress? Science 285:1870-1874.

Markram H, Helm PJ, and Sakmann B. 1995. Dendritic calcium transients evoked by single back-propagating action potentials in rat neocortical pyramidal neurons. J Physiol 485 (Pt 1):1-20.

Martin KC, Barad M, and Kandel ER. 2000. Local protein synthesis and its role in synapse-specific plasticity. Curr Opin Neurobiol 10:587-592.

Mazzoni A, Broccard FD, Garcia-Perez E, Bonifazi P, Ruaro ME, and Torre V. 2007. On the dynamics of the spontaneous activity in neuronal networks. PLoS ONE 2:e439.

McKay BE, McRory JE, Molineux ML, Hamid J, Snutch TP, Zamponi GW, and Turner RW. 2006. Ca(V)3 T-type calcium channel isoforms differentially distribute to somatic and dendritic compartments in rat central neurons. Eur J Neurosci 24:2581-2594.

Metz AE, Jarsky T, Martina M, and Spruston N. 2005. R-type calcium channels contribute to afterdepolarization and bursting in hippocampal CA1 pyramidal neurons. J Neurosci 25:5763-5773.

Murphy LO and Blenis J. 2006. MAPK signal specificity: the right place at the right time. Trends Biochem Sci 31:268-275.

Newcomb R, Szoke B, Palma A, Wang G, Chen X, Hopkins W, Cong R, Miller J, Urge L, Tarczy-Hornoch K, Loo JA, Dooley DJ, Nadasdi L, Tsien RW, Lemos J, and Miljanich G. 1998. Selective peptide antagonist of the class E calcium channel from the venom of the tarantula Hysterocrates gigas. Biochemistry 37:15353-15362.

Pinato G and Midtgaard J. 2003. Regulation of granule cell excitability by a low-threshold calcium spike in turtle olfactory bulb. J Neurophysiol 90:3341-3351.

Piriz J, Rosato S, Pagani R, and Uchitel OD. 2003. Nifedipine-mediated mobilization of intracellular calcium stores increases spontaneous neurotransmitter release at neonatal rat motor nerve terminals. J Pharmacol Exp Ther 306:658-663.

Rao VR, Pintchovski SA, Chin J, Peebles CL, Mitra S, and Finkbeiner S. 2006. AMPA receptors regulate transcription of the plasticity-related immediate-early gene Arc. Nat Neurosci 9:887-895.

Raymond CR. 2007. LTP forms 1, 2 and 3: different mechanisms for the "long" in long-term potentiation. Trends Neurosci 30:167-175.

Remy S and Spruston N. 2007. Dendritic spikes induce single-burst long-term potentiation. Proc Natl Acad Sci U S A 104:17192-17197.

Ruaro ME, Bonifazi P, and Torre V. 2005. Toward the neurocomputer: image processing and pattern recognition with neuronal cultures. IEEE Trans Biomed Eng 52:371-383.

Schiller Y. 2004. Activation of a calcium-activated cation current during epileptiform discharges and its possible role in sustaining seizure-like events in neocortical slices. J Neurophysiol 92:862-872.

Schuman EM. 1997. Synapse specificity and long-term information storage. Neuron 18:339-342.

Sidach SS and Mintz IM. 2002. Kurtoxin, a gating modifier of neuronal high- and low-threshold ca channels. J Neurosci 22:2023-2034.

Straub H, Speckmann EJ, Bingmann D, and Walden J. 1990. Paroxysmal depolarization shifts induced by bicuculline in CA3 neurons of hippocampal slices: suppression by the organic calcium antagonist verapamil. Neurosci Lett 111:99-101.

Timofeev I, Grenier F, and Steriade M. 2004. Contribution of intrinsic neuronal factors in the generation of cortically driven electrographic seizures. J Neurophysiol 92:1133-1143.

Tottene A, Moretti A, and Pietrobon D. 1996. Functional diversity of P-type and R-type calcium channels in rat cerebellar neurons. J Neurosci 16:6353-6363.

Tottene A, Volsen S, Pietrobon D. 2000. alpha(1E) subunits form the pore of three cerebellar R-type calcium channels with different pharmacological and permeation properties. J Neurosci 20:171-178.

Traub RD, Miles R, and Jefferys JG. 1993. Synaptic and intrinsic conductances shape picrotoxin-induced synchronized after-discharges in the guinea-pig hippocampal slice. J Physiol 461:525-547.

Uchida I, Cestari IN, and Yang J. 1996. The differential antagonism by bicuculline and SR95531 of pentobarbitone-induced currents in cultured hippocampal neurons. Eur J Pharmacol 307:89-96.

Vinet J and Sik A. 2006. Expression pattern of voltage-dependent calcium channel subunits in hippocampal inhibitory neurons in mice. Neuroscience 143:189-212.

Westenbroek RE, Ahlijanian MK, and Catterall WA. 1990. Clustering of L-type Ca^{2+} channels at the base of major dendrites in hippocampal pyramidal neurons. Nature 347:281-284.

Westenbroek RE, Hell JW, Warner C, Dubel SJ, Snutch TP, and Catterall WA. 1992. Biochemical properties and subcellular distribution of an N-type calcium channel alpha 1 subunit. Neuron 9:1099-1115.

Wu GY, Deisseroth K, and Tsien RW. 2001. Activity-dependent CREB phosphorylation: convergence of a fast, sensitive calmodulin kinase pathway and a slow, less sensitive mitogen-activated protein kinase pathway. Proc Natl Acad Sci U S A 98:2808-2813.

Xiang G, Pan L, Xing W, Zhang L, Huang L, Yu J, Zhang R, Wu J, Cheng J, and Zhou Y. 2007. Identification of activity-dependent gene expression profiles reveals specific subsets of genes induced by different routes of Ca^{2+} entry in cultured rat cortical neurons. J Cell Physiol 212:126-136.

Zhang SJ, Steijaert MN, Lau D, Schutz G, Delucinge-Vivier C, Descombes P, and Bading H. 2007. Decoding NMDA receptor signaling: identification of genomic programs specifying neuronal survival and death. Neuron 53:549-562.

Figure legends

Fig.1. A: Fluorescence image of a neuronal culture stained with the membrane permeable calcium dye Oregon Green 488-BAPTA-1-AM. Four regions of interest (ROIs) are marked with colored spots. B: optical signals (DF/F) recorded from the soma of four distinct neurons corresponding to the ROIs indicated in A. C: as in B but in the presence of 20 μM gabazine. D: DF/F from the soma of three different neurons in control conditions (black traces) and in the presence of a blocker (red traces): 20 μM nifedipine (first column), 100 μM $NiCl_2$ (second column), 500 nM SNX-482 (third column), 1 μM of ω-conotoxinMVIIC (fourth column) and 20 μM APV (fifth column). The last row in each column reports optical signals obtained by averaging DF/F obtained from 15, 10, 30, 22 and 21 soma in control conditions (black traces) and in the presence of the blocker (red traces).

Fig.2. A: histogram of the fractional reduction of the peak of DF/F observed during GabT induced burst of electrical activity caused by the addition of 20 μM nifedipine. Collected data from the soma of 77 neurons.
B: histogram of the fractional reduction of the peak of DF/F observed during GabT induced burst of electrical activity caused by the addition of 100 μM $NiCl_2$. Collected data from the soma of 71 neurons.
C: histogram of the fractional reduction of the peak of DF/F observed during GabT induced burst of electrical activity caused by the addition of 1 μM ω-conotoxinMVIIC. Collected data from the soma of 43 neurons.
D: histogram of the fractional reduction of the peak of DF/F observed during GabT induced burst of electrical activity caused by the addition of 20 μM APV. Collected data from the soma of 132 neurons.
E: Simultaneous somatic calcium imaging (top traces) and electrophysiological recordings from different experiments showing the effects of APV on dissociated

hippocampal cultures treated with 20 μM gabazine. Black traces are recordings in control conditions (GabT), red traces, after APV.

Fig.3. A: GabT induced Ca^{2+}transients in control (black trace) and after nifedipine (red traces), measured with the calcium dye Oregon green 488-BAPTA-2 (OGB-2-AM) which has a higher value of K_D of 580 nM with respect of 488-BAPTA-1-AM (K_D of 170 nM). Optical traces were averaged over a large area to increase signal to noise ratio. B: as in A but testing the effect of APV.

Fig.4. A: somatic optical signals DF/F during injection of a depolarizing step of current evoking 9 spikes (upper trace, electrophysiological recording) in control conditions (black traces) and in the presence of 20 μM nifedipine (red trace). B: as in A but evoking 6 spikes and testing 100 μM $NiCl_2$. C: as in A but testing the effect of 1 μM ω-conotoxinMVIIC. D: as in A but evoking 4 spikes and testing the effect of 100 μM $NiCl_2$ and 100 μM Cd^{2+}.

Fig.5. A: voltage recording of the membrane potential of a neuron (black trace) during GabT induced bursts. The neuron was loaded with the membrane impermeable calcium dye Oregon Green 488-BAPTA-1-AM included in the patch pipette and was imaged in B and D. Red and green traces are optical signals DF/F recorded from the soma and the dendrite indicated by arrows of the same color in B.
B: color coded map of the amplitude of DF/F at the time t_1 indicated in A.
C: as in A, but after the addition of 20 μM nifedipine.
D: as in B, but after the addition of 20 μM nifedipine, at the time t_2 indicated in C.

Fig.6. A: voltage recording of the membrane potential of a neuron (black trace) during GabT induced bursts. The neuron was loaded with the membrane impermeable calcium dye Oregon Green 488-BAPTA-1-AM included in the patch pipette and was imaged in B and D. Red and green traces are optical signals DF/F

recorded from the soma and the dendrite indicated by arrows of the same color in B. B: color coded map of DF/F obtained in the presence of 20 μM gabazine at the time t_1 indicated in A. C: as in A but after the addition of 1 μM ω-conotoxinMVIIC. D: as in B but after the addition of 1 μM ω-conotoxinMVIIC, at the time t_2 indicated in C.

Fig.7. A: voltage recording of the membrane potential of a neuron (black trace) during GabT induced burst. The neuron was loaded with the membrane impermeable calcium dye Oregon Green 488-BAPTA-1- and was imaged in B and D. Red and green traces are optical signals DF/F recorded from the soma and the dendrite indicated by the arrows with the same color as in A.
B: color coded map of the amplitude of DF/F at the time t_1 indicated in A.
C: as in A but after the addition of 20 μM APV.
D: as in B but after the addition of 20 μM APV, at the time t_2 indicated in C.

Fig.8. A-C: optical signals (DF/F) recorded from the soma of three neurons composing the culture used for the genomic analysis shown in the following panels. In the presence of 20 μM gabazine (A), + 20 μM APV (B) and + 20 μM nifedipine (C). D-G: pie charts illustrating the number of up-regulated (D and E) and down-regulated (F and G) genes 1.5 and 3 hours after GabT. The pie charts illustrate the fraction of genes sensitive or not sensitive to APV and/or nifedipine treatments. The color white indicates genes controlled primarily by activation of NMDA receptors (GenesNMDA), i.e. their up-regulation (down-regulation) being blocked by APV. The color black indicates genes controlled primarily by Ca^{2+} entry through L-type Ca^{2+} channels (GenesL), i.e. their up-regulation (down-regulation) being blocked by nifedipine. Pale grey indicates genes which were up-regulated (down-regulated) either in the presence of APV or nifedipine (GenesNMDAorL). Dark grey indicates genes whose up-regulation (down-regulation) was blocked either by APV or by nifedipine (GenesNMDAandL). The pie charts indicated also the number of genes belonging to each group.

Fig.9. mRNA expression fold changes measured with qRT-PCR for Nr4a1 in the absence (white bars) or presence (black bars) of the membrane permeable calcium dye Oregon Green 488-BAPTA-1-AM. Untreated hippocampal dissociated cultures (C), cultures treated with 20 μM gabazine alone (GBZ), or in the presence of 20 μM APV (APV+GBZ) or 20 μM nifedipine (nifedipine+GBZ).

Fig.10. A-B: effect of APV and nifedipine on gene up-regulated after 1.5 h GabT measured with qRT-PCR. Results are expressed in fold change signal between untreated hippocampal dissociated cultures(C) and cultures treated with 20 μM gabazine alone (GBZ) or in the presence of 20 μM APV (APV+GBZ) or 20 μM nifedipine (nifedipine+GBZ). Analyzed genes were Nr4a1, Bdnf (exon 9), Arc, Egr2, Nr4a and Homer1a. The analysis was performed using Gapdh as a housekeeping gene. Bars represent means ± SEM (n=6-4).

Fig.11. A: Genes up-regulated 3 hours after GabT and blocked by nifedipine; red represents the proportion of genes also blocked by ω-conotoxinMVIIC. B: Genes up-regulated 3 hours after GabT and not blocked by nifedipine; red representes the proportion of genes also not blocked by ω-conotoxinMVIIC.

Table 1. Up-regulated genes 1.5 hours after GabT. Classification in four groups is determined by their sensitivity to APV and nifedipine.

Group 1-GenesNMDA 1.5 h after GabT

Up-regulated genes in GBZ and GBZ+nifedipine but not in GBZ+APV

Affy ID	Gene Symbol	Gene Name
1368144_at	Rgs2	regulator of G-protein signaling 2
1368146_at	Dusp1	dual specificity phosphatase 1
1368223_at	Adamts1	a disintegrin-like and metallopeptidse (reprolysin type) with thrombospondin type 1 motif, 1
1368488_at	Nfil3	nuclear factor, interleukin 3 regulated
1368527_at	Ptgs2	prostaglandin-endoperoxide synthase 2
1368662_at	Rnf39	ring finger protein 39
1369217_at	Nr4a3	nuclear receptor subfamily 4, group A, member 3
1369268_at	Atf3	activating transcription factor 3
1370652_at	Ntrk2	neurotrophic tyrosine kinase, receptor, type 2
1370997_at	Homer1	homer homolog 1 (Drosophila)
1371019_at	Trib1	tribbles homolog 1 (Drosophila)
1373035_at	---	Transcribed locus
1373759_at	---	Transcribed locus
1374446_at	Tiparp_predicted	TCDD-inducible poly(ADP-ribose) polymerase (predicted)
1376275_at	---	Transcribed locus
1378393_at	RGD1306214_predicted	similar to TGF-beta induced apotosis protein 2 (predicted)
1378489_at	---	Transcribed locus
1378925_at	Crem	CAMP responsive element modulator
1380229_at	---	Transcribed locus
1380383_at	Arf4l_predicted	ADP-ribosylation factor 4-like (predicted)
1381903_at	Fbxo33_predicted	F-box only protein 33 (predicted)
1383860_at	Fosl2	fos-like antigen 2
1385691_at	RGD1560454_predicted	similar to RIKEN cDNA 5830435K17 (predicted)
1386935_at	Nr4a1	nuclear receptor subfamily 4, group A, member 1
1387068_at	Arc	activity regulated cytoskeletal-associated protein
1387260_at	Klf4	kruppel-like factor 4 (gut)
1387337_at	Cort	Cortistatin
1387442_at	Egr4	early growth response 4

1389402_at	---	Transcribed locus
1391643_at	---	---
1392152_at	---	Transcribed locus
1392791_at	---	Transcribed locus
1393119_at	---	Transcribed locus
1393550_at	---	Transcribed locus
1393782_at	---	Transcribed locus
1394012_at	---	Transcribed locus, moderately similar to XP_001094447.1 zinc finger, SWIM domain containing 5 [Macaca mulatta]
1394039_at	Klf5	kruppel-like factor 5
1394689_at	---	Transcribed locus
1394940_at	RGD1311381_predicted	similar to hypothetical protein FLJ20037 (predicted)
1396545_at	---	Transcribed locus
1396563_at	---	Transcribed locus

Group 2-GenesL 1.5 h after GabT

Up-regulated genes in GBZ and GBZ+APV but not in GBZ+nifedipine

Affy ID	Gene Symbol	Gene Name
1373403_at	LOC684871	similar to Protein C8orf4 (Thyroid cancer protein 1) (TC-1)
1380400_at	---	Transcribed locus

Group 3-GenesNMDAorL 1.5 h after GabT

Up-regulated genes either in GBZ or GBZ+APV or GBZ+nifedipine

Affy ID	Gene Symbol	Gene Name
1368487_at	Serpinb2	serine (or cysteine) proteinase inhibitor, clade B, member 2
1368677_at	Bdnf	brain derived neurotrophic factor
1369871_at	Areg	Amphiregulin
1370454_at	Homer1	homer homolog 1 (Drosophila)
1373093_at	Errfi1	ERBB receptor feedback inhibitor 1
1387306_a_at	Egr2	early growth response 2
1387410_at	Nr4a2	nuclear receptor subfamily 4, group A, member 2
1389211_at	---	Transcribed locus
1392108_at	---	RM2 mRNA, partial sequence

Group 4-GenesNMDAandL 1.5 h after GabT

Up-regulated genes in GBZ but not in GBZ+APV and GBZ+nifedipine

Affy ID	Gene Symbol	Gene Name
1368892_at	---	adenylate cyclase activating polypeptide 1 (Adcyap1) mRNA, 3' UTR
1369130_at	Rasgrp1	RAS guanyl releasing protein 1
1370509_at	Pdp2	pyruvate dehydrogenase phosphatase isoenzyme 2
1374257_at	Tiam1	T-cell lymphoma invasion and metastasis 1
1375179_at	---	---
1377663_at	Rnd3	Rho family GTPase 3
1378654_at	---	Transcribed locus
1380063_at	Ch25h	cholesterol 25-hydroxylase
1380138_at	RGD1564397_predicted	Similar to heparan sulfate 6-O-sulfotransferase 2 isoform S (predicted)
1382009_at	Chd1_predicted	chromodomain helicase DNA binding protein 1 (predicted)
1382291_at	---	Transcribed locus, strongly similar to XP_001081628.1 similar to Transcription factor SOX-9 [Rattus norvegicus]
1382850_at	Syn2	synapsin II
1382898_at	Cacnb4	calcium channel, voltage-dependent, beta 4 subunit
1385578_at	---	Transcribed locus
1385903_at	---	Transcribed locus, moderately similar to XP_001094447.1 zinc finger, SWIM domain containing 5 [Macaca mulatta]
1386396_at	Dusp8_predicted	dual specificity phosphatase 8 (predicted)
1388000_at	Slc24a2	solute carrier family 24 (sodium/potassium/calcium exchanger), member 2
1389864_at	---	---
1390205_at	---	---
1391418_at	---	---
1391771_at	Atp2a2	ATPase, Ca++ transporting, cardiac muscle, slow twitch 2
1392157_at	Plxna2_predicted	plexin A2 (predicted)
1393910_at	RGD1309807	similar to Fam13a1 protein
1397194_at	Txndc13	thioredoxin domain containing 13

Table 2. Up-regulated genes 3 hours after GabT. Classification in four groups is determined by their sensitivity to APV and nifedipine.

Group 1-GenesNMDA 3 h after GabT

Up-regulated genes in GBZ and GBZ+nifedipine but not in GBZ+APV

Affy ID	Gene Symbol	Gene Name
1368146_at	Dusp1	dual specificity phosphatase 1
1368321_at	Egr1	early growth response 1
1368527_at	Ptgs2	prostaglandin-endoperoxide synthase 2
1370454_at	Homer1	homer homolog 1 (Drosophila)
1370997_at	Homer1	homer homolog 1 (Drosophila)
1372016_at	Gadd45b	growth arrest and DNA-damage-inducible 45 beta
1373559_at	Nptx2	neuronal pentraxin II
1373759_at	---	Transcribed locus
1373807_at	---	Transcribed locus
1375043_at	Fos	FBJ murine osteosarcoma viral oncogene homolog
1380383_at	Arf4l_predicted	ADP-ribosylation factor 4-like (predicted)
1380967_at	Nts	Neurotensin
1386935_at	Nr4a1	nuclear receptor subfamily 4, group A, member 1
1387068_at	Arc	activity regulated cytoskeletal-associated protein
1387219_at	Adm	Adrenomedullin
1387306_a_at	Egr2	early growth response 2
1387410_at	Nr4a2	nuclear receptor subfamily 4, group A, member 2
1387442_at	Egr4	early growth response 4
1387788_at	Junb	jun-B oncogene
1390626_at	---	Transcribed locus
1392108_at	---	RM2 mRNA, partial sequence
1396823_at	---	Transcribed locus

Group 2-GenesL 3 h after GabT

Up-regulated genes in GBZ and GBZ+APV but not in GBZ+nifedipine

Affy ID	Gene Symbol	Gene Name
1367973_at	Ccl2	chemokine (C-C motif) ligand 2

1368073_at	Irf1	interferon regulatory factor 1
1368308_at	Myc	myelocytomatosis viral oncogene homolog (avian)
1368489_at	Fosl1	fos-like antigen 1
1368490_at	Cd14	CD14 antigen
1370177_at	PVR	poliovirus receptor
1370371_a_at	Ceacam1 /// Ceacam10	CEA-related cell adhesion molecule 1 /// CEA-related cell adhesion molecule 10
1373403_at	LOC684871	similar to Protein C8orf4 (Thyroid cancer protein 1) (TC-1)
1373421_at	Tgif	TG interacting factor
1373485_at	RGD1561238_predicted	Similar to ring finger protein 122 homolog (predicted)
1375617_at	---	Transcribed locus
1376908_at	Ifit3	interferon-induced protein with tetratricopeptide repeats 3
1377092_at	---	Transcribed locus
1377340_at	Tfpi2	tissue factor pathway inhibitor 2
1379365_at	Cxcl11	chemokine (C-X-C motif) ligand 11
1379935_at	Ccl7	chemokine (C-C motif) ligand 7
1380229_at	---	Transcribed locus
1384415_at	---	Transcribed locus
1386160_at	Thh_predicted	trichohyalin (predicted)
1387260_at	Klf4	kruppel-like factor 4 (gut)
1387316_at	Cxcl1	chemokine (C-X-C motif) ligand 1
1387870_at	Zfp36	zinc finger protein 36
1387969_at	Cxcl10	chemokine (C-X-C motif) ligand 10
1388587_at	Ier3	immediate early response 3
1389230_at	---	Transcribed locus
1397929_at	---	Transcribed locus
1398655_at	Myod1	myogenic differentiation 1

Group 3-GenesNMDAorL 3 h after GabT

Up-regulated genes in GBZ and GBZ+APV and GBZ+nifedipine

Affy ID	Gene Symbol	Gene Name
1368224_at	Serpina3n	serine (or cysteine) peptidase inhibitor, clade A, member 3N
1369268_at	Atf3	activating transcription factor 3
1369415_at	Bhlhb2	basic helix-loop-helix domain containing, class B2
1383242_a_at	---	Transcribed locus

1394948_at	---	Transcribed locus

Group 4-GenesNMDAandL 3 h after GabT

Up-regulated genes in GBZ but neither in GBZ+APV nor GBZ+nifedipine

Affy ID	Gene Symbol	Gene Name
1368124_at	Dusp5	dual specificity phosphatase 5
1368223_at	Adamts1	a disintegrin-like and metallopeptidse (reprolysin type) with thrombospondin type 1 motif, 1
1368290_at	Cyr61	cysteine rich protein 61
1368650_at	Klf10	kruppel-like factor 10
1368674_at	Pygl	liver glycogen phosphorylase
1381565_at	---	Transcribed locus
1382138_at	LOC499745 /// LOC688240	similar to Notch-regulated ankyrin repeat protein
1383519_at	Hk2	hexokinase 2
1385641_at	---	Transcribed locus
1388189_at	Grm3	glutamate receptor, metabotropic 3
1389402_at	---	Transcribed locus
1390391_at	---	Transcribed locus
1393728_at	---	Transcribed locus
1394423_at	---	Transcribed locus

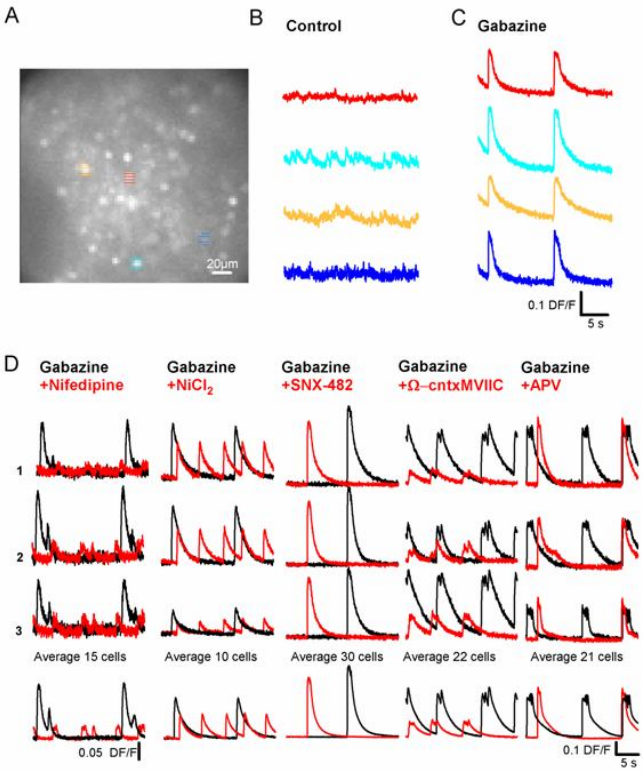
A
B
Control
C
Gabazine
20μm
0.1 DF/F
5 s
D
Gabazine
+Nifedipine
Gabazine
+NiCl2
Gabazine
+SNX-482
Gabazine
+Ω–cntxMVIIC
Gabazine
+APV
1
2
3
Average 15 cells
Average 10 cells
Average 30 cells
Average 22 cells
Average 21 cells
0.05 DF/F
0.1 DF/F
5 s

Fig.1

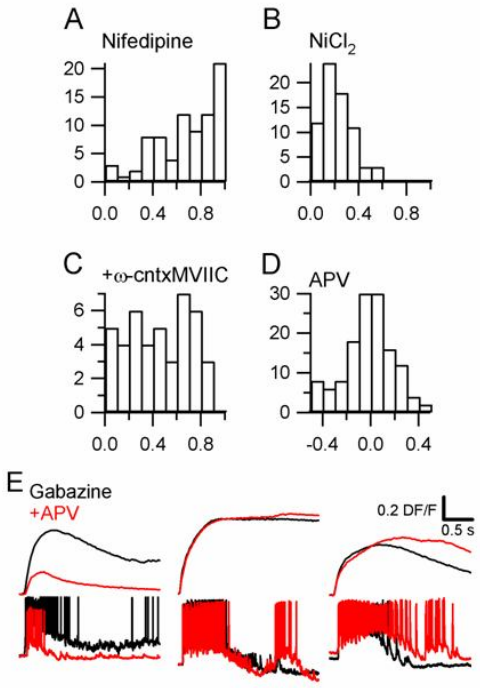
A
Nifedipine
B
NiCl2
C
+ω-cntxMVIIC
D
APV
E
Gabazine
+APV
0.2 DF/F
0.5 s

Fig.2

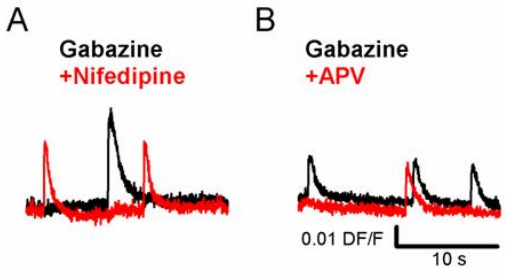
A
Gabazine
+Nifedipine
B
Gabazine
+APV
0.01 DF/F
10 s

Fig.3

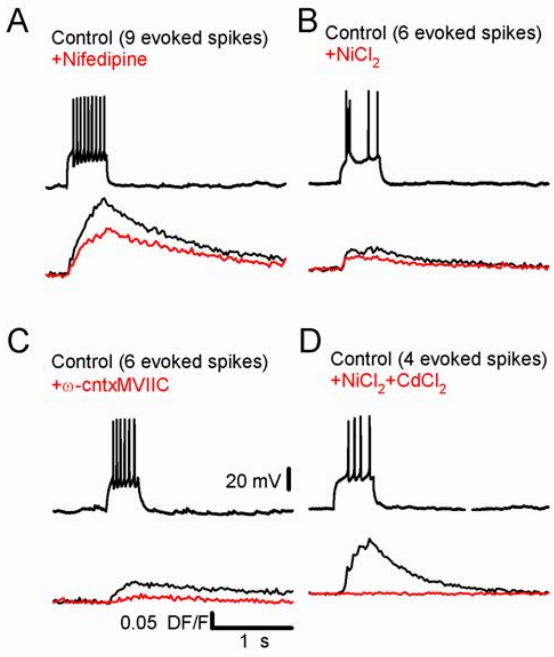
A
Control (9 evoked spikes)
+Nifedipine
B
Control (6 evoked spikes)
+NiCl2
C
Control (6 evoked spikes)
+ω-cntxMVIIC
D
Control (4 evoked spikes)
+NiCl2+CdCl2
20 mV
0.05 DF/F
1 s

Fig.4

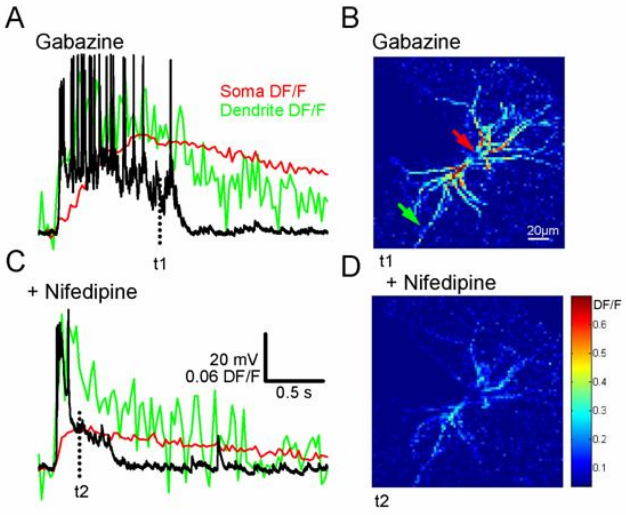
A
Gabazine
Soma DF/F
Dendrite DF/F
t1
B
Gabazine
20μm
t1
C
+ Nifedipine
20 mV
0.06 DF/F
0.5 s
t2
D
+ Nifedipine
DF/F
0.6
0.5
0.4
0.3
0.2
0.1
t2

Fig.5

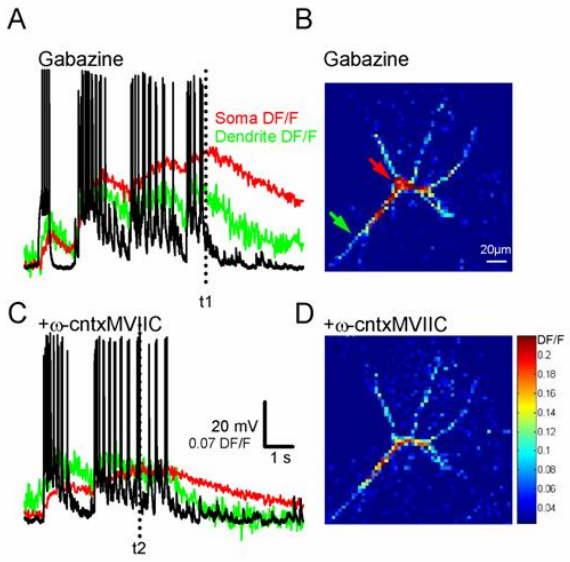
A
Gabazine
Soma DF/F
Dendrite DF/F
t1
B
Gabazine
20μm
C
+ω-cntxMVIIC
20 mV
0.07 DF/F
1 s
t2
D
+ω-cntxMVIIC
DF/F

Fig.6

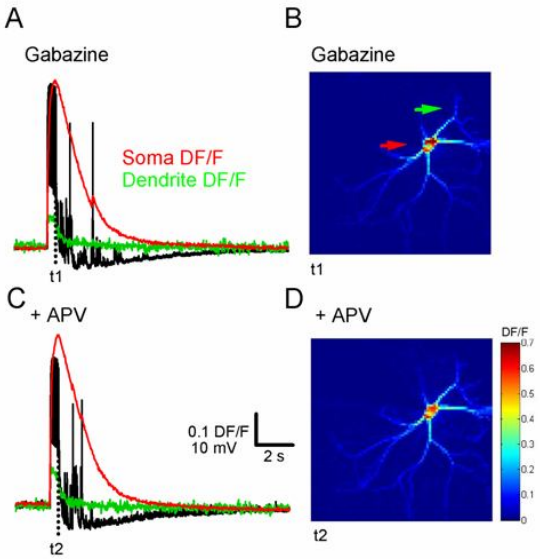
A
Gabazine
Soma DF/F
Dendrite DF/F
t1
B
Gabazine
t1
C
+ APV
0.1 DF/F
10 mV
2 s
t2
D
+ APV
DF/F

Fig.7

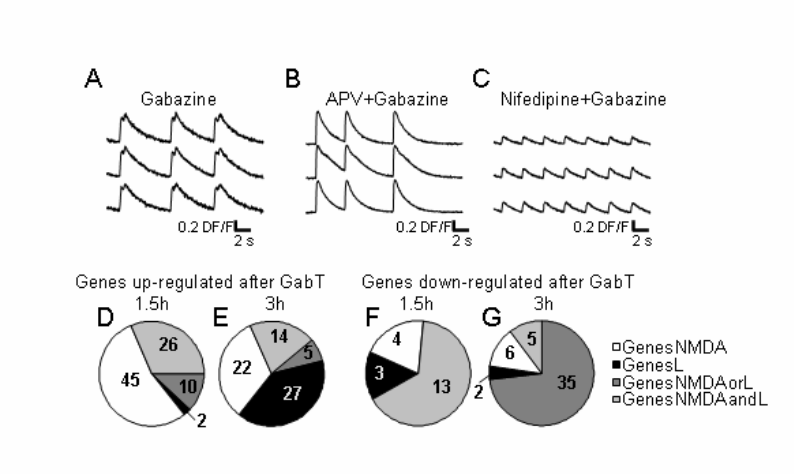
A
Gabazine
0.2 DF/F
2 s
B
APV+Gabazine
0.2 DF/F
2 s
C
Nifedipine+Gabazine
0.2 DF/F
2 s
Genes up-regulated after GabT
Genes down-regulated after GabT
D
1.5h
26
45
10
2
E
3h
14
5
22
27
F
1.5h
4
3
13
2
G
3h
5
6
35
GenesNMDA
GenesL
GenesNMDAorL
GenesNMDAandL

Fig.8

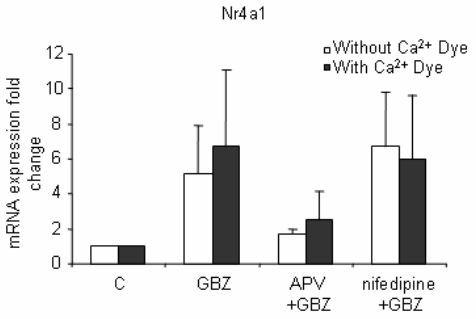
Nr4a1
Without Ca2+ Dye
With Ca2+ Dye
mRNA expression fold change
12
10
8
6
4
2
0
C
GBZ
APV +GBZ
nifedipine +GBZ

Fig.9

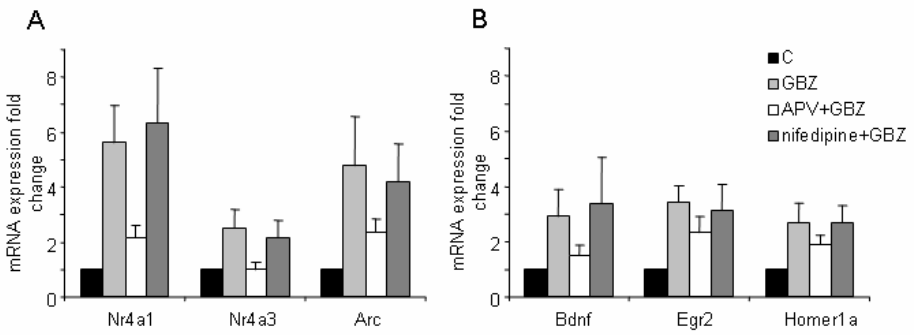
A
B
mRNA expression fold change
0
2
4
6
8
Nr4a1
Nr4a3
Arc
Bdnf
Egr2
Homer1a
C
GBZ
APV+GBZ
nifedipine+GBZ

Fig.10

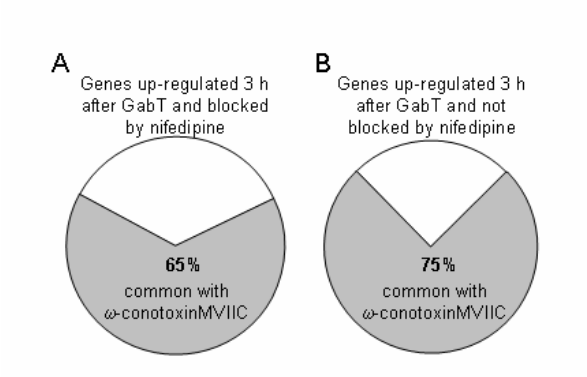
A
Genes up-regulated 3 h after GabT and blocked by nifedipine
65%
common with ω-conotoxinMVIIC
B
Genes up-regulated 3 h after GabT and not blocked by nifedipine
75%
common with ω-conotoxinMVIIC

Fig.11

4 Conclusions

The aim of my thesis was to study the network properties of dissociated cultures from rat hippocampus after blockage of the inhibitory synaptic pathways mediated by $GABA_A$ receptors. This neuronal system provides a good model of activity-induced changes in network properties and it allows the study of network functions related to neuronal plasticity. In my work I have also combined the use of genome-wide analysis, MEA technology and calcium imaging in order to analyze network functions at three main levels: transcriptional profile, network electrical activity and calcium dynamics. Therefore this thesis establishes a useful model for the study of concomitant changes at different network levels and for the investigation of activity-regulated changes in gene expression underlying synaptic plasticity.

The major results consist of the integration of transcriptome, calcium contribution and network electrical activity profiles for a functional genomic approach aimed at studying activity-dependent modification of neuronal networks. In recent years, genome-wide analyses have been made to detect activity-regulated genes in neurons (Altar et al., 2004; Hong et al., 2004; Li et al., 2004; Park et al., 2006). These studies revealed that several hundreds of genes are regulated in response to extracellular stimuli that change the electrical activity of the neurons. But the activation of this new transcriptional program seems to be complicated. In fact, two features of the activity-regulated transcriptional program have emerged from these studies: the new gene transcription can be activated through several mechanisms mediated principally by Ca^{2+}, and with different kinetics.

The first achievement of this research was the characterization of an activity-regulated gene expression program in response to the transiently blockage of the $GABA_A$ receptors by pharmacological inhibitors, such as bicuculline or gabazine. In hippocampal dissociated neurons, blockage of $GABA_A$ receptors triggers large synchronous bursts of electrical activity. Interestingly, after $GABA_A$ receptor blockers washout, the network activity changed into a new state characterized by a synchronous bursting pattern of activity. Moreover, disinhibiting the network with gabazine was sufficient to induce long-term modification of both the evoked and

spontaneous activity for several hours. In fact, after pharmacological manipulation, the neuronal network displayed a bursting synchronous activity that persists for hours, up to several days. In addition, the evoked activity was potentiated for several hours. These features indicated that a form of plasticity was induced during pharmacological manipulation. Furthermore, the long-lasting changes in the spontaneous network activity were mediated by new gene transcription, since the transcription inhibitors were able to block this late component. The microarray technology allowed a genome-wide analysis of the gene expression changes that took place in the above described conditions. By using this technique I was able to verify that hundreds of genes were regulated. The transcriptional program activated was very complex. In fact, here it is also shown that, apart from the genes involved in the regulation of the gene transcription, a large number of genes encoding for proteins that have an important role in pre-synaptic or post-synaptic functions or have a structural role in cellular function, were regulated. The results suggest that this transcriptional program consists of two parts: the induction of transcription factors that coordinate the expression of the effector genes and the induction of genes, with a pre- or post-synaptic or structural role, that directly regulates the synaptic properties and morphological changes. Therefore, these findings indicate a complex molecular cascade participating in the regulation and orchestration of the plasticity changes induced.

The second achievement of this work comprises the temporal dissection of the activity-regulated gene expression program. First we analyzed the spontaneous and evoked network electrical activity at different times after the pharmacological manipulation. Principally, we identified several sequential phases underlying this form of neuronal plasticity: an early component of synchronization initiated immediately after termination of the stimulation (E-Sync) dependent on the MAPK/ERK pathway, and a late component - from 6 to 24 hours - (L-Sync) dependent on the new gene transcription. In addition, an intermediate phase (from 1 hour to 6 hours) was characterized by an increased in the evoked response (M-LTP).

Then, it was shown that also the gene expression program was dynamically regulated in time. In fact, the gene expression profile revealed three main clusters of genes that displayed a similar temporal expression profile. A first component of gene expression was primarily composed of transcription factors, and then a second wave of gene transcription was temporally associated with the potentiation of the evoked electrical response. Moreover, when the spontaneous electrical activity became more synchronous, a down-regulation of genes coding for several K^+ channels appeared evident. The time course profiling of the activity-regulated gene expression would provide a mean to uncover the dynamics of molecular processes during the different phases emerged from the network activity. Considered all together, these results provide the possibility to relate specific events occurring during neuronal plasticity to changes of expression of specific gene clusters. Although previous works identified several activity-regulated genes in different models of neuronal plasticity, a comprehensive description of the molecular events is still incomplete. In this work, the concomitant analysis of the network activity and of the gene expression profile could provide some definitions describing the cellular and molecular events that underlie synaptic activity modification.

The third achievement of this thesis consists of elucidating the diffent routes by which Ca^{2+} regulates the gene expression program activated after disinhibition. During the large bursts of spontaneous synchronous spikes induced by blockage of $GABA_A$ receptors, also large Ca^{2+} transients occur synchronously in the network neurons. The pharmacological dissection of the cytoplasmic Ca^{2+} concentration increase during these events revealed that the VGCCs, in particular L-, N- and P/Q-type, predominated over NMDA receptors. Nevertheless, in this work it is also shown that Ca^{2+} entry through NMDA receptors mostly mediated the changes in gene expression.

However, the results obtained proved that NMDA receptors were not the only pathway by which gene expression was regulated. In fact, also Ca^{2+} entry through VGCCs, L, N and P/Q-types, had a role in the gene expression induction. Previous

works demonstrated that the signalling through NMDA receptors had an important role in inducing and maintaining the synchronous bursting pattern of activity (Arnold et al., 2005). In agreement with this observation, the conclusion that can be drawn here is that Ca^{2+} entry through NMDA receptors is a key event in mediating gene expression, in the used model of neuronal plasticity. Moreover, the communication between the synapse and the nucleus was more intricated, and beside NMDA receptors also L, N and P/Q-types VGCCs mediated in a composite and time dependent way the gene expression program that coordinated each synaptic changes occurring in the neurons. Therefore, these results demonstrate that the complexity of the gene expression program activated was not only characterized by the intricate molecular cascade of genes expression and by their temporal regulation, but also by the signalling pathways that mediate their induction.

In summary, these results show that this neuronal system is a good and simple model to study the network properties at different levels and in particular to study the neuronal plasticity at the network level. In addition, they also show that the activity-regulated transcriptional program is dynamically modulated by Ca^{2+} ions.

5 References

Abegg M. H., Savic N., Ehrengruber M. U., McKinney R. A., and Gahwiler B. H. (2004) Epileptiform activity in rat hippocampus strengthens excitatory synapses. *J Physiol* **554,** 439-448.

Abraham W. C. (2003) How long will long-term potentiation last? *Philos Trans R Soc Lond B Biol Sci* **358,** 735-744.

Abraham W. C., Mason S. E., Demmer J., Williams J. M., Richardson C. L., Tate W. P., Lawlor P. A., and Dragunow M. (1993) Correlations between immediate early gene induction and the persistence of long-term potentiation. *Neuroscience* **56,** 717-727.

Aid T., Kazantseva A., Piirsoo M., Palm K., and Timmusk T. (2007) Mouse and rat BDNF gene structure and expression revisited. *J Neurosci Res* **85,** 525-535.

Allbritton N. L., Meyer T., and Stryer L. (1992) Range of messenger action of calcium ion and inositol 1,4,5-trisphosphate. *Science* **258,** 1812-1815.

Altar C. A., Laeng P., Jurata L. W., Brockman J. A., Lemire A., Bullard J., Bukhman Y. V., Young T. A., Charles V., and Palfreyman M. G. (2004) Electroconvulsive seizures regulate gene expression of distinct neurotrophic signaling pathways. *J Neurosci* **24,** 2667-2677.

Arnold F. J., Hofmann F., Bengtson C. P., Wittmann M., Vanhoutte P., and Bading H. (2005) Microelectrode array recordings of cultured hippocampal networks reveal a simple model for transcription and protein synthesis-dependent plasticity. *J Physiol* **564,** 3-19.

Bading H., Ginty D. D., and Greenberg M. E. (1993) Regulation of gene expression in hippocampal neurons by distinct calcium signaling pathways. *Science* **260,** 181-186.

Bading H., Segal M. M., Sucher N. J., Dudek H., Lipton S. A., and Greenberg M. E. (1995) N-methyl-D-aspartate receptors are critical for mediating the effects of glutamate on intracellular calcium concentration and immediate early gene expression in cultured hippocampal neurons. *Neuroscience* **64,** 653-664.

Bartel D. P., Sheng M., Lau L. F., and Greenberg M. E. (1989) Growth factors and membrane depolarization activate distinct programs of early response gene expression: dissociation of fos and jun induction. *Genes Dev* **3,** 304-313.

Ben Ari Y. and Gho M. (1988) Long-lasting modification of the synaptic properties of rat CA3 hippocampal neurones induced by kainic acid. *J Physiol* **404,** 365-384.

Ben Ari Y. and Represa A. (1990) Brief seizure episodes induce long-term potentiation and mossy fibre sprouting in the hippocampus. *Trends Neurosci* **13,** 312-318.

Benke T. A., Jones O. T., Collingridge G. L., and Angelides K. J. (1993) N-Methyl-D-aspartate receptors are clustered and immobilized on dendrites of living cortical neurons. *Proc Natl Acad Sci U S A* **90,** 7819-7823.

Berridge M. J. (1998) Neuronal calcium signaling. *Neuron* **21,** 13-26.

Berridge M. J. (2006) Calcium microdomains: organization and function. *Cell Calcium* **40,** 405-412.

Berridge M. J., Lipp P., and Bootman M. D. (2000) The versatility and universality of calcium signalling. *Nat Rev Mol Cell Biol* **1,** 11-21.

Bito H., Deisseroth K., and Tsien R. W. (1996) CREB phosphorylation and dephosphorylation: a Ca(2+)- and stimulus duration-dependent switch for hippocampal gene expression. *Cell* **87,** 1203-1214.

Bito H., Deisseroth K., and Tsien R. W. (1997) Ca2+-dependent regulation in neuronal gene expression. *Curr Opin Neurobiol* **7,** 419-429.

Bliss T. V. and Collingridge G. L. (1993) A synaptic model of memory: long-term potentiation in the hippocampus. *Nature* **361,** 31-39.

Bloodgood B. L. and Sabatini B. L. (2007) Ca(2+) signaling in dendritic spines. *Curr Opin Neurobiol* **17,** 345-351.

Bolshakov V. Y., Golan H., Kandel E. R., and Siegelbaum S. A. (1997) Recruitment of new sites of synaptic transmission during the cAMP-dependent late phase of LTP at CA3-CA1 synapses in the hippocampus. *Neuron* **19,** 635-651.

Bottai D., Guzowski J. F., Schwarz M. K., Kang S. H., Xiao B., Lanahan A., Worley P. F., and Seeburg P. H. (2002) Synaptic activity-induced conversion of intronic to exonic sequence in Homer 1 immediate early gene expression. *J Neurosci* **22,** 167-175.

Bradley J. and Finkbeiner S. (2002) An evaluation of specificity in activity-dependent gene expression in neurons. *Prog Neurobiol* **67,** 469-477.

Calin-Jageman I. and Lee A. (2008) Ca(v)1 L-type Ca2+ channel signaling complexes in neurons. *J Neurochem* **105,** 573-583.

Cao X. M., Koski R. A., Gashler A., McKiernan M., Morris C. F., Gaffney R., Hay R. V., and Sukhatme V. P. (1990) Identification and characterization of the Egr-1 gene product, a

DNA-binding zinc finger protein induced by differentiation and growth signals. *Mol Cell Biol* **10,** 1931-1939.

Carrion A. M., Link W. A., Ledo F., Mellstrom B., and Naranjo J. R. (1999) DREAM is a Ca2+-regulated transcriptional repressor. *Nature* **398,** 80-84.

Catterall W. A. (2000) Structure and regulation of voltage-gated Ca2+ channels. *Annu Rev Cell Dev Biol* **16,** 521-555.

Chawla S., Hardingham G. E., Quinn D. R., and Bading H. (1998) CBP: a signal-regulated transcriptional coactivator controlled by nuclear calcium and CaM kinase IV. *Science* **281,** 1505-1509.

Chen C. and Regehr W. G. (2000) Developmental remodeling of the retinogeniculate synapse. *Neuron* **28,** 955-966.

Cheng H. Y., Pitcher G. M., Laviolette S. R., Whishaw I. Q., Tong K. I., Kockeritz L. K., Wada T., Joza N. A., Crackower M., Goncalves J., Sarosi I., Woodgett J. R., Oliveira-dos-Santos A. J., Ikura M., van der K. D., Salter M. W., and Penninger J. M. (2002) DREAM is a critical transcriptional repressor for pain modulation. *Cell* **108,** 31-43.

Christy B. and Nathans D. (1989) DNA binding site of the growth factor-inducible protein Zif268. *Proc Natl Acad Sci U S A* **86,** 8737-8741.

Clayton D. F. (2000) The genomic action potential. *Neurobiol Learn Mem* **74,** 185-216.

Cole A. J., Saffen D. W., Baraban J. M., and Worley P. F. (1989) Rapid increase of an immediate early gene messenger RNA in hippocampal neurons by synaptic NMDA receptor activation. *Nature* **340,** 474-476.

Colman H., Nabekura J., and Lichtman J. W. (1997) Alterations in synaptic strength preceding axon withdrawal. *Science* **275,** 356-361.

Crabtree G. R. and Olson E. N. (2002) NFAT signaling: choreographing the social lives of cells. *Cell* **109 Suppl,** S67-S79.

Curtis J. and Finkbeiner S. (1999) Sending signals from the synapse to the nucleus: possible roles for CaMK, Ras/ERK, and SAPK pathways in the regulation of synaptic plasticity and neuronal growth. *J Neurosci Res* **58,** 88-95.

Debanne D., Thompson S. M., and Gahwiler B. H. (2006) A brief period of epileptiform activity strengthens excitatory synapses in the rat hippocampus in vitro. *Epilepsia* **47,** 247-256.

Debarbieux F., Brunton J., and Charpak S. (1998) Effect of bicuculline on thalamic activity: a direct blockade of IAHP in reticularis neurons. *J Neurophysiol* **79,** 2911-2918.

Deisseroth K., Heist E. K., and Tsien R. W. (1998) Translocation of calmodulin to the nucleus supports CREB phosphorylation in hippocampal neurons. *Nature* **392,** 198-202.

Dolmetsch R. E., Lewis R. S., Goodnow C. C., and Healy J. I. (1997) Differential activation of transcription factors induced by Ca2+ response amplitude and duration. *Nature* **386,** 855-858.

Dolmetsch R. E., Pajvani U., Fife K., Spotts J. M., and Greenberg M. E. (2001) Signaling to the nucleus by an L-type calcium channel-calmodulin complex through the MAP kinase pathway. *Science* **294,** 333-339.

Dolmetsch R. E., Xu K., and Lewis R. S. (1998) Calcium oscillations increase the efficiency and specificity of gene expression. *Nature* **392,** 933-936.

Donai H., Sugiura H., Ara D., Yoshimura Y., Yamagata K., and Yamauchi T. (2003) Interaction of Arc with CaM kinase II and stimulation of neurite extension by Arc in neuroblastoma cells expressing CaM kinase II. *Neurosci Res* **47,** 399-408.

Ernfors P., Wetmore C., Olson L., and Persson H. (1990) Identification of cells in rat brain and peripheral tissues expressing mRNA for members of the nerve growth factor family. *Neuron* **5,** 511-526.

Finkbeiner S. and Greenberg M. E. (1998) Ca2+ channel-regulated neuronal gene expression. *J Neurobiol* **37,** 171-189.

Fleck M. W., Palmer A. M., and Barrionuevo G. (1992) Potassium-induced long-term potentiation in rat hippocampal slices. *Brain Res* **580,** 100-105.

Frey U., Huang Y. Y., and Kandel E. R. (1993) Effects of cAMP simulate a late stage of LTP in hippocampal CA1 neurons. *Science* **260,** 1661-1664.

Fujimoto T., Tanaka H., Kumamaru E., Okamura K., and Miki N. (2004) Arc interacts with microtubules/microtubule-associated protein 2 and attenuates microtubule-associated protein 2 immunoreactivity in the dendrites. *J Neurosci Res* **76,** 51-63.

Gallin W. J. and Greenberg M. E. (1995) Calcium regulation of gene expression in neurons: the mode of entry matters. *Curr Opin Neurobiol* **5,** 367-374.

Ghosh A., Ginty D. D., Bading H., and Greenberg M. E. (1994) Calcium regulation of gene expression in neuronal cells. *J Neurobiol* **25,** 294-303.

Ghosh A. and Greenberg M. E. (1995) Calcium signaling in neurons: molecular mechanisms and cellular consequences. *Science* **268,** 239-247.

Ginty D. D., Bading H., and Greenberg M. E. (1992) Trans-synaptic regulation of gene expression. *Curr Opin Neurobiol* **2,** 312-316.

Graef I. A., Mermelstein P. G., Stankunas K., Neilson J. R., Deisseroth K., Tsien R. W., and Crabtree G. R. (1999) L-type calcium channels and GSK-3 regulate the activity of NF-ATc4 in hippocampal neurons. *Nature* **401,** 703-708.

Greenberg M. E. and Ziff E. B. (1984) Stimulation of 3T3 cells induces transcription of the c-fos proto-oncogene. *Nature* **311,** 433-438.

Greenberg M. E., Ziff E. B., and Greene L. A. (1986) Stimulation of neuronal acetylcholine receptors induces rapid gene transcription. *Science* **234,** 80-83.

Gu X. and Spitzer N. C. (1995) Distinct aspects of neuronal differentiation encoded by frequency of spontaneous Ca2+ transients. *Nature* **375,** 784-787.

Guzowski J. F., McNaughton B. L., Barnes C. A., and Worley P. F. (1999) Environment-specific expression of the immediate-early gene Arc in hippocampal neuronal ensembles. *Nat Neurosci* **2,** 1120-1124.

Hardingham G. E., Arnold F. J., and Bading H. (2001) Nuclear calcium signaling controls CREB-mediated gene expression triggered by synaptic activity. *Nat Neurosci* **4,** 261-267.

Hardingham G. E. and Bading H. (2002) Coupling of extrasynaptic NMDA receptors to a CREB shut-off pathway is developmentally regulated. *Biochim Biophys Acta* **1600,** 148-153.

Herdegen T., Kiessling M., Bele S., Bravo R., Zimmermann M., and Gass P. (1993) The KROX-20 transcription factor in the rat central and peripheral nervous systems: novel expression pattern of an immediate early gene-encoded protein. *Neuroscience* **57,** 41-52.

Hong S. J., Li H., Becker K. G., Dawson V. L., and Dawson T. M. (2004) Identification and analysis of plasticity-induced late-response genes. *Proc Natl Acad Sci U S A* **101,** 2145-2150.

Hughes P. and Dragunow M. (1995) Induction of immediate-early genes and the control of neurotransmitter-regulated gene expression within the nervous system. *Pharmacol Rev* **47,** 133-178.

Impey S., Mark M., Villacres E. C., Poser S., Chavkin C., and Storm D. R. (1996) Induction of CRE-mediated gene expression by stimuli that generate long-lasting LTP in area CA1 of the hippocampus. *Neuron* **16,** 973-982.

Inokuchi K., Murayama A., and Ozawa F. (1996) mRNA differential display reveals Krox-20 as a neural plasticity-regulated gene in the rat hippocampus. *Biochem Biophys Res Commun* **221,** 430-436.

Inoue Y., Udo H., Inokuchi K., and Sugiyama H. (2007) Homer1a regulates the activity-induced remodeling of synaptic structures in cultured hippocampal neurons. *Neuroscience* **150,** 841-852.

Jonas P. and Burnashev N. (1995) Molecular mechanisms controlling calcium entry through AMPA-type glutamate receptor channels. *Neuron* **15,** 987-990.

Kang H. and Schuman E. M. (1995) Long-lasting neurotrophin-induced enhancement of synaptic transmission in the adult hippocampus. *Science* **267,** 1658-1662.

Kato A., Ozawa F., Saitoh Y., Hirai K., and Inokuchi K. (1997) vesl, a gene encoding VASP/Ena family related protein, is upregulated during seizure, long-term potentiation and synaptogenesis. *FEBS Lett* **412,** 183-189.

Lemaire P., Revelant O., Bravo R., and Charnay P. (1988) Two mouse genes encoding potential transcription factors with identical DNA-binding domains are activated by growth factors in cultured cells. *Proc Natl Acad Sci U S A* **85,** 4691-4695.

Lerea L. S., Butler L. S., and McNamara J. O. (1992) NMDA and non-NMDA receptor-mediated increase of c-fos mRNA in dentate gyrus neurons involves calcium influx via different routes. *J Neurosci* **12,** 2973-2981.

Li H., Gu X., Dawson V. L., and Dawson T. M. (2004) Identification of calcium- and nitric oxide-regulated genes by differential analysis of library expression (DAzLE). *Proc Natl Acad Sci U S A* **101,** 647-652.

Link W., Konietzko U., Kauselmann G., Krug M., Schwanke B., Frey U., and Kuhl D. (1995) Somatodendritic expression of an immediate early gene is regulated by synaptic activity. *Proc Natl Acad Sci U S A* **92,** 5734-5738.

Lipscombe D., Madison D. V., Poenie M., Reuter H., Tsien R. W., and Tsien R. Y. (1988a) Imaging of cytosolic Ca2+ transients arising from Ca2+ stores and Ca2+ channels in sympathetic neurons. *Neuron* **1,** 355-365.

Lipscombe D., Madison D. V., Poenie M., Reuter H., Tsien R. Y., and Tsien R. W. (1988b) Spatial distribution of calcium channels and cytosolic calcium transients in growth cones and cell bodies of sympathetic neurons. *Proc Natl Acad Sci U S A* **85,** 2398-2402.

Lisman J., Schulman H., and Cline H. (2002) The molecular basis of CaMKII function in synaptic and behavioural memory. *Nat Rev Neurosci* **3,** 175-190.

Lyford G. L., Yamagata K., Kaufmann W. E., Barnes C. A., Sanders L. K., Copeland N. G., Gilbert D. J., Jenkins N. A., Lanahan A. A., and Worley P. F. (1995) Arc, a growth factor and activity-regulated gene, encodes a novel cytoskeleton-associated protein that is enriched in neuronal dendrites. *Neuron* **14,** 433-445.

Mack K., Day M., Milbrandt J., and Gottlieb D. I. (1990) Localization of the NGFI-A protein in the rat brain. *Brain Res Mol Brain Res* **8,** 177-180.

Malinow R. and Malenka R. C. (2002) AMPA receptor trafficking and synaptic plasticity. *Annu Rev Neurosci* **25,** 103-126.

Maren S. and Quirk G. J. (2004) Neuronal signalling of fear memory. *Nat Rev Neurosci* **5,** 844-852.

Marom S. and Eytan D. (2005) Learning in ex-vivo developing networks of cortical neurons. *Prog Brain Res* **147,** 189-199.

Matthews R. P., Guthrie C. R., Wailes L. M., Zhao X., Means A. R., and McKnight G. S. (1994) Calcium/calmodulin-dependent protein kinase types II and IV differentially regulate CREB-dependent gene expression. *Mol Cell Biol* **14,** 6107-6116.

McKay B. E., McRory J. E., Molineux M. L., Hamid J., Snutch T. P., Zamponi G. W., and Turner R. W. (2006) Ca(V)3 T-type calcium channel isoforms differentially distribute to somatic and dendritic compartments in rat central neurons. *Eur J Neurosci* **24,** 2581-2594.

Means A. R., VanBerkum M. F., Bagchi I., Lu K. P., and Rasmussen C. D. (1991) Regulatory functions of calmodulin. *Pharmacol Ther* **50,** 255-270.

Mellstrom B. and Naranjo J. R. (2001) Mechanisms of Ca(2+)-dependent transcription. *Curr Opin Neurobiol* **11,** 312-319.

Milbrandt J. (1987) A nerve growth factor-induced gene encodes a possible transcriptional regulatory factor. *Science* **238,** 797-799.

Morgan J. I., Cohen D. R., Hempstead J. L., and Curran T. (1987) Mapping patterns of c-fos expression in the central nervous system after seizure. *Science* **237,** 192-197.

Morgan J. I. and Curran T. (1986) Role of ion flux in the control of c-fos expression. *Nature* **322,** 552-555.

Morgan S. L. and Teyler T. J. (2001) Epileptic-like activity induces multiple forms of plasticity in hippocampal area CA1. *Brain Res* **917,** 90-96.

Murphy T. H., Worley P. F., and Baraban J. M. (1991) L-type voltage-sensitive calcium channels mediate synaptic activation of immediate early genes. *Neuron* **7,** 625-635.

Nedivi E., Hevroni D., Naot D., Israeli D., and Citri Y. (1993) Numerous candidate plasticity-related genes revealed by differential cDNA cloning. *Nature* **363,** 718-722.

Neher E. (1998) Vesicle pools and Ca2+ microdomains: new tools for understanding their roles in neurotransmitter release. *Neuron* **20,** 389-399.

Nguyen P. V., Abel T., and Kandel E. R. (1994) Requirement of a critical period of transcription for induction of a late phase of LTP. *Science* **265,** 1104-1107.

Nisch W., Bock J., Egert U., Hammerle H., and Mohr A. (1994) A thin film microelectrode array for monitoring extracellular neuronal activity in vitro. *Biosens Bioelectron* **9,** 737-741.

Osawa M., Tong K. I., Lilliehook C., Wasco W., Buxbaum J. D., Cheng H. Y., Penninger J. M., Ikura M., and Ames J. B. (2001) Calcium-regulated DNA binding and oligomerization of the neuronal calcium-sensing protein, calsenilin/DREAM/KChIP3. *J Biol Chem* **276,** 41005-41013.

Otani S. and Abraham W. C. (1989) Inhibition of protein synthesis in the dentate gyrus, but not the entorhinal cortex, blocks maintenance of long-term potentiation in rats. *Neurosci Lett* **106,** 175-180.

Otmakhov N., Khibnik L., Otmakhova N., Carpenter S., Riahi S., Asrican B., and Lisman J. (2004) Forskolin-induced LTP in the CA1 hippocampal region is NMDA receptor dependent. *J Neurophysiol* **91,** 1955-1962.

Otto T., Eichenbaum H., Wiener S. I., and Wible C. G. (1991) Learning-related patterns of CA1 spike trains parallel stimulation parameters optimal for inducing hippocampal long-term potentiation. *Hippocampus* **1,** 181-192.

Park C. S., Gong R., Stuart J., and Tang S. J. (2006) Molecular network and chromosomal clustering of genes involved in synaptic plasticity in the hippocampus. *J Biol Chem* **281,** 30195-30211.

Pastalkova E., Serrano P., Pinkhasova D., Wallace E., Fenton A. A., and Sacktor T. C. (2006) Storage of spatial information by the maintenance mechanism of LTP. *Science* **313,** 1141-1144.

Patterson S. L., Pittenger C., Morozov A., Martin K. C., Scanlin H., Drake C., and Kandel E. R. (2001) Some forms of cAMP-mediated long-lasting potentiation are associated with release of BDNF and nuclear translocation of phospho-MAP kinase. *Neuron* **32,** 123-140.

Pine J. (1980) Recording action potentials from cultured neurons with extracellular microcircuit electrodes. *J Neurosci Methods* **2,** 19-31.

Potter S. M. (2001) Distributed processing in cultured neuronal networks. *Prog Brain Res* **130,** 49-62.

Racine R. J., Milgram N. W., and Hafner S. (1983) Long-term potentiation phenomena in the rat limbic forebrain. *Brain Res* **260,** 217-231.

Rajan I. and Cline H. T. (1998) Glutamate receptor activity is required for normal development of tectal cell dendrites in vivo. *J Neurosci* **18,** 7836-7846.

Rao A. and Craig A. M. (1997) Activity regulates the synaptic localization of the NMDA receptor in hippocampal neurons. *Neuron* **19,** 801-812.

Redmond L., Kashani A. H., and Ghosh A. (2002) Calcium regulation of dendritic growth via CaM kinase IV and CREB-mediated transcription. *Neuron* **34,** 999-1010.

Reichardt L. F. (2006) Neurotrophin-regulated signalling pathways. *Philos Trans R Soc Lond B Biol Sci* **361,** 1545-1564.

Reymann K. G. and Frey J. U. (2007) The late maintenance of hippocampal LTP: requirements, phases, 'synaptic tagging', 'late-associativity' and implications. *Neuropharmacology* **52,** 24-40.

Rizzuto R. and Pozzan T. (2006) Microdomains of intracellular Ca2+: molecular determinants and functional consequences. *Physiol Rev* **86,** 369-408.

Rosen L. B., Ginty D. D., and Greenberg M. E. (1995) Calcium regulation of gene expression. *Adv Second Messenger Phosphoprotein Res* **30,** 225-253.

Rosenblum K., Futter M., Voss K., Erent M., Skehel P. A., French P., Obosi L., Jones M. W., and Bliss T. V. (2002) The role of extracellular regulated kinases I/II in late-phase long-term potentiation. *J Neurosci* **22,** 5432-5441.

Ruaro M. E., Bonifazi P., and Torre V. (2005) Toward the neurocomputer: image processing and pattern recognition with neuronal cultures. *IEEE Trans Biomed Eng* **52,** 371-383.

Saffen D. W., Cole A. J., Worley P. F., Christy B. A., Ryder K., and Baraban J. M. (1988) Convulsant-induced increase in transcription factor messenger RNAs in rat brain. *Proc Natl Acad Sci U S A* **85,** 7795-7799.

Sala C., Futai K., Yamamoto K., Worley P. F., Hayashi Y., and Sheng M. (2003) Inhibition of dendritic spine morphogenesis and synaptic transmission by activity-inducible protein Homer1a. *J Neurosci* **23,** 6327-6337.

Sanes J. R. and Lichtman J. W. (1999) Development of the vertebrate neuromuscular junction. *Annu Rev Neurosci* **22,** 389-442.

Sato M., Suzuki K., and Nakanishi S. (2001) NMDA receptor stimulation and brain-derived neurotrophic factor upregulate homer 1a mRNA via the mitogen-activated protein kinase cascade in cultured cerebellar granule cells. *J Neurosci* **21,** 3797-3805.

Siebler M., Koller H., Stichel C. C., Muller H. W., and Freund H. J. (1993) Spontaneous activity and recurrent inhibition in cultured hippocampal networks. *Synapse* **14,** 206-213.

Steward O., Wallace C. S., Lyford G. L., and Worley P. F. (1998) Synaptic activation causes the mRNA for the IEG Arc to localize selectively near activated postsynaptic sites on dendrites. *Neuron* **21,** 741-751.

Steward O. and Worley P. F. (2001a) A cellular mechanism for targeting newly synthesized mRNAs to synaptic sites on dendrites. *Proc Natl Acad Sci U S A* **98,** 7062-7068.

Steward O. and Worley P. F. (2001b) Selective targeting of newly synthesized Arc mRNA to active synapses requires NMDA receptor activation. *Neuron* **30,** 227-240.

Sutton K. G., McRory J. E., Guthrie H., Murphy T. H., and Snutch T. P. (1999) P/Q-type calcium channels mediate the activity-dependent feedback of syntaxin-1A. *Nature* **401,** 800-804.

Sutton M. A. and Schuman E. M. (2005) Local translational control in dendrites and its role in long-term synaptic plasticity. *J Neurobiol* **64,** 116-131.

Sutton M. A. and Schuman E. M. (2006) Dendritic protein synthesis, synaptic plasticity, and memory. *Cell* **127,** 49-58.

Sweatt J. D. (2001) The neuronal MAP kinase cascade: a biochemical signal integration system subserving synaptic plasticity and memory. *J Neurochem* **76,** 1-10.

Tao X., Finkbeiner S., Arnold D. B., Shaywitz A. J., and Greenberg M. E. (1998) Ca2+ influx regulates BDNF transcription by a CREB family transcription factor-dependent mechanism. *Neuron* **20,** 709-726.

Tappe A., Klugmann M., Luo C., Hirlinger D., Agarwal N., Benrath J., Ehrengruber M. U., During M. J., and Kuner R. (2006) Synaptic scaffolding protein Homer1a protects against chronic inflammatory pain. *Nat Med* **12,** 677-681.

Thoenen H. (1995) Neurotrophins and neuronal plasticity. *Science* **270,** 593-598.

Thomas G. M. and Huganir R. L. (2004) MAPK cascade signalling and synaptic plasticity. *Nat Rev Neurosci* **5,** 173-183.

Valor L. M., Charlesworth P., Humphreys L., Anderson C. N., and Grant S. G. (2007) Network activity-independent coordinated gene expression program for synapse assembly. *Proc Natl Acad Sci U S A* **104,** 4658-4663.

Varoqueaux F., Sigler A., Rhee J. S., Brose N., Enk C., Reim K., and Rosenmund C. (2002) Total arrest of spontaneous and evoked synaptic transmission but normal synaptogenesis in the absence of Munc13-mediated vesicle priming. *Proc Natl Acad Sci U S A* **99,** 9037-9042.

Vinet J. and Sik A. (2006) Expression pattern of voltage-dependent calcium channel subunits in hippocampal inhibitory neurons in mice. *Neuroscience* **143,** 189-212.

Watt S. D., Gu X., Smith R. D., and Spitzer N. C. (2000) Specific frequencies of spontaneous Ca2+ transients upregulate GAD 67 transcripts in embryonic spinal neurons. *Mol Cell Neurosci* **16,** 376-387.

West A. E., Chen W. G., Dalva M. B., Dolmetsch R. E., Kornhauser J. M., Shaywitz A. J., Takasu M. A., Tao X., and Greenberg M. E. (2001) Calcium regulation of neuronal gene expression. *Proc Natl Acad Sci U S A* **98,** 11024-11031.

Westenbroek R. E., Ahlijanian M. K., and Catterall W. A. (1990) Clustering of L-type Ca2+ channels at the base of major dendrites in hippocampal pyramidal neurons. *Nature* **347,** 281-284.

Westenbroek R. E., Hell J. W., Warner C., Dubel S. J., Snutch T. P., and Catterall W. A. (1992) Biochemical properties and subcellular distribution of an N-type calcium channel alpha 1 subunit. *Neuron* **9,** 1099-1115.

Whitlock J. R., Heynen A. J., Shuler M. G., and Bear M. F. (2006) Learning induces long-term potentiation in the hippocampus. *Science* **313,** 1093-1097.

Williams J., Dragunow M., Lawlor P., Mason S., Abraham W. C., Leah J., Bravo R., Demmer J., and Tate W. (1995) Krox20 may play a key role in the stabilization of long-term potentiation. *Brain Res Mol Brain Res* **28,** 87-93.

Wu G. Y., Deisseroth K., and Tsien R. W. (2001) Activity-dependent CREB phosphorylation: convergence of a fast, sensitive calmodulin kinase pathway and a slow, less sensitive mitogen-activated protein kinase pathway. *Proc Natl Acad Sci U S A* **98,** 2808-2813.

Yamada H., Kuroki T., Nakahara T., Hashimoto K., Tsutsumi T., Hirano M., and Maeda H. (2007) The dopamine D1 receptor agonist, but not the D2 receptor agonist, induces gene expression of Homer 1a in rat striatum and nucleus accumbens. *Brain Res* **1131,** 88-96.

Yamagata K., Kaufmann W. E., Lanahan A., Papapavlou M., Barnes C. A., Andreasson K. I., and Worley P. F. (1994) Egr3/Pilot, a zinc finger transcription factor, is rapidly regulated by activity in brain neurons and colocalizes with Egr1/zif268. *Learn Mem* **1,** 140-152.

Acknowledgments

First of all, I would like to thank my supervisor, Vincent Torre for his continuous and constructive support during my PhD.

I thank all the "bicuculline team": Elisabetta for…all!..for scientific and personal support! Giulietta, for the calcium imaging, electrophysiological experiments, for teaching me and for her patience. Frederic for the MEA analysis and especially for his friendship & the chocolate!..that made my days more nice! Giada for preparing a lot of cultures and mainly for listening me! Daniele and Claudio, for the useful discussions about the microarray analyses.

I thank: Manuela for carefully reading my thesis, Jelena for her optimistic view of the life and for creating the "panino day"!!!, my dear friends Helena and Tullio…and remember "SuperSilvia sara' sempre con voi"!!!, all the "Torre's family" for making the days in the lab, very nice days!

I thank my parents…

I thank Andrea…my love…